

UNIVERSITY OF SYDNEY



---

## Final Design Report

---

### AERO4460 AEROSPACE DESIGN 3

*Prepared for:*

DRIES VERSTRAETE  
DERRICK HO

*Prepared by:*

JIE CAO  
TIANPENG GOU  
LORENA GIL MONTERROSO  
SULLIVAN MAI  
HAO YUAN MA  
MINH HOANG DUNG NGUYEN  
HAO WEN WU

# Executive Summary

This report finalises and details the component design for the Autonomous Delivery Vehicle (ADV) proposed by team AviCargo for the Flying Donkey Challenge. The Flying Donkey Challenge is a design competition for an unmanned aerial vehicle with the purpose of cargo delivery around Mount Kenya. The challenge specifically requests for a fixed wing design with high payload capabilities.

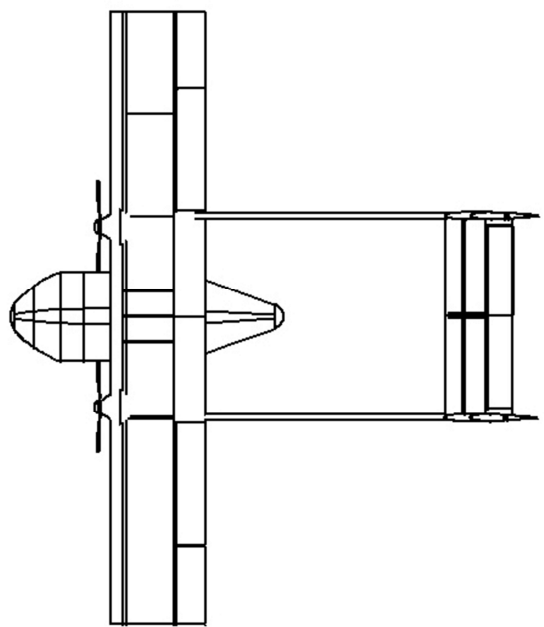
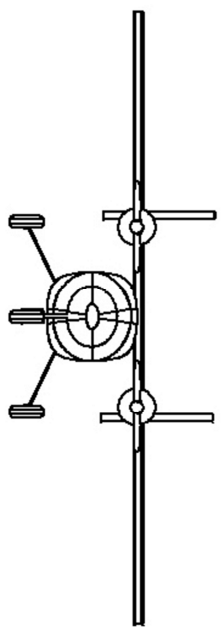
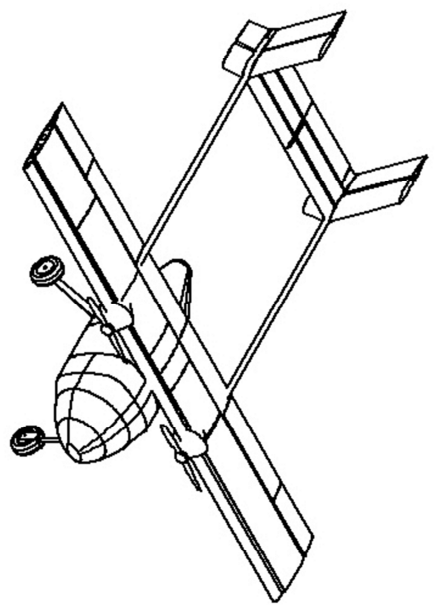
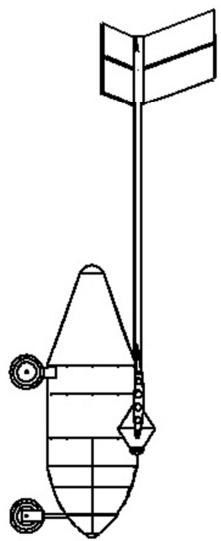
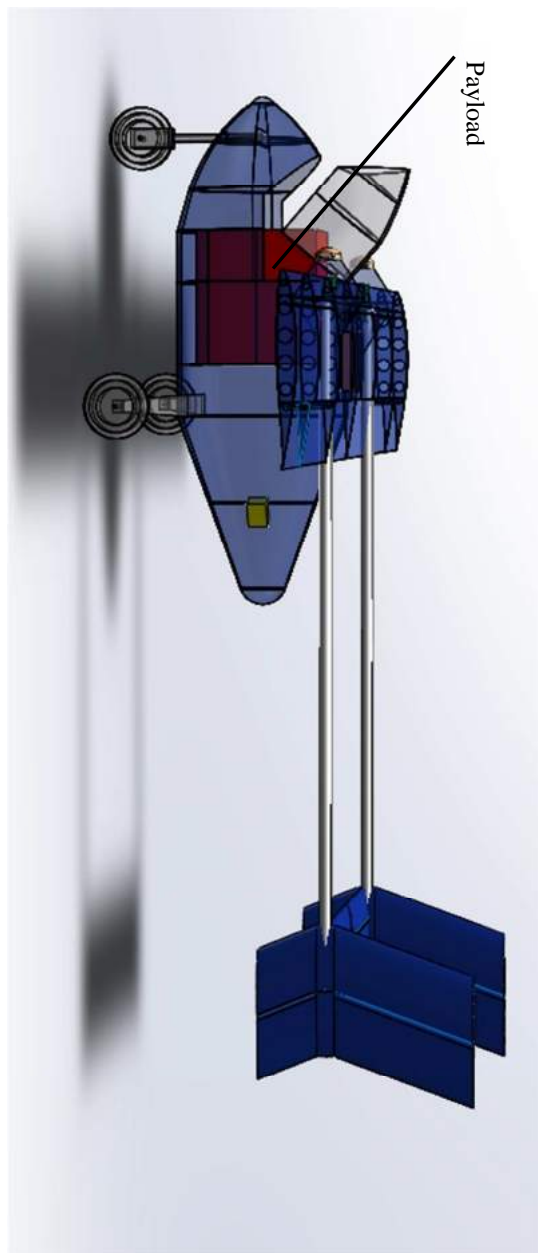
The table below summarises the main design criteria specified by the client and outlines how Avicargo have addressed each issue during the design process of the ADV.

*ADV Design and RFP Considerations*

Design Criteria	Specification	Effect	ADV
Low GTOW	60 kg	Structural Design Loads to be satisfied with lightest possible weight impact.	59.3 kg Structurally designed to FAR load cases
Take Off Run	50 m	High L/D, Powerful Engine (>12kW), Take off run aim for 40 m	Clears 4.41m at 35m runway distance. Landing max 49.6m
Range	50 km	Minimum design range of 50 km	50 km range achieved with 2.66 kg fuel
Max Payload	20 kg	CG sensitivity, Ease of cargo loading	Static Margin: 7%-18%, Top Loading
Location	Mt Kenya	Robustness, Versatility, Ease of Use	Simplified design, Simplified operation

The proposed ADV features design characteristics which are suited for the target mission. Initial performance constraints were found to be the take-off power requirement and this was addressed with employing twin engines with high power to weight ratios. Space requirements due to the large cargo size was addressed by employing high mounted wings which also played a role in minimising FOD from the cleared dirt runways.

Versatility with the operation conditions were the next concern. Due to the isolated geography of the primary design mission, the concept ADV needed to address the possibility of fuel shortages, a lack of available maintenance personnel and harsh operating conditions. The ADV achieves these qualities by simplifying the structural design and this can be seen in the figure on the following page. Engines selected for the ADV are also versatile in the available fuels.



The final design report of the Autonomous Delivery Vehicle has the purpose of addressing the design criteria for a high payload, fixed wing UAV. This report establishes AviCargo's submission to the challenge and will provide details on:

- How the ADV plans to achieve design criteria specified by the customer
- Performance analysis with an emphasis on take-off performance
- Analysis of aerodynamics characteristics and performance
- Optimisation of propulsive system and propeller for operation at high altitude conditions
- Stability analysis of the ADV and control authority check
- Sizing of control surfaces to effectively maintain stability and control
- Optimisation of structural design of wing and undercarriage
- Payload bay design considerations
- Autonomous system implementation of the UAV

The final stages of design of the ADV have produced the following design parameters which sum up the aircraft characteristics:

<b>Final Design Parameters</b>			
GTOW	59.3 kg	OEW	37.1 kg
Total Fuel Weight	2.82 kg	Wing Loading	16.7 kg/m <sup>2</sup>
Height	1.61 m	Power (2xDA-100L)	14.6 kW
Wing Span	4.78 m	Specific Fuel Consumption	2.5 g/min
Length	3.80 m	$C_{Lmax(TO)}$	1.7
Take-Off Distance	49 m	Cruise Speed	25 m/s
AR	6.5	Production Cost (per unit)	\$61,668
L/D <sub>(max)</sub>	110	Sale Price (per unit)	\$86,400

# AviCargo Design Group

*AERO4460 – Aerospace Design 3, 2014*

## Member Roster

<i>Members</i>	<i>Role</i>	<i>Signature</i>
JIE CAO	Aircraft Performance	
TIANPENG GOU	Flight Mechanics and Mission Analysis	
LORENA GIL MONTERROSO	Aerodynamics, Cost Analysis	
SULLIVAN MAI	Undercarriage, Weights and Balance	
HAO YUAN MA	Propulsion	
MINH HOANG DUNG NGUYEN	Team Leader, Structural Design	
HAO WEN WU	Aircraft Systems and Configuration	

---

---

## Table of Contents

<b>List of Figures .....</b>	<b>x</b>
<b>List of Tables.....</b>	<b>xiii</b>
<b>1    Introduction .....</b>	<b>1</b>
<b>2    Analysis of RFP .....</b>	<b>2</b>
<b>2.1    RFP requirements.....</b>	<b>2</b>
<b>2.2    Compliance with RFP.....</b>	<b>3</b>
<b>3    Design Review .....</b>	<b>4</b>
<b>3.1    Comparison with Existing Aircraft.....</b>	<b>4</b>
<b>3.2    Configuration Review .....</b>	<b>6</b>
<b>4    Mission Analysis .....</b>	<b>9</b>
<b>4.1    Geographical Location .....</b>	<b>9</b>
<b>4.2    Cargo Delivery Challenge – Full Mission Outline .....</b>	<b>10</b>
<b>5    Aircraft Suitability for Mission.....</b>	<b>12</b>
<b>5.1    Cargo Loading.....</b>	<b>12</b>
<b>5.2    Simplified Solution.....</b>	<b>13</b>
<b>6    Performance.....</b>	<b>14</b>
<b>6.1    Take Off .....</b>	<b>14</b>
<b>6.2    Climb.....</b>	<b>18</b>
<b>6.3    Cruise .....</b>	<b>21</b>
<b>6.4    Turn.....</b>	<b>22</b>
<b>6.5    Descent and Landing .....</b>	<b>23</b>
<b>6.6    Summary of Performance .....</b>	<b>24</b>
<b>7    Aerodynamics .....</b>	<b>25</b>
<b>7.1    Aerofoil Selection .....</b>	<b>25</b>
<b>7.2    Wing Geometry and High Lift Devices .....</b>	<b>27</b>
<b>7.3    Aircraft Lift .....</b>	<b>28</b>
<b>7.4    Aircraft Drag.....</b>	<b>29</b>
<b>7.4.1    Component Drag.....</b>	<b>29</b>
<b>7.4.2    High Lift Devices Drag .....</b>	<b>31</b>
<b>8    Propulsion .....</b>	<b>33</b>
<b>8.1    Engine .....</b>	<b>33</b>
<b>8.1.1    Engine Selection.....</b>	<b>33</b>
<b>8.1.2    Engine Performance .....</b>	<b>34</b>

---

<b>8.2 Propeller .....</b>	<b>37</b>
8.2.1 ADV Propeller.....	37
8.2.2 Propeller Design .....	37
8.2.3 Propeller Characteristics.....	40
<b>8.3 Propulsion System Performance.....</b>	<b>41</b>
8.3.1 Take-Off, Climb and Cruise .....	41
8.3.2 Operational Engine Conditions.....	41
<b>9 Structures.....</b>	<b>42</b>
<b>9.1 V-N Diagram .....</b>	<b>42</b>
<b>9.2 Load Cases for Structural Design.....</b>	<b>43</b>
<b>9.3 Sizing of Tail Booms .....</b>	<b>44</b>
9.3.1 Boom Material and Final Sizing.....	44
<b>9.4 Sizing of Wing .....</b>	<b>45</b>
9.4.1 Wing Material and Final Sizing.....	48
<b>9.5 Payload Bay .....</b>	<b>50</b>
<b>9.6 Undercarriage .....</b>	<b>51</b>
9.6.1 Landing Gear .....	51
9.6.2 Detailed Undercarriage Structural Analysis .....	53
<b>9.7 Materials Summary .....</b>	<b>56</b>
<b>10 Weights and Balance.....</b>	<b>57</b>
<b>10.1 Component Weight Summary .....</b>	<b>57</b>
<b>10.2 Centre of Gravity .....</b>	<b>59</b>
<b>11 Flight Mechanics .....</b>	<b>60</b>
<b>11.1 Control Surface Sizing.....</b>	<b>61</b>
<b>11.2 CG Travel Limit and Static Margin.....</b>	<b>62</b>
<b>11.3 Longitudinal Stability .....</b>	<b>64</b>
11.3.1 Longitudinal Stability Derivatives .....	64
11.3.2 Longitudinal Elevator Trim with Speed Variation.....	64
11.3.3 Longitudinal State Responses to Elevator Input (Most Forward CG).....	65
<b>11.4 Lateral Stability .....</b>	<b>66</b>
11.4.1 Lateral Static Stability .....	66
11.4.2 Lateral State Responses to Rudder Input (Most Forward CG).....	67
<b>11.5 Control Authority .....</b>	<b>68</b>
11.5.1 Take-off Rotation Elevator Control Authority (Most Forward CG) .....	68
11.5.2 One Engine Inoperative (Most Forward CG, $\beta = 0^\circ$ ) .....	69
11.5.3 Cross Wind Landing (Most Forward CG, $\beta = 15^\circ$ ).....	70

---

11.5.4	Roll Authority Check .....	70
11.6	Handling Quality and Regulations .....	71
11.7	Summary.....	71
<b>12</b>	<b>Aircraft Systems .....</b>	<b>72</b>
12.1	Avionics.....	72
12.2	Actuation.....	73
12.3	Control System.....	73
12.3.1	GPS .....	73
12.3.2	Fuel Systems .....	74
12.3.3	Ground Control .....	74
<b>13</b>	<b>Cost and Development .....</b>	<b>75</b>
13.1	Airplane Cost: Development and Acquisition Cost .....	76
13.2	Operational and Maintenance Cost and Life Cycle Cost .....	80
<b>14</b>	<b>Conclusion.....</b>	<b>82</b>
<b>A</b>	<b>Appendix – Aerodynamics.....</b>	<b>84</b>
a)	Validation of XFLR5.....	84
<b>B</b>	<b>Appendix – Propulsion.....</b>	<b>85</b>
b)	Evolution of Engine Selection.....	85
c)	Operational Engine Conditions at different altitudes.....	86
d)	Estimation of Propeller Diameter and Pitch.....	89
e)	Validation of Xrotor.....	93
<b>C</b>	<b>Appendix – Flight Mechanics.....</b>	<b>95</b>
a)	Initial Sizing.....	95
b)	Vertical Tail Sizing.....	96
c)	Vertical Tail Design.....	96
d)	State Response – Longitudinal and Lateral Control Input .....	97
e)	Elevator Take-off Control Authority and Trim with Speed Variation .....	97
f)	AVL Modelling .....	98
g)	Dynamic Mode and Eigen Characteristics (Most Adverse CG) .....	99
h)	Validation – Cessna 172.....	100
<b>D</b>	<b>Appendix – Structural Design of Wing and Booms .....</b>	<b>102</b>
a)	V-N Diagram Construction and Load Considerations .....	102
b)	AVL Simulation – Lift Distribution.....	103
c)	Component Loads due to Weight.....	106
d)	Sizing of Booms – Loads and Bending Moments.....	107

---

I.	Boom material.....	108
<b>E</b>	<b>Appendix - Undercarriage.....</b>	<b>109</b>
a)	Landing Gear Geometric Layout.....	109
b)	Tyre Selection .....	110
c)	Shock Absorber Types .....	111
d)	Stroke Length Calculation.....	111
e)	Design Approach .....	112
f)	Stress Analysis .....	112
	<b>References .....</b>	<b>118</b>

## List of Figures

Figure 3-1 STOL aircraft Weight/GTOW and AR comparison.....	4
Figure 3-2 STOL aircraft Wing loading and Power loading comparison.....	5
Figure 3-3Dimensions of ADV (in mm) .....	7
Figure 3-4 ADV components layout .....	8
Figure 4-1 Missions map.....	9
Figure 4-2 Altitude and distance of whole mission travels.....	10
Figure 5-1 Payload Access.....	12
Figure 5-2 Depiction of Cargo Loading Mechanism .....	12
Figure 5-3 Component Layout .....	13
Figure 6-1 Thrust, Drag and Lift during Take-Off 2500m .....	14
Figure 6-2 Climb angle (deg) for take off stage at critical altitude (2500m) .....	15
Figure 6-3 Climb rate (m/s) during take-off stage at critical altitude (2500m).....	15
Figure 6-4 Design point for take-off at critical altitude (2500m) .....	16
Figure 6-5 Climb angle at different throttle settings during climb .....	18
Figure 6-6 Climb rate at different throttle settings during climb .....	19
Figure 6-7ROC at different altitude and full throttle, 0 degrees flaps .....	20
Figure 6-8 Drag and thrust along speed on cruise section .....	21
Figure 6-9 Turn Radius vs. Speed at different throttle settings .....	22
Figure 6-10 Bank angle vs. speed at different throttle settings .....	22
Figure 6-11 Landing Detail Map.....	23
Figure 7-1 NACA 65410 profile .....	26
Figure 7-2 Wing lift coefficient over angle of attack.....	28
Figure 7-3 Drag coefficient over flap deflection.....	32
Figure 8-1 Evaluation of Engine Selection .....	33
Figure 8-2 Contour of Engine Power (WOT) with variation of Altitude.....	35
Figure 8-3 Contour of Engine Torque (WOT) with variation of Altitude .....	35
Figure 8-4 Engine Fuel Consumption .....	36
Figure 8-5 Propeller Thrust and Aircraft Drag.....	38
Figure 8-6 Evaluation of Performance of Various Propellers.....	38
Figure 8-7 Engine Torque (WOT) Condition with '31x12' Propeller .....	39
Figure 8-8 Comparison of Propeller Thrust in WOT Take-off .....	40
Figure 8-9 a) Propeller Power Coefficient b) Propeller Thrust Coefficient c) Propeller Efficiency .....	40

---

Figure 9-1 V-N Diagram .....	42
Figure 9-2 Shear Force - Cruise Aileron Down .....	45
Figure 9-3 Moment Diagram - Cruise Aileron Down.....	45
Figure 9-4 Shear Force - Diving .....	46
Figure 9-5 Moment Diagram - Diving .....	46
Figure 9-6 Shear Force - Landing .....	47
Figure 9-7 Moment Diagram - Landing.....	47
Figure 9-8 Wing Ribs and Spar Layout .....	48
Figure 9-9 Wing and Tail Boom Materials Summary.....	49
Figure 9-10 a) Cargo Tray Design b) Fuselage Structure accommodating landing gear.....	50
Figure 9-11 a) ADV Landing Gear Geometry- Overturn Angle and Wheel Track b) Positioning and clearances .....	52
Figure 9-12 a) Nose Gear System b) Main Gear System.....	52
Figure 9-13 Leaf Spring FEA - Total Deformation .....	54
Figure 9-14 Leaf Spring FEA - Maximum Shear Stress .....	54
Figure 9-15 Leaf Spring FEA - Equivalent Stress .....	55
Figure 9-16 Materials Summary .....	56
Figure 10-1 Component Layout .....	57
Figure 10-2 CG Travel .....	59
Figure 11-1 Control Surface Size and Vertical Tail Features .....	61
Figure 11-2 Horizontal Tail Sizing for CG Travel Limit – Scissor Plot.....	62
Figure 11-3 Longitudinal Elevator Trim with Speed Variation for two CG cases .....	64
Figure 11-4 Longitudinal State Responses at Initial Climb with 5o Elevator Input for 5 seconds .....	65
Figure 11-5 Longitudinal State Responses at Cruise with 5o Elevator Input for 5 seconds.....	65
Figure 11-6 Longitudinal State Responses at Approach with 5o Elevator Input for 5 seconds ...	65
Figure 11-7 Lateral State Responses at Initial Climb with 5o Rudder Input for 5 seconds.....	67
Figure 11-8 Lateral State Responses at Cruise with 5o Rudder Input for 5 seconds.....	67
Figure 11-9 Lateral State Responses at Approach with 5o Rudder Input for 5 seconds.....	67
Figure 11-10 Take-off Rotation Elevator Control Authority .....	68
Figure 11-11 One Engine Inoperative Lateral Trim.....	69
Figure 11-12 Cross Wing Landing Lateral Trim .....	70
Figure 11-13 Roll Authority Check .....	70
Figure 12-1 Avionics System Architecture .....	72

---

Figure 12-2 Fuel System .....	74
Figure 13-1 Comparison of cost per unit (RDTE + acquisition) produced (USA vs. China).....	77
Figure 13-2 Cost per unit (RDTE + acquisition) over aircraft quantity produced China Labour Cost.....	78
Figure 13-3 Contribution of elements to total airplane cost.....	79
Figure 13-4 Variation of operational and maintenance cost with number of flights .....	80
Figure A-1 Lift Coefficient vs. angle of attack XFLR5 .....	84
Figure B-1 33x9 and 27x10 Ideal Propeller Thrust Comparison .....	90
Figure B-2 Ideal Thrust and Required Torque for Propellers with varying geometry.....	91
Figure B-3 Comparison of Propeller Thrust in Flight Operation by Engine .....	91
Figure B-4 31x12 and 32x11 Propeller Efficiency Comparison.....	92
Figure B-5 X-Rotor Validation of Airscrew Propellers .....	94
Figure C-1 Vertical Tail Design.....	96
Figure D-1 Cruising maximum negative elevator deflection (elevator up 25 degree).....	103
Figure D-2 Cruising maximum positive elevator deflection (elevator down 25 degree).....	104
Figure D-3 Cruising maximum positive rudder deflection (30 degree).....	104
Figure D-4 Cruising right aileron maximum deflection down (-25 degree) .....	105
Figure D-5 Diving no control surface deflection .....	105
Figure D-6 Landing full flap deployed (50 degree) .....	106
Figure E-1 One Wheel Landing - SolidWorks.....	113
Figure E-2 Braked Roll - SolidWorks.....	114
Figure E-3 Braked Roll - ANSYS.....	115
Figure E-4 Side Loading - SolidWorks.....	116
Figure E-5 Side Loading - ANSYS.....	117

## List of Tables

Table 2-1 Compliance with RFP requirements .....	3
Table 3-1 Concept ADV parameters in response to RFP requirements.....	6
Table 4-1 Mission stations location coordinates .....	9
Table 4-2 Fuel burn needed in each channel between stations .....	11
Table 6-1 Design point break down of take-off at critical altitude .....	17
Table 6-2 Maximum Climb Performance Summary.....	19
Table 6-3 Summary of cruise phase.....	21
Table 6-4 Design Point for Turn .....	22
Table 6-5 Landing detail .....	23
Table 7-1 Wing aerofoil aerodynamic characteristics.....	25
Table 7-2 Wing geometry characteristics.....	27
Table 7-3 Flaps dimensions.....	27
Table 7-4 Lift coefficients for flight phases.....	28
Table 7-5 Detailed component drag .....	31
Table 7-6 Drag at TO and landing with flaps configuration .....	31
Table 8-1 Engine Specification .....	34
Table 8-2 Propeller Specifications .....	37
Table 8-3 Propulsive performance under different flight phases .....	41
Table 8-4 2500 meters Elevation: Engine Condition in Operation by Throttle Position .....	41
Table 9-1 Load Case Summary .....	43
Table 9-2 Structural Design - Load Cases .....	43
Table 9-3 Boom Sizing Results.....	44
Table 9-4 Max shear and bending moment from load cases.....	47
Table 9-5 Wing Structure Summary .....	48
Table 9-6 Wing Caps Summary .....	49
Table 9-7 Summary of Undercarriage System.....	51
Table 9-8 Undercarriage Load Cases (tick indicates compliance).....	53
Table 10-1 Component Weight Summary .....	58
Table 11-1 Control Surface Dimensions .....	62
Table 11-2 CG Travel Limit vs. CG Travel in Flight and Static Margin.....	63
Table 11-3 Longitudinal Stability at Most Forward CG Location.....	64
Table 11-4 Longitudinal Stability at Most Aft CG Location .....	64
Table 11-5 Lateral Stability at Most Forward CG Location .....	66

---

Table 11-6 Lateral Stability at Most Afterward CG Location .....	66
Table 11-7 Handling Quality Check with Regulations .....	71
Table 12-1 Avionics Components.....	73
Table 13-1 Cost analysis summary .....	75
Table 13-2 Breakdown for RDTE cost .....	76
Table 13-3 Breakdown for acquisition cost .....	78
Table 13-4 Breakdown for operational and maintenance cost.....	81
Table B-1 Potential Engine Choices .....	85
Table B-2 2150 meters Elevation: Engine Condition in Operation by Throttle Position .....	86
Table B-3 2085 meters Elevation: Engine Condition in Operation by Throttle Position .....	86
Table B-4 2003 meters Elevation: Engine Condition in Operation by Throttle Position .....	87
Table B-5 1981 meters Elevation: Engine Condition in Operation by Throttle Position .....	87
Table B-6 1970 meters Elevation: Engine Condition in Operation by Throttle Position .....	87
Table B-7 1831 meters Elevation: Engine Condition in Operation by Throttle Position .....	88
Table B-8 1770 meters Elevation: Engine Condition in Operation by Throttle Position .....	88
Table B-9 1621 meters Elevation: Engine Condition in Operation by Throttle Position .....	88
Table B-10 Measurement of 27x10 Sport Prop Type A .....	89
Table B-11 Geometry of Master Airscrew Propellers .....	93
Table C-1 Horizontal and Vertical Tail Sizing .....	95
Table C-2 Control Surface Sizing .....	95
Table C-3 Initial Climb Dynamic Mode and Eigen Characteristics .....	99
Table C-4 Cruise Dynamic Mode and Eigen Characteristics .....	99
Table C-5 Approach Dynamic Mode and Eigen Characteristics .....	99
Table C-6 Cessna 172 Longitudinal Static Trim.....	100
Table C-7 Initial Climb Dynamic Mode and Eigen Characteristics .....	100
Table C-8 Cruise Dynamic Mode and Eigen Characteristics .....	100
Table C-9 Approach Dynamic Mode and Eigen Characteristics .....	101
Table D-1 Major aircraft parameters.....	102
Table D-2 Load factor under new condition .....	102
Table D-3 Limit component weights at 1g and corresponding load factors .....	106
Table D-4 Ultimate loads at corresponding load factors created by control surface deflection .	107
Table D-5 Moment acting at right boom.....	107
Table D-6 Listed properties of Aluminum in English units.....	108
Table D-7 Boom diameters and mass .....	108

---

Table E-1 Tyre Type .....	110
Table E-2 Load Cases for Undercarriage Design.....	112

## 1 Introduction

This final design report presents a solution to the request for proposal specified by the Flying Donkey Challenge. The design of the ADV is an iterative process in which, each design department is integrated into forming one design solution with the aim of satisfying the main design criteria specified by the customer. This report details the design approach conducted to produce the ADV and summarises key design factors of each department.

Section 2 of this document analyses the RFP, specifying the critical design criteria to which the ADV is subject and identifying the criteria to which the final design has satisfied. The following section 3 aims to compare the final design with similar aircraft and summarise the design decisions which led to the fruition of the ADV. Section 4 will summarise the mission in which the ADV is designed for, specifying the operating conditions around Mount Kenya and the potential missions in which the ADV will have to perform. Section 5 will look at the ADV as a final product, justifying the design decisions and reviewing critical components of each department and the purpose these components serve towards complying with the RFP.

Section 6 summarises the aircraft performance and details the flight phases to which the ADV is subjected during its mission. Section 7 details aerodynamic performance of the aircraft and introduces the high lift devices which the ADV requires to meet take-off requirements. Section 8 will then detail the design of the propulsion system and the effects of engine performance at high operating altitudes.

Section 9 details the full structural design of wing, tail boom and undercarriage of the ADV with a focus on optimisation of the main undercarriage system. Section 10 summarises the component weight build-up of the ADV and will explore the centre of gravity travel for the aircraft. Section 11 of this report will detail the static and dynamic stability of the ADV in addition to a performance of control authority checks specified by the costumer. Finally section 12 will detail the aircraft systems and section 13 will outline the cost and development required in producing the ADV for commercial use.

The design philosophy behind AviCargo as a company is to provide a simplified solution to the consumer. AviCargo's aim is to produce a design in which robustness, reliability, ease of use and cost effectiveness are key. AviCargo believes that the Flying Donkey Challenge calls for a simplified solution which will stand against the complex operating conditions to which the ADV is subject.

## 2 Analysis of RFP

The Flying Donkey Challenge aims to implement large scale unmanned civilian air cargo delivery services in Africa and beyond.

The mission requires a minimum of three 20 kg payload deliveries around Mount Kenya within 24 hour period. The UAV will be required to take off within 50 m and have a MTOW of 60 kg.

### 2.1 RFP requirements

The total mission specifications required by the Flying Donkey Challenge are:

- Maximum Take-off Weight of 60 Kg
- Maximum payload 20 Kg
- Total distance ~200 km
- Ground Stations around the route: 6
- Minimum delivery and collections missions: 3
- Maximum distance between ground stations 50 km
- Minimum hold cargo volume of  $0.126 \text{ m}^3$  to fit two suitcases with easy access
- Maximum suitcase dimensions: 45x25x56 cm
- Ground station maximum slope 5% and 10 m wide and 50 m long
- Ground station maximum altitude 2500 m above sea level
- $15^\circ$  approach/departing sectors
- Flight corridor minimum width 200 m. Minimum altitude 50 m and maximum altitude 300 m (above ground level)
- Visual flight rules: 500 m clear of cloud
- As cost-effective as possible

All the requirements were fixed by AviCargo team. The more restrictive ones were the MTOW of 60 kg and the maximum take-off distance of 50 m. Special focus was done throughout all the design process to meet a cost-effective design. This is of high importance for AviCargo to allow the ADV to be afforded by low resources areas.

## 2.2 Compliance with RFP

This section summarises the compliance of the ADV with the RFP requirements, which is presented in Table 2-1.

*Table 2-1 Compliance with RFP requirements*

Design Criteria	RFP Specification	ADV	Compliance
Max GTOW	60 kg	59.3 kg	✓
Max Take Off Run	50 m	49.6m	✓
Min Range	50 km	50 km range achieved with 2.66 kg fuel	✓
Max Payload	20 kg	20 kg	✓
Max width	10 m	4.78 m	✓
Min turn radius	100 m	100	✓
Min delivery and collections	3	6	✓
Max suitcase dimensions	45x25x56 cm	45x25x56 cm	✓
Location	Mt Kenya	Simplified design and operation Low cost	✓

### 3 Design Review

#### 3.1 Comparison with Existing Aircraft

In committing to the design of an aircraft with short take-off and landing characteristics, aspect ratio considerations were accounted for. Aspect ratio determination relied on historical data of UAV similar in weight as well as the data obtained from a variety of STOL aircraft. Generally, higher aspect ratio aircraft have long and thin wings and this was problematic due to the impact a small chord length has on fitting structural components. However aspect ratios in the range of 6-7 did display good lift to drag characteristics and this was an important design criterion that was specified by the RFP. Figure 3-1 shows the comparison of ADV to various STOL aircraft's aspect ratio and their empty weight to gross take-off weight ratio.

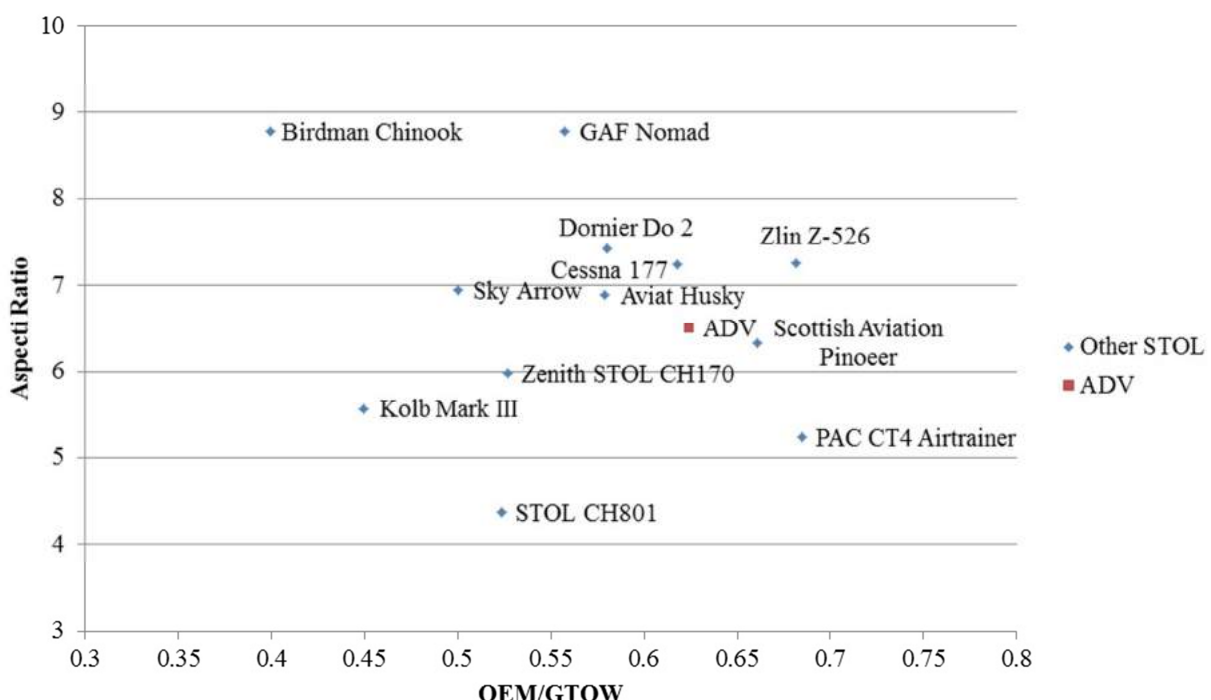


Figure 3-1 STOL aircraft Weight/GTOW and AR comparison

Such comparison gives guidance to the design of Aircraft's configuration of this particular category. As the design evolves, ADV has been designed to have moderate aspect ratio to its similar kinds.

Comparison has also been established on power loading and wing loading of various UAVs of the similar configuration. Figure 3-2 shows the comparison of power loading and wing loading between ADV and other similar aircrafts. It is outstanding that the ADV is a STOL aircraft with lower average power and wing loading parameters. This is due to the low GTOW of this UAV compared to the existing typical aircraft weights. It could be said that a new generation of STOL aircraft has been made out.

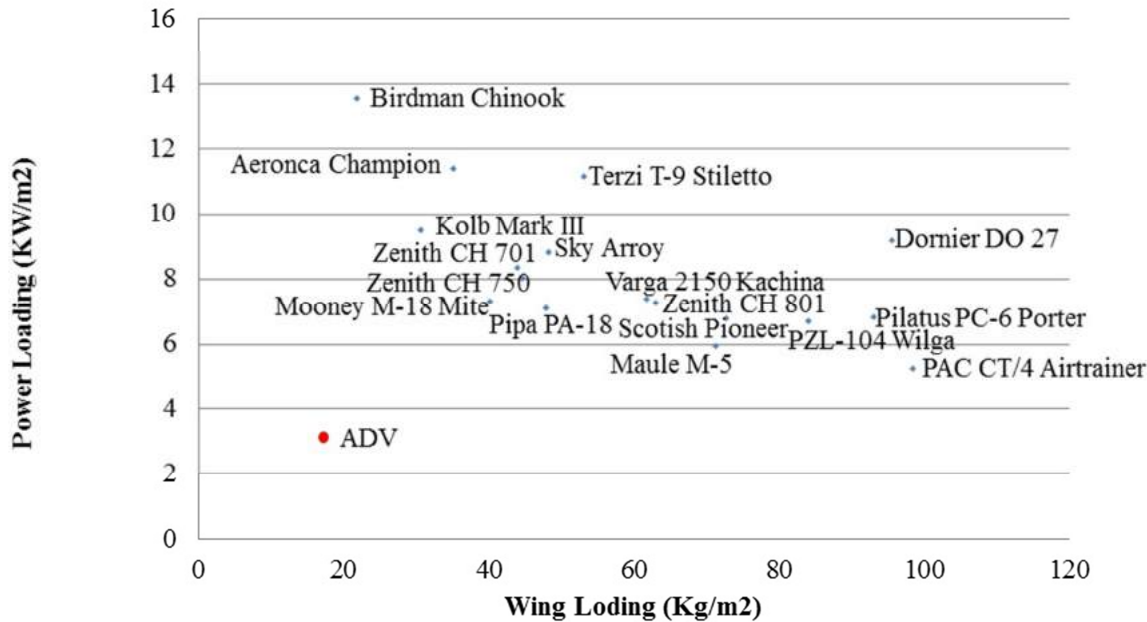


Figure 3-2 STOL aircraft Wing loading and Power loading comparison

### 3.2 Configuration Review

The design of the ADV was done with the aim of achieving the design criteria specified by the Flying Donkey Challenge.

Table 3-1 outlines how AviCargo have addressed each issue during the design process of the ADV.

*Table 3-1 Concept ADV parameters in response to RFP requirements*

Design Criteria	Specification	Effect	ADV
Low GTOW	60 kg	Structural Design Loads to be satisfied with lightest possible weight impact.	59.3 kg Structurally designed to FAR load cases
Take Off Run	50 m	High L/D, Powerful Engine (>12kW), Take off run aim for 40 m	Clears 4.41m at 35m runway distance. Landing max 49.6m
Range	50 km	Minimum design range of 50 km	50 km range achieved with 2.66 kg fuel
Max Payload	20 kg	CG sensitivity, Ease of cargo loading	Static Margin: 7%-18%, Top Loading
Location	Mt Kenya	Robustness, Versatility, Ease of Use	Simplified design, Simplified operation

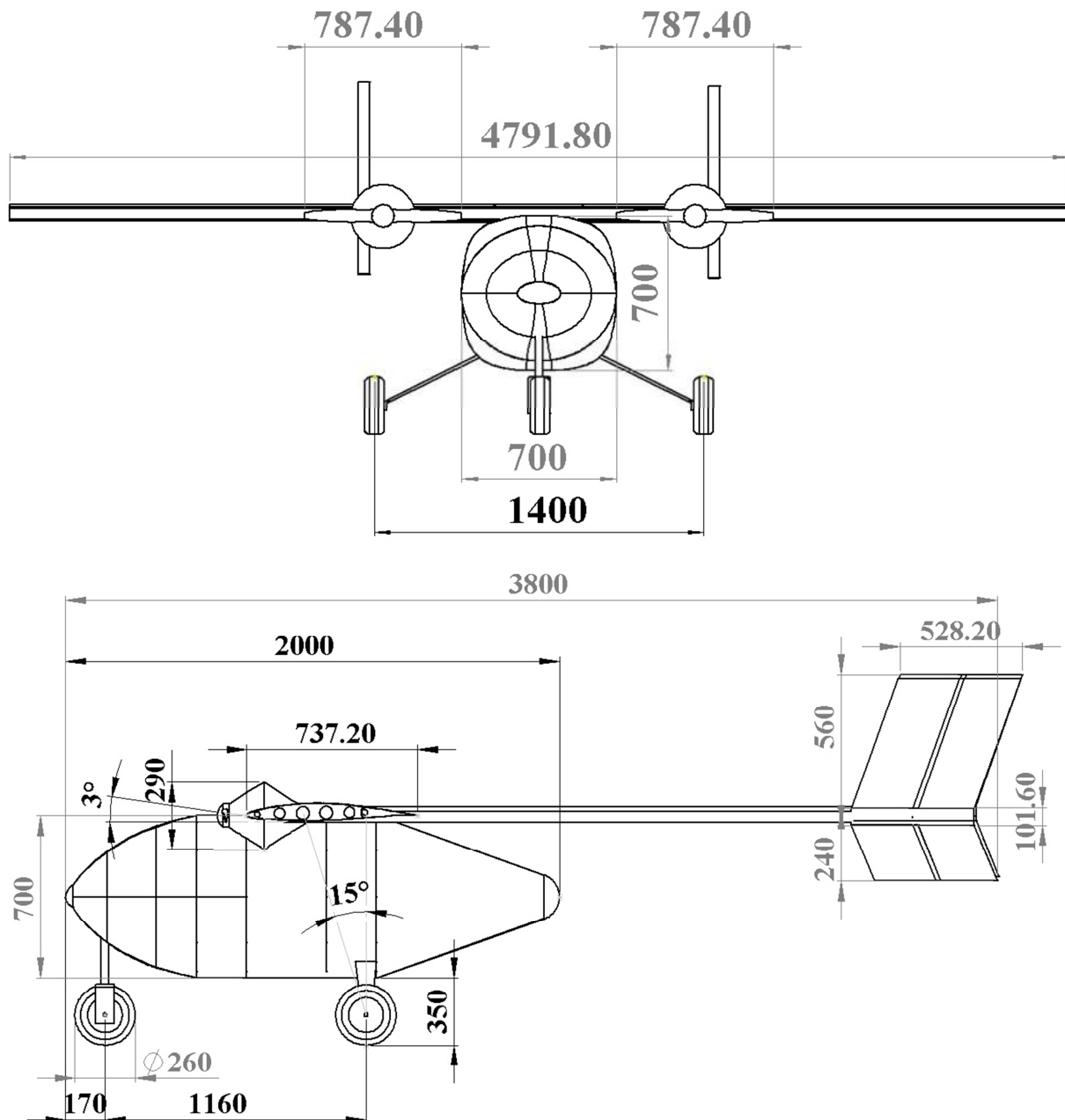


Figure 3-3 Dimensions of ADV (in mm)

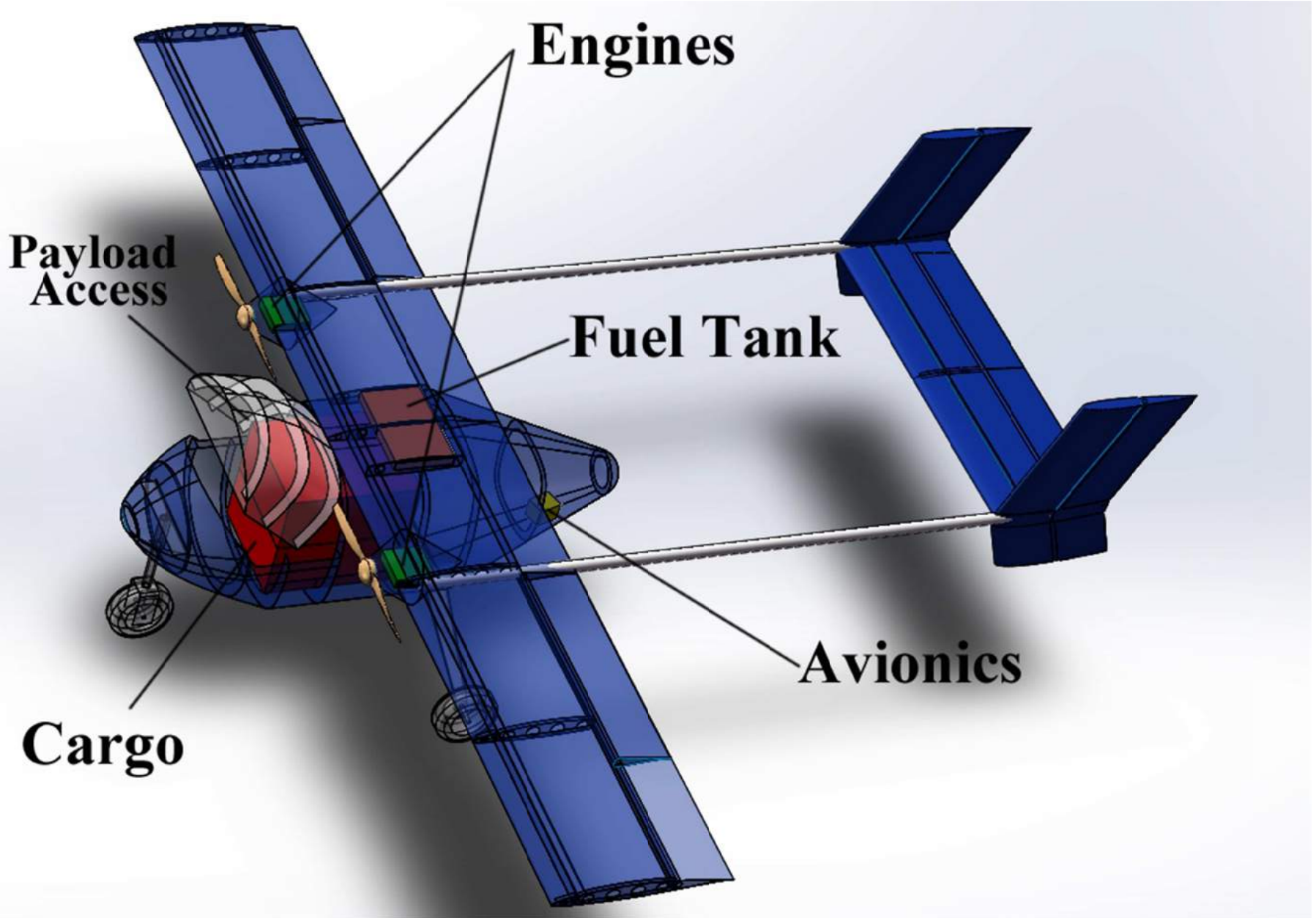


Figure 3-4 ADV components layout

## 4 Mission Analysis

The focus on this section is to show the mission profile that has been adopted for the ADV in response to the RFP and outline the performance capabilities of the UAV at each mission segment. The latter will include distance, time and fuel burn within each section.

### 4.1 Geographical Location

The mission profile adopted for the ADV is shown in Figure 4-1. It is composed of a total of 6 stations around the highest altitude point in Mount Kenya. Specific details about altitude and longitude and latitude coordinates of each of the stations is outlined in Table 4-1.

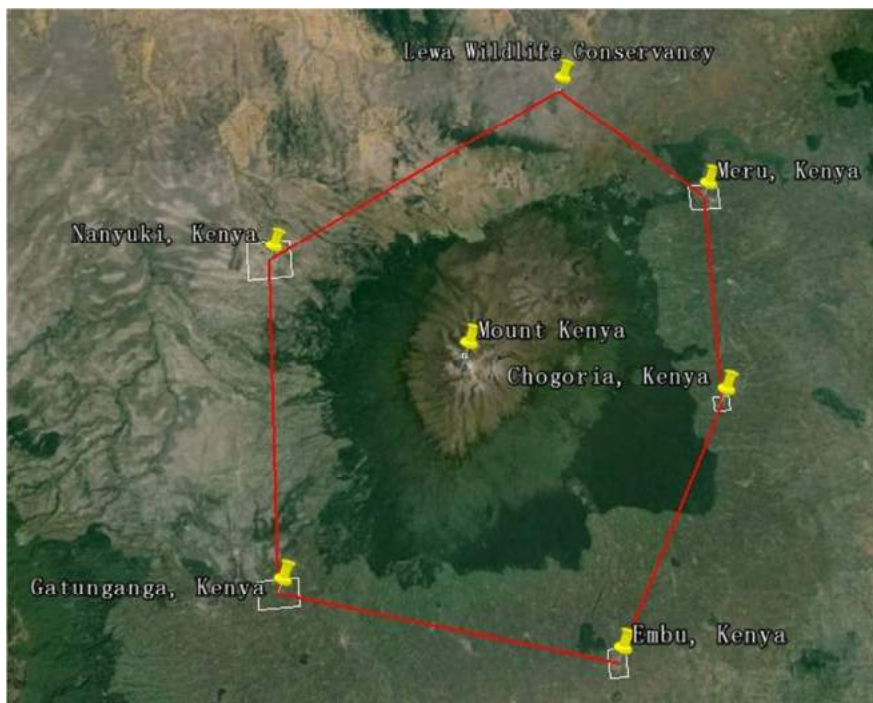


*Figure 4-1 Missions map*

*Table 4-1 Mission stations location coordinates*

Name	North (deg)	East (deg)	Elevation (m)
Lewa	0.218667	37.470125	1681
Meru	0.051381	37.64585	1660
Chogoria	-0.228017	37.630694	1531
Embu	-0.538856	37.459653	1321
Gatunganga	-0.416683	37.05	1703
Nanyuki	0.016656	37.066669	1922

## 4.2 Cargo Delivery Challenge – Full Mission Outline

The RFP specifies that the flight height varies between 300 meters and 100 meters over the ground, so it means that the level altitude on flight changes during the travel over variable ground stations. Figure 4-2 outlines the mission height and distance profile between the six ground stations selected for the challenge mission. At each station, refuelling takes place as well as the required load and unload operations as needed.

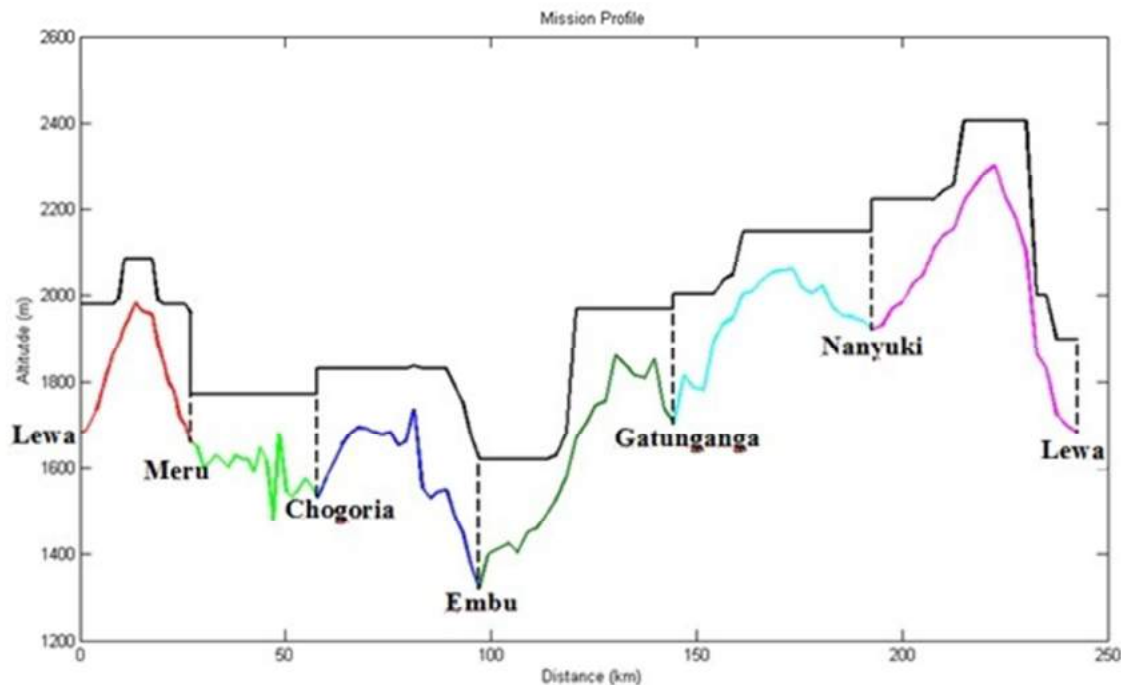


Figure 4-2 Altitude and distance of whole mission travels

There are in total 13 section of level flight on one cycle travel. The 6 different colours show the 6 different channels. From Figure 4-2, the first three level flights are included in the first channel. To find further details of each flight level phase, the 6 channels can be solved out as the following Table 4-2.

For the fuel burn, a safe margin is already added, which is 5 % of fuel used. It is also included the take-off section, which spends only 0.006 kg of fuel. For the maximum distance of 50 m, the aircraft needs to carry the maximum fuel weight (2.66 kg) during that flight.

*Table 4-2 Fuel burn needed in each channel between stations*

Stage	Distance (m)	Time (min)	Fuel burn (kg)
1	25550	21.5	1.91
2	32250	27.4	2.18
3	39200	33.2	2.75
4	47500	40.3	2.59
5	48100	40.3	2.66
6	50000	41.6	2.66

## 5 Aircraft Suitability for Mission

### 5.1 Cargo Loading

AviCargo's aim was to provide a solution in which was simplified for the consumer and this is reflective in the cargo loading mechanism of the ADV. The ADV is an unmanned vehicle during flight and the operational human interface of the aircraft is first and foremost the cargo access. Design of the cargo bay features a hinged access panel which opens up and automatically spring-locked. The cargo then can be accessed from the front of the aircraft. Utilising a tricycle landing gear for the aircraft was ideal in this situation as it allowed ease of loading for the payload due to a level height platform (figure 5-2). More details on the structural design of the cargo bay is outlined in section 9.



Figure 5-1 Payload Access



Figure 5-2 Depiction of Cargo Loading Mechanism

## 5.2 Simplified Solution

The ADV is designed to operate around Mount Kenya, and the simplified approach to designing the aircraft minimises the risk of damage, lowers cost of maintenance and repair as well as reducing the difficulty in operation.

Figure 5-3 shows the layout of parts of the ADV, it can be seen from here the placement of crucial components such as the avionics is moved to the aft of the fuselage to prevent damage during the loading and unloading of payload. Payload access is placed at the front of the aircraft to ensure ease of operation whilst the engines are wing mounted and moved from the fuselage, removing the risk of damage of crucial components when handling heavy cargo.

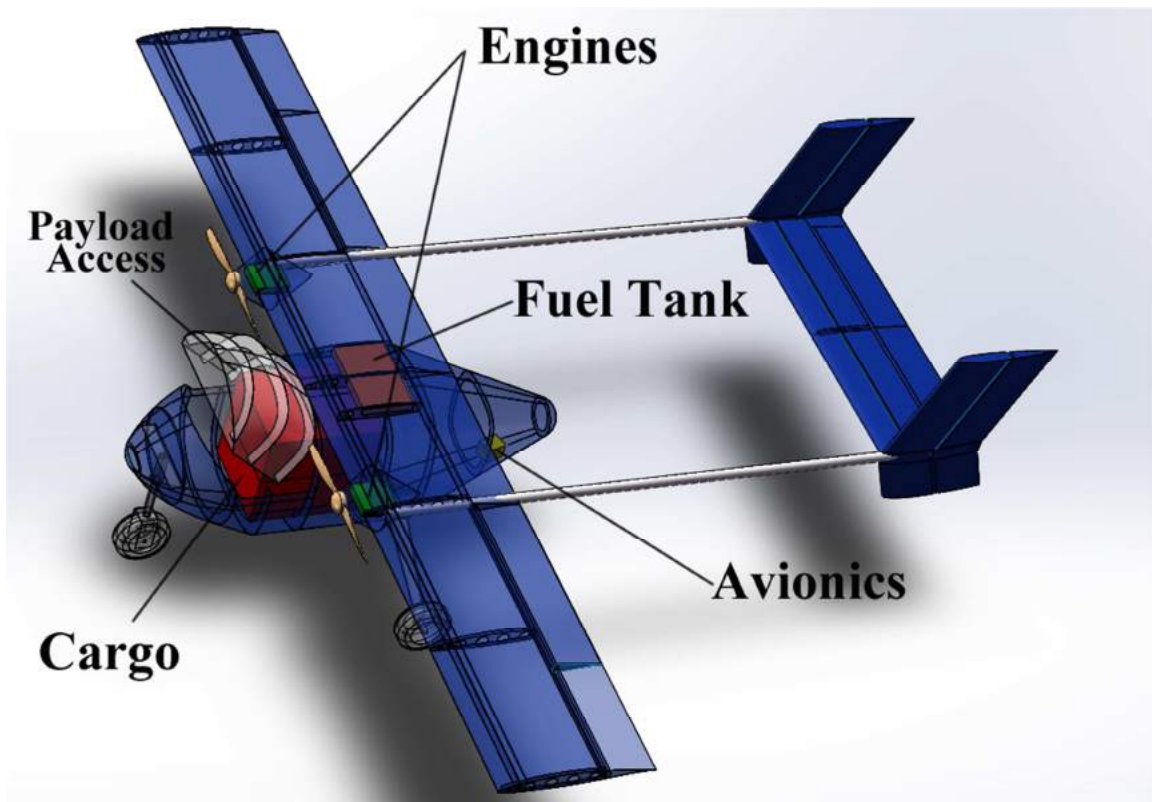


Figure 5-3 Component Layout

## 6 Performance

### 6.1 Take Off

Take off performance refers to the distance required for the aircraft to accelerate from warm up to lift-off, as well as the required distance to the initial steady climb. Hence in this section, maximum design runway distance is 50m which incorporates all stages of take-off including a 4.41 m obstacle at the end.

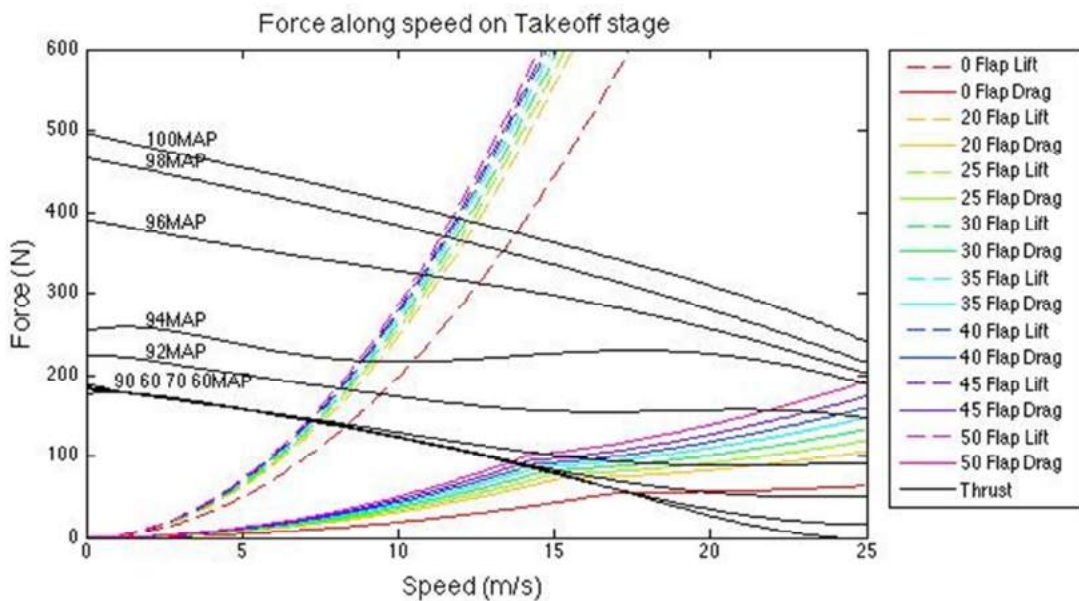


Figure 6-1 Thrust, Drag and Lift during Take-Off 2500m

Figure 6-1 details the forces that are present at 2500m during the take-off phase. The forces on the plot include: lift under variable flap angle, drag under variable flap angle and thrust under variable throttle. For the trend of drag, there are turning points which occur at the stall speed of each relative flap angle. From figure 6-1 it can be seen easily that 100% throttle is the best choice to produce the most thrust for take-off for short runway distance. The take-off run is characterised by the ground run followed by an immediate flap actuation to the take-off setting to achieve desired lift. A deploy time of one second is required to extend 35 degrees flaps before lift-off.

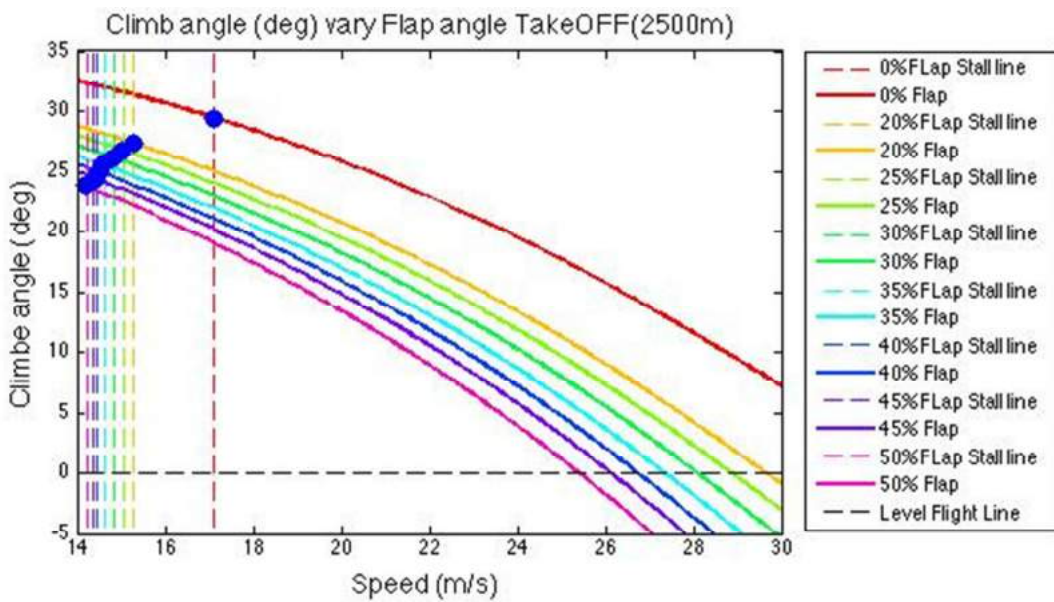


Figure 6-2 Climb angle (deg) for take off stage at critical altitude (2500m)

On figure 6-2, the blue points represent the maximum climb angle at each flap setting. These maximum values always occur at their stall speed. The stall speeds are shown as the vertical dash line. It is because the lower speed can produce more thrust and receive less drag, so it has much more extra force to maintain large pitch angle. With increasing speed, pitch angle decreases. The conditions below the red line are all viable for the ADV. The trends of the lines are decreasing along the speed, so aircraft will be hard to climb at high velocity.

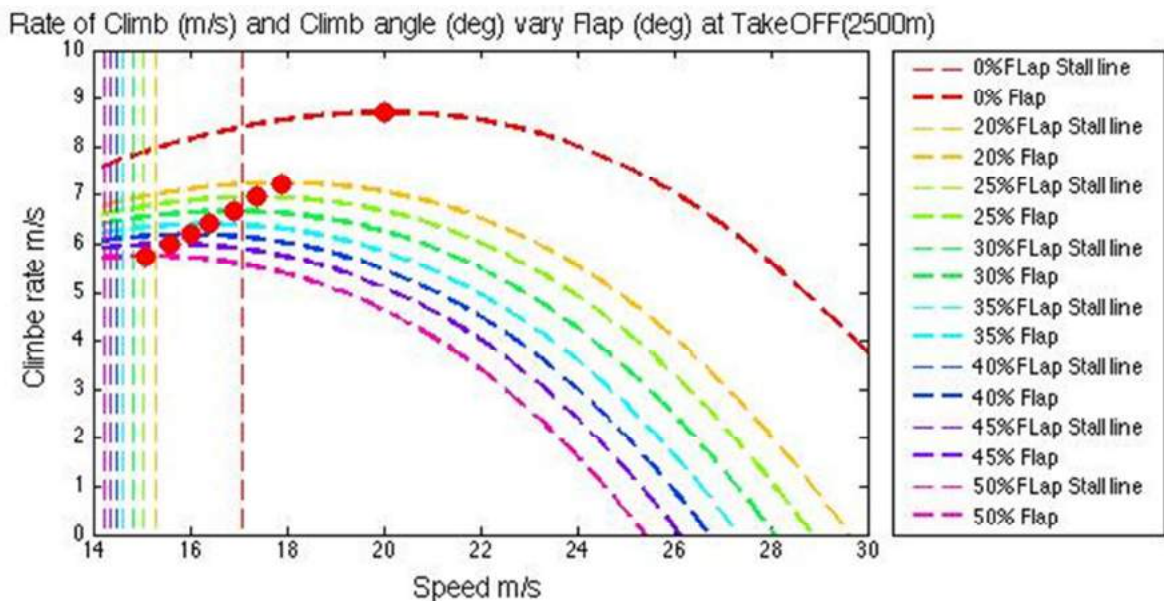


Figure 6-3 Climb rate (m/s) during take-off stage at critical altitude (2500m)

Figure 6-3 is similar with that of climb angle, but its maximum values occur on the peak of curves. The main function of figure 6-2 and 6-3 are to make sure the pitch condition is under the safe line. The maximum climb angle is 29 degree from figure 6-2, but its speed is close the stall speed; it is dangerous climb at this angle.

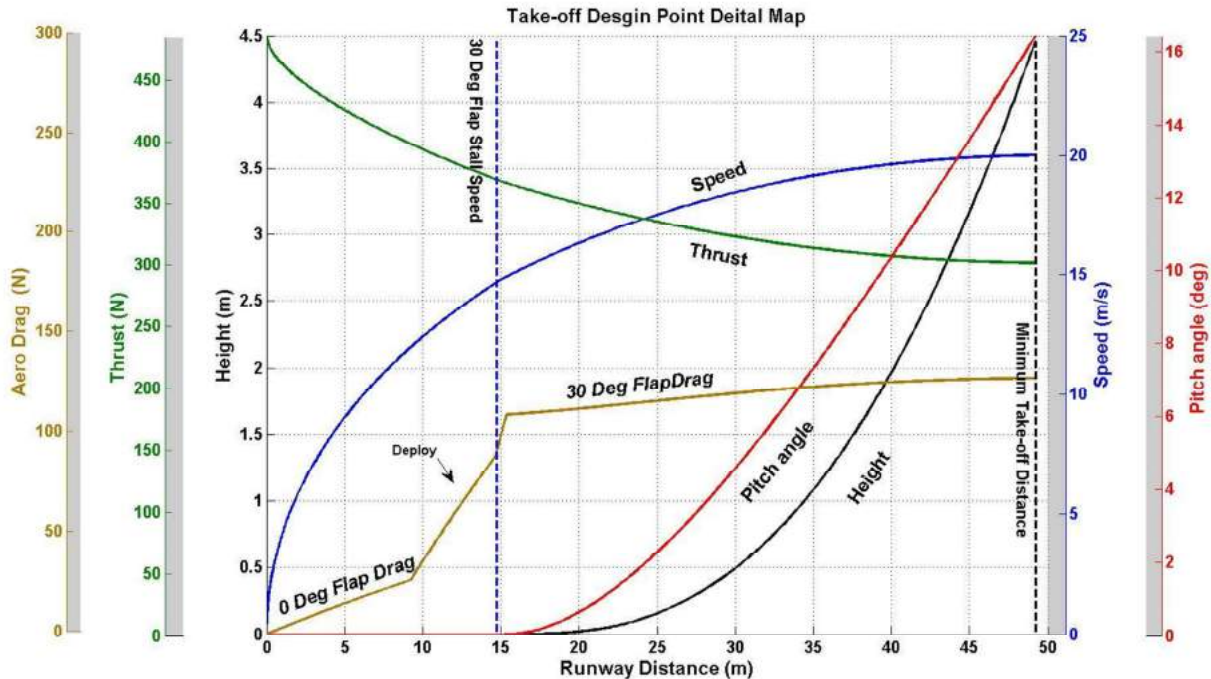


Figure 6-4 Design point for take-off at critical altitude (2500m)

Figure 6-4 summarises the take-off run performance of the UAV by showing the relationship between multiple variables during the phase of flight. The take-off phase clears the end of runway obstacle just after 30 metres therefore satisfying the performance requirement specified by the RFP.

The take-off run as seen in figure 6-4 assumes a zero flap setting then deploys flaps during the acceleration phase. A large flap setting is selected due to the climb angle being reduced as can be seen from figure 6-2. Larger flap angle can increase lift with slight increasing drag therefore allowing the ADV to take off as soon as possible, so therefore the 30-degree flap is selected to satisfy the STOL requirement. The critical points during the take-off phase are shown on the following table:

*Table 6-1 Design point break down of take-off at critical altitude*

	<b>Beginning</b>	<b>Lift off</b>	<b>End</b>
Distance (m)	0	15.40	49.2
Height (m)	0	0	4.41
Speed (m)	0	14.9	20
Pitch Angle (m)	0	0	18
Thrust (m)	496.9	365.4	300.2
Throttle (m)	100	100	100
Drag (N)	0	82.5	128.2
Flap angle (deg)	0	30	30
CL	1.17	1.599	1.599
Stall Speed (m/s)	17.1	14.6	14.6
Friction Coefficient	0.04	0	0

## 6.2 Climb

The following two figures are shown how rapidly or how steeply a UAV can climb. Therefore it is necessary to estimate the maximum rate of climb and the angle of climb.

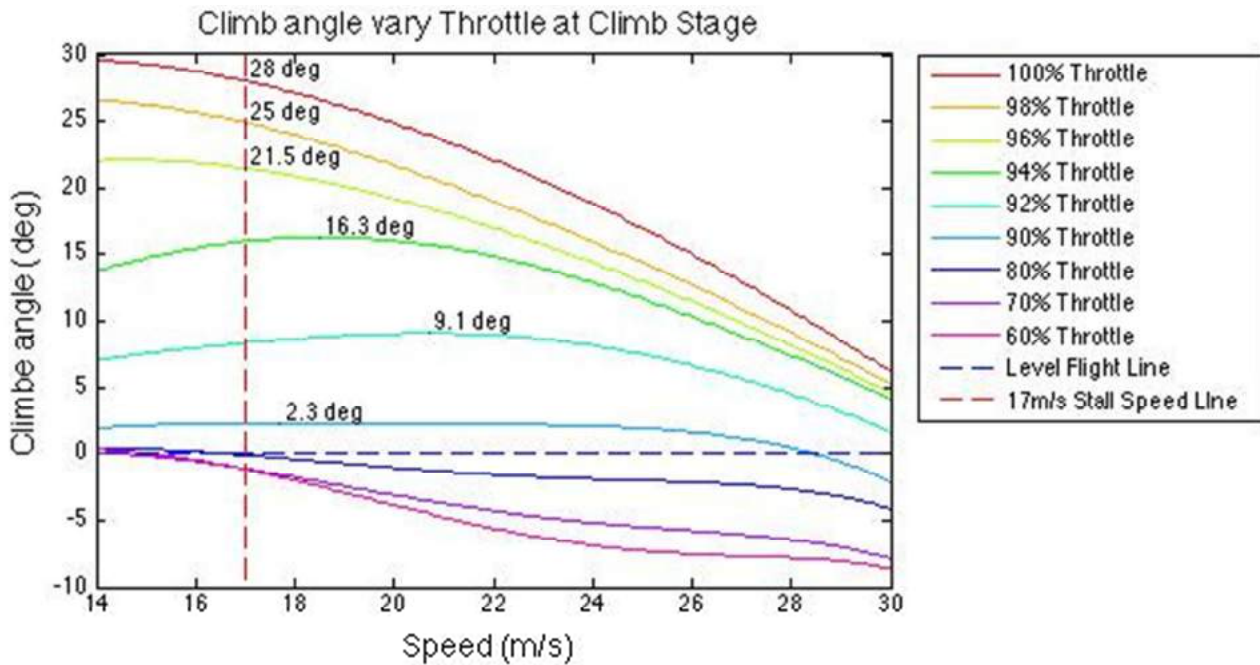


Figure 6-5 Climb angle at different throttle settings during climb

Due to the variable thrust depended on the speed, throttle can be set to control the climb condition. The climb conditions of these two graphs (figure 6-5 and 6-6) are all at 2800 meters altitude specified by the RFP. The blue point in the figures 6-5 shows the maximum climb angle on each throttle stage. Therefore, the maximum climb angle occurs at the intersection point of stall speed line and the operation line of 100% throttle, but it is close on the stall line.

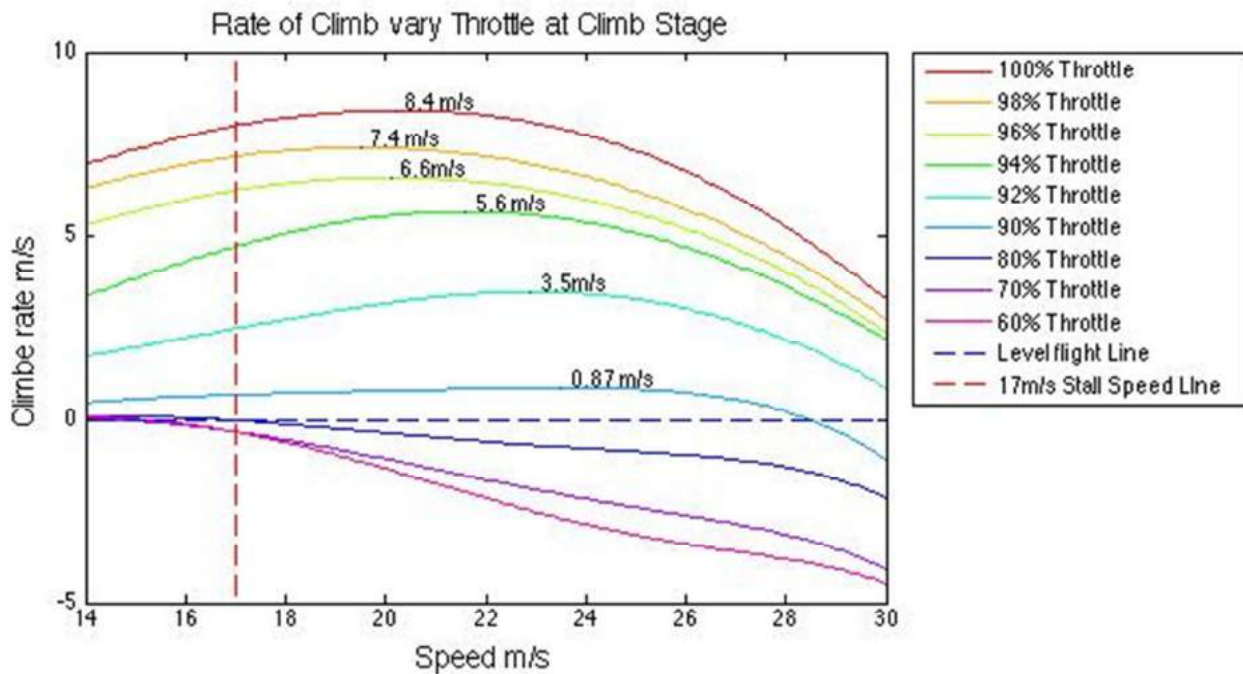


Figure 6-6 Climb rate at different throttle settings during climb

When figure 6-6 is compared with figure 6-5, it can be easily seen that the UAV have the maximum climb angle, but it doesn't mean it has the maximum climb rate. So its maximum climb rate is 8.4 m/s at 100% throttle, and it is efficiency at this throttle setting. Therefore the maximum climb rate can be as the guideline on climbing.

Table 6-2 Maximum Climb Performance Summary

	Climb angle (deg)	Climb rate (m/s)	Speed (m/s)	Throttle (%)
Max climb angle	28	8	17.2	100
Max climb rate	24.5	8.4	20.3	100

At the end of take-off, the velocity is 20m/s. Hence the design point is selected on the 94% throttle, and then the climb rate is 5.6 m/s with 15-degree climb angle.

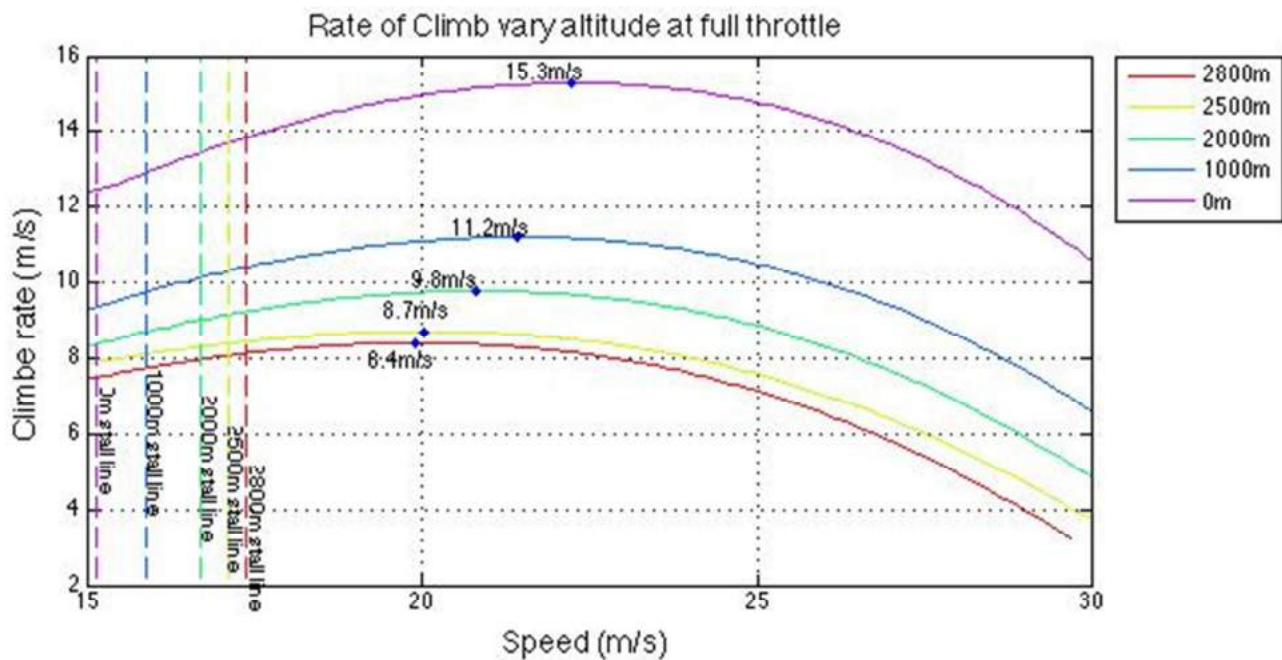


Figure 6-7 ROC at different altitude and full throttle, 0 degrees flaps

Climb angle and climb rate also be effected by the altitude. Actual measured data of the flight altitudes around Mount Kenya shows a variation of altitude from around 1700 to 2400, so the climb angle and climb rate increases with decreasing altitude. This figure can be useful to estimate fuel flow of climb part on mission in which altitude varies frequently.

### 6.3 Cruise

The cruise performance of the ADV can be summarised by the relationship shown in figure 6-8. Based on the graph, it is shown that the optimal cruise speed varies according to the value of throttle and drag or thrust. The black point is the minimum drag on each flap setting. The maximum design cruise speed is 32.7 m/s for the ADV. Drag is minimised at a 0 degrees flap setting with a corresponding cruise speed of 20.5 m/s. The results are summarised in table

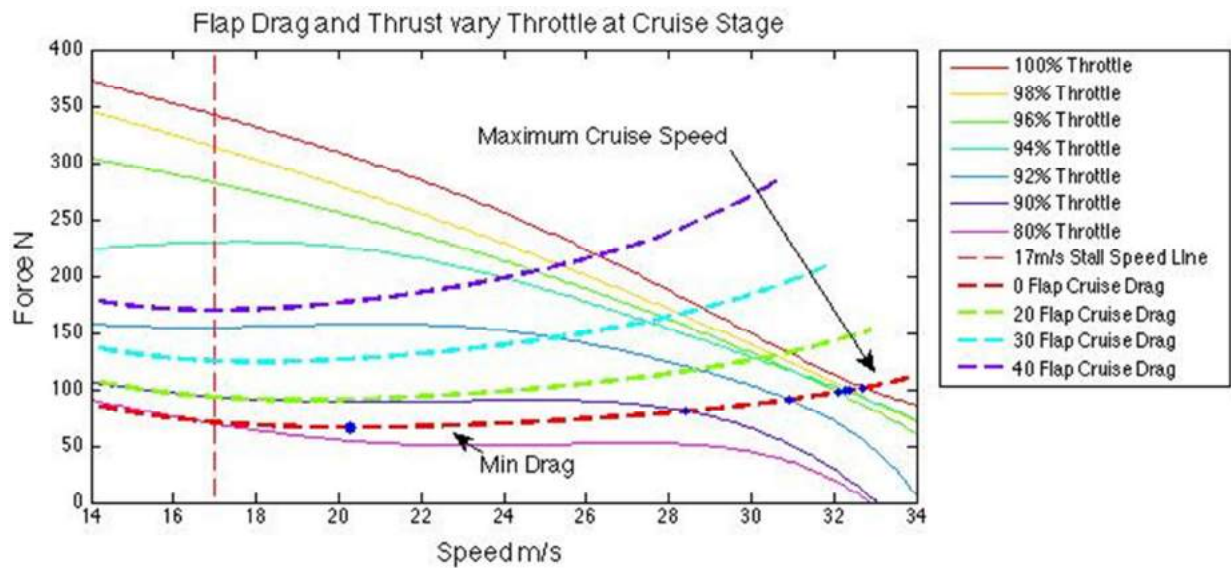


Figure 6-8 Drag and thrust along speed on cruise section

Table 6-3 Summary of cruise phase

	Force N	Speed m/s	Throttle %	Flap angle deg
<b>Minimum Drag</b>	66	20.5	89	0
<b>Maximum Speed</b>	102	32.7	100%	0

## 6.4 Turn

Turn performance requires a turn radius of less than 100 metres due to a minimum flight corridor specified by the RFP. Figure 6-9 illustrates the minimum design point for turn performance as represented by the blue dash. The ADV satisfies the minimum turn performance required at zero flap settings with a throttle setting of 90% and above.

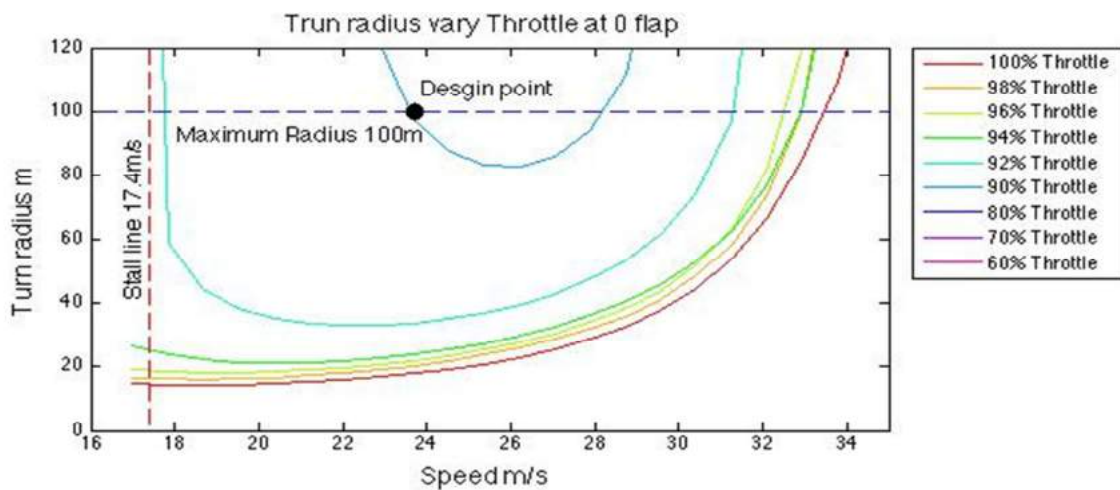


Figure 6-9 Turn Radius vs. Speed at different throttle settings

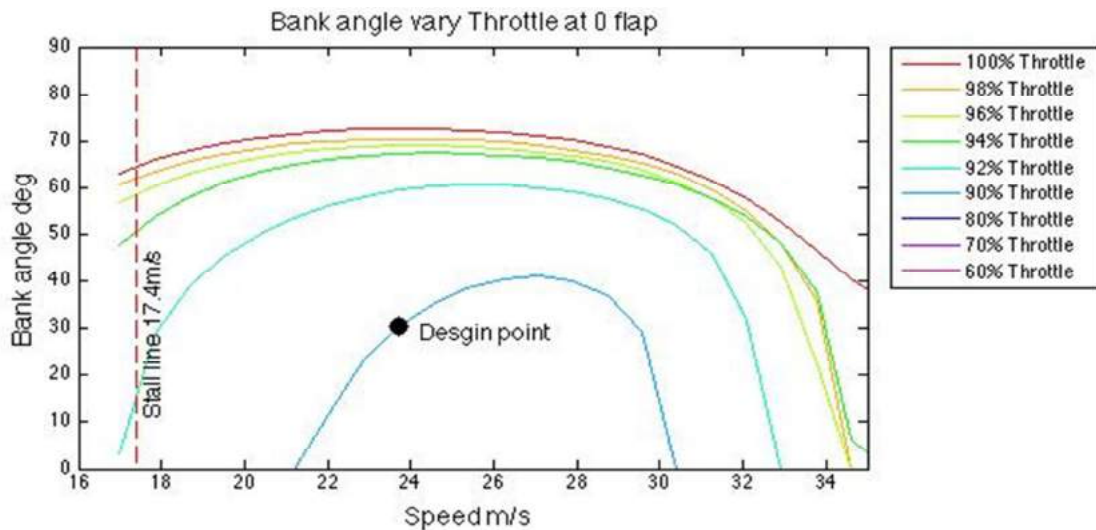


Figure 6-10 Bank angle vs. speed at different throttle settings

According above two figures, black points shown in the graphs has the least bank angle, but it still be able to turn within a 100 metre radius.

Table 6-4 Design Point for Turn

	Turning Speed	Turning Radius	Bank Angle	Throttle	Load Factor
Design point	23.7 m/s	100 m	30.5deg	92 %	1.14

## 6.5 Descent and Landing

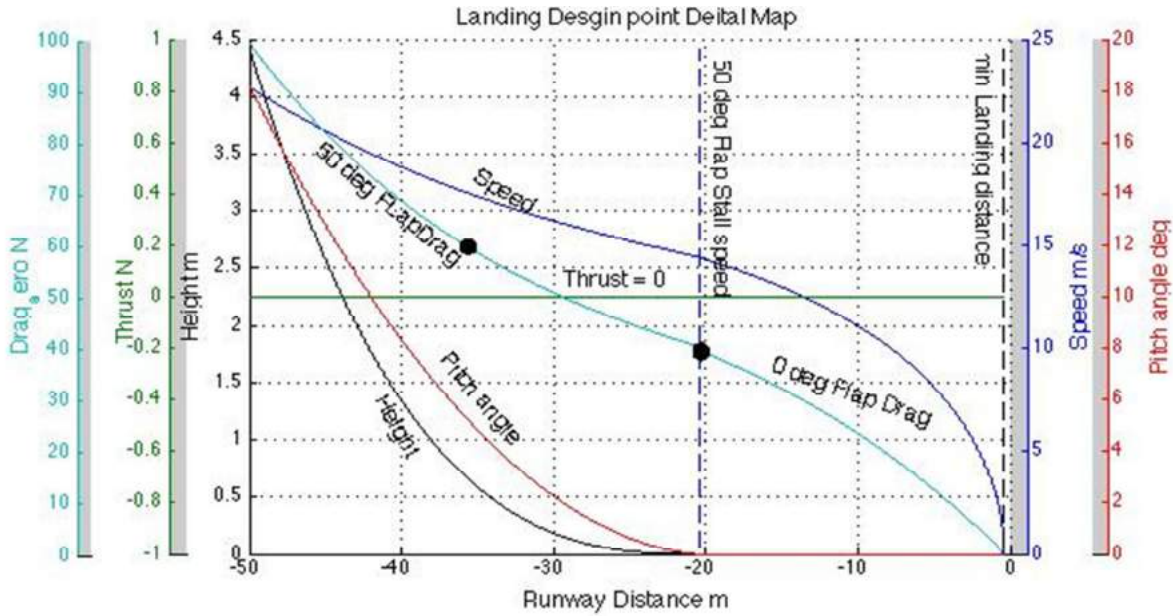


Figure 6-11 Landing Detail Map

The first design is to set our maximum flap angle, 50-degree, in the landing. This flap can increases drag to reduce the speed for landing, and produces more lift to maintain the lift lost by the decreasing speed. On landing, it is assumed that there is zero thrust.

Table 6-5 Landing detail

Moment	Approach	Touch Ground	End
<b>Distance (m)</b>	0	20	49.6
<b>Height (m)</b>	4.41	0	0
<b>Speed (m/s)</b>	22.6	14.5	0
<b>Pitch Angle (deg)</b>	18.2	0	0
<b>Thrust (N)</b>	0	0	0
<b>Throttle (%)</b>	0	0	0
<b>Drag (N)</b>	255.9	40	0
<b>Flap angle (deg)</b>	50	0	0
<b>CL</b>	1.63	1.17	1.17
<b>Stall Speed (m/s)</b>	14.2	17.1	17.1
<b>Friction Coefficient</b>	0	0.5	0.5

The approach speed was designed to be at a maximum of 22.6 m/s for the landing phase. In other words, any speed, under 22.6m/ and larger than 17.1m/s (0 flap stall speed), the ADV is able to land within the 50 metres.

## 6.6 Summary of Performance

At 30 degrees flaps, the ADV takes off and transitions into climb at 49 metres of the runway, clearing the obstacle well before the 50 metre requirement. The velocity reaches 20m/s at end of take-off. After this stage, the speed and 94 % throttle is used to keep constant climb rate (5.6 m/s) until the ADV reaches a 2800 metre cruise altitude. The UAV then accelerates to 25m/s to get cruise speed and keep this speed with around 90% throttle. At last, the stage of flight, velocity is to reduce to 22m/s or less to approach runway to land. Fuel burnt during the longest stage of flight requires 2.66 kg of fuel from take-off to landing.

## 7 Aerodynamics

This section is focused on the presentation of the main aerodynamic characteristics critical for the compliance with the requirements of the RFP. Aerofoil selection, wing geometry, high lift devices, lift characteristics, and a detailed drag analysis for all flight phases are specified.

### 7.1 Aerofoil Selection

Aerofoil selection was based on a number of design requirements coming from aerodynamic and structural considerations to meet the RFP requirements. These requirements are listed below.

- High lift over drag ratio to meet the maximum take-off and landing distance requirement (50 m).
- High maximum thickness to chord ratio to lower structural weight and meet the maximum GTOW requirement (60 Kg).
- Maximum stall angle of 15° for approach and departing sectors climb angle requirement.
- Low pitching moment for trim performance.

A trade-off study was performed for several candidate aerofoils based on the above criteria. The candidate aerofoils selected were: NACA 23015, NACA 23012, NACA 65410, NACA 64<sub>3</sub>618, and NACA 747a315 [1] [2] [3]. These aerofoils were tested in XFLR5 and their main aerodynamic characteristics were compared ( $C_{l\max}$ ,  $C_{d\min}$ ,  $(C_l/C_d)_{\max}$ ,  $\alpha_{stall}$ ,  $\alpha_{Cl=0}$ ,  $C_m$ , t/c). A score-base criterion was used to find the absolute best performing aerofoil. The aerofoil with the highest overall score was selected. Note that the requirement of high lift to drag ratio and high thickness to chord ratio are opposed to the low pitching moment. The score base method allows finding the equilibrium to fulfil all the requirements.

The aerofoil selected for the wing was the NACA 65410. The aerofoil profile is represented in Figure 7-1. Table 7-1 summarises the aerodynamic characteristics of the NACA 65410.

*Table 7-1 Wing aerofoil aerodynamic characteristics*

$C_{l\max}$	$C_{d\min}$	$(C_l/C_d)_{\max}$	$\alpha_{Cl=0}$	$\alpha_{stall}$	$C_{m,cruise}$
1.3	0.0074	110	-3.3°	12°	-0.08

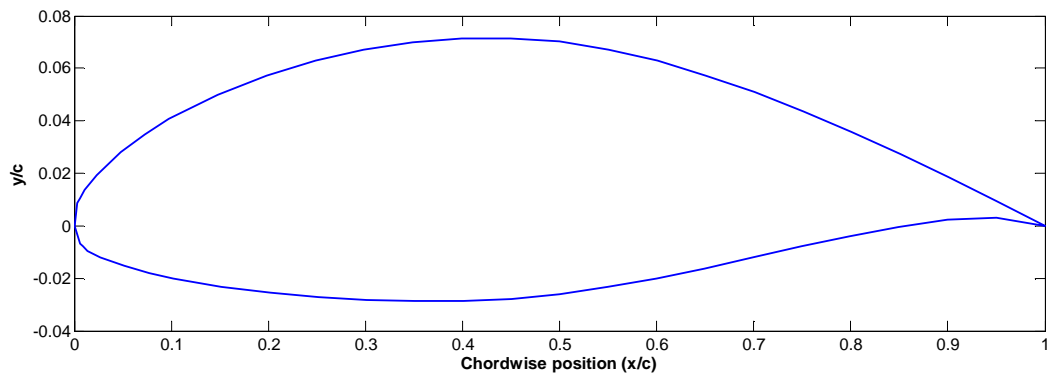


Figure 7-1 NACA 65410 profile

For the vertical and horizontal tails only symmetric profiles were considered for performance reasons. Aerofoil thickness needs to be chosen so that it allows enough moment balance while it is not oversized and contributes to increase drag. NACA 0010 was chosen for the empennage with the right performance in stability and trim.

## 7.2 Wing Geometry and High Lift Devices

Wing geometry determines the basic aerodynamic performance of the aircraft. Its selection was based on the following constraints criteria:

- Maximum wing span requirement (10 m).
- Wing loading operating point ( $16.7 \text{ kg/m}^2$ ).
- AR from historical data collected for UAV and STOL data (see Appendix)
- Manufacturing ease and low cost.

With these factors considered, the wing geometry was chosen to have a square planform with notwist angle. The final parameters are summarised in Table 7-2.

*Table 7-2 Wing geometry characteristics*

$S_{ref}(\text{m}^2)$	$b(\text{m})$	$c(\text{m})$	$AR$	$(t/c)_{max}$
3.5	4.8	0.73	6.5	10%

To meet the take-off and landing distance requirement, high lift devices were employed in these phases. The plain leading-edge flap was the one implemented because it is the simplest and most cost-effective method to meet the 50 m take-off and landing requirement. Final flaps dimensions are shown in Table 7-3 based on 40% of wing span and 30% of wing chord [4].

*Table 7-3 Flaps dimensions*

	$b(\text{m})$	$c(\text{m})$
<b>Flaps (each)</b>	0.96	0.24

### 7.3 Aircraft Lift

Aerodynamic performance is an important factor when considering the RFP criterion. A maximum lift coefficient is critical to meet the required take-off distance. Figure 5-2 shows the 3D coefficient of lift over angle of attack for the main flight phase conditions. It is notable that flaps have been used for take-off and landing conditions.

The clean maximum lift coefficient, roughly 1.2, was not enough to meet the 50 m take-off and landing distance requirement. Therefore, high lift devices were employed to increase the aerodynamic performance during these phases. The increase in lift due to flaps was estimated based on Stinton [5]. Drag increase is presented in section 7.4.2. From performance the best L/D increase was found at 30° flaps deflection for take-off and 50° for landing.

Table 7-4 summarises the lift coefficients for the different flight phases.

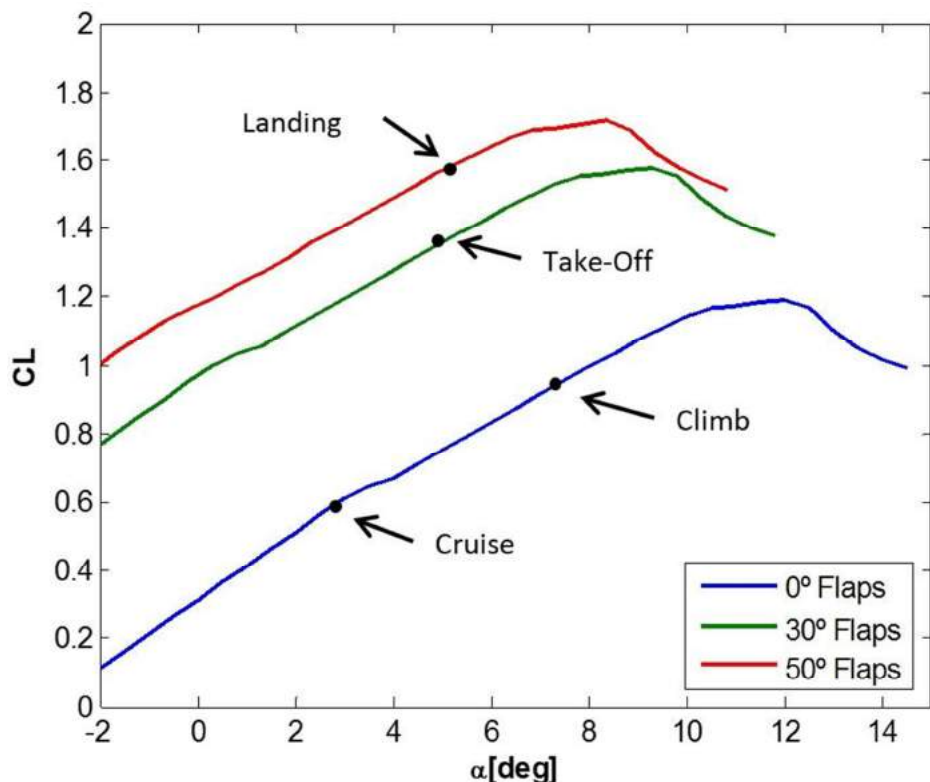


Figure 7-2 Wing lift coefficient over angle of attack

Table 7-4 Lift coefficients for flight phases

	<i>TO</i>	<i>Climb</i>	<i>Cruise</i>	<i>Landing</i>
<i>CL</i>	1.35	0.9	0.6	1.6

## 7.4 Aircraft Drag

### 7.4.1 Component Drag

Determining the total drag of the UAV is essential to assess performance and therefore the compliance with the RFP requirements. Drag directly affects the take-off and landing distance requirement. It also influences on parameters such as the fuel consumption and drives aircraft limit range or operational cost.

The total drag is composed of parasitic drag,  $C_{D0}$ , and induced drag due to lift,  $C_{Di} = K C_L^2$ . Parasitic drag is influenced by several factors: form drag, skin friction and interference of components drag. A full component analysis on the parasite drag was carried out [4] with adjustments and corrections for low speed aircrafts [2].

The influence of each component over the total parasite drag allowed for an assessment of its impact and thus optimisation considerations of the component. The components taken into consideration for the build-up drag are: wing; horizontal and vertical tail; fuselage; non-retractable landing gear; booms; engine nacelles; engine: cooling (effect of engine temperature on the flow) and miscellaneous. The components parasitic drag is based on  $S_{ref} = 3.5 \text{ m}^2$ .

Table 7-5 summarises the detailed component parasite drag and the total drag for the main flight phases. Take-off and landing phases coefficients are computed without the effect of flaps deflection. It can be observed that the main components influencing the drag coefficient are the wing, landing gear and the cooling engine drag.

Table 7-5 Detailed component drag

COMPONENTS	$C_{D0}$		
Wing	0.0074		
Horizontal Tail	0.0021		
Vertical Tail	0.0028		
Fuselage	0.0134		
Landing Gear	0.0074		
Booms	0.0002		
Engine Nacelle	0.0009		
Engine Cooling	0.0068		
Miscellaneous engine	0.0008		
Take-Off/ Landing	Climb	Cruise	
<b><math>total C_{D0}</math></b>	<b>0.1054</b>	<b>0.0485</b>	<b>0.044</b>
<b><math>K</math></b>	<b>0.0680</b>	<b>0.0680</b>	<b>0.0680</b>
<b><math>C_{Di}</math></b>	<b>0.0687</b>	<b>0.0385</b>	<b>0.0212</b>
<b><math>total C_D</math></b>	<b>0.1742</b>	<b>0.087</b>	<b>0.0652</b>

#### 7.4.2 High Lift Devices Drag

High lift devices were used to increase the maximum lift coefficient for take-off and landing performance. Plain flaps were chosen for simplicity in the manufacturing process and low cost.

The detailed determination of the effect of drag increase is critical for accurate take-off and landing distances. The method used for the estimation of drag increase was based on Stinton [5], and was compared with the one found at Gudmundsson [2], obtaining similar results.

Figure 7-3 shows the variation of the total drag coefficient, the parasite drag coefficient and the induced drag coefficient over flap angle deflection for take-off and landing conditions. The drag coefficient values for the actual take-off and landing configuration is presented in Table 7-6.

Table 7-6 Drag at TO and landing with flaps configuration

	Take-Off	Landing
<b><math>total C_D</math></b>	<b>0.295</b>	<b>0.383</b>

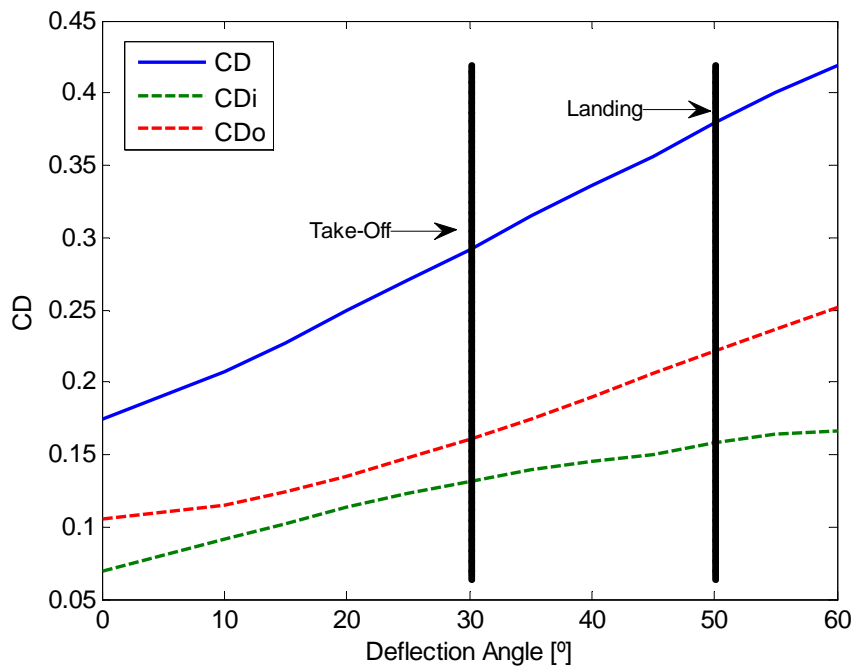


Figure 7-3 Drag coefficient over flap deflection

## 8 Propulsion

### 8.1 Engine

This section will focus on the development of the propulsion system of the aircraft, which includes the performance of the selected engine, a summary of the propeller design and propeller characteristics. Final performance of the propulsion system at various operational conditions are also included and presented in section 8.3.2.

#### 8.1.1 Engine Selection

Due to the design criteria specified by the request for proposal, it is critical for the propulsion system to have a high power to weight ratio to satisfy the short lift-off distance requirements. High altitude operation conditions in Mount Kenya also mean that engine power is reduced by 25 % [6]. Hence the engine selection process is guided by some core requirements which address the critical design factors and are defined below:

- Engine Performance
  - high power to weight ratio
  - high altitude operating conditions
  - low fuel consumption
- Engine/Aircraft Integration (Engine Size)
- Cost

The total power required for take-off is 13KW and the ADV incorporates two engines. Thus the selection process considered 6 potential engines rated between 7kW to 9kW. The evaluation of engine specifications are detailed in the Appendix and figure 8-1 outlines the potential candidates.

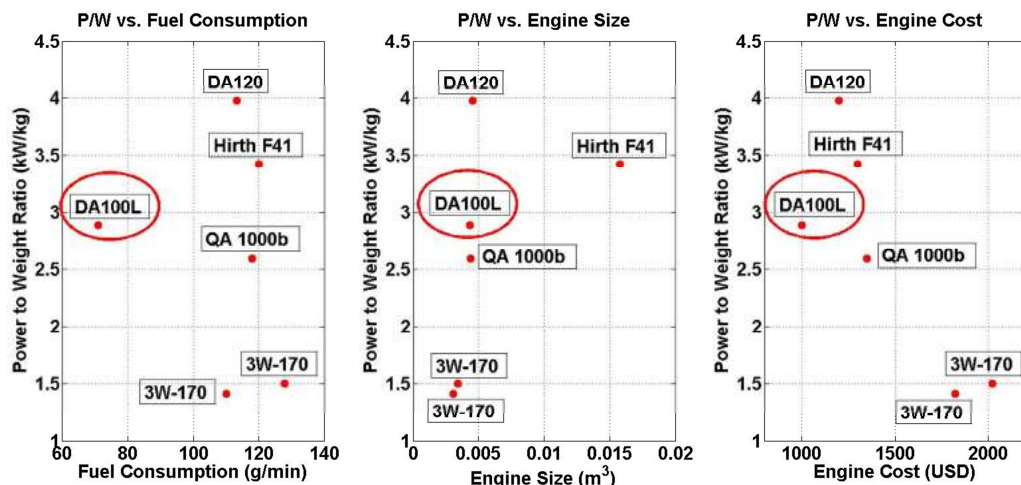


Figure 8-1 Evaluation of Engine Selection

The above selected engines have been examined by evaluating its power to weight ratio with fuel consumption, engine size and unit cost. Results are plotted in Figure 6-1 on which the choice of engine for this mission has been circled in red.

Ideally, the selected engine should have the highest power to weight ratio with lowest fuel consumption, minimum cost and is the smallest in size, however, trade-offs had to be made. When considering the engine performance being the top priority (High Power to weight ratio) , the Desert Aircraft DA-100L is the most suitable engine of all the candidates as it has a reasonable power to weight ratio and the lowest fuel consumption and cost.

*Table 8-1 Engine Specification*

<b>Manufacture</b>	Desert Aircraft
<b>Model</b>	DA-100L
<b>Engine Type</b>	2 Stroke, Gas
<b>Weight (kg)</b>	2.53
<b>Max. Engine Power (kW) Sea level</b>	7.31@6500RPM
<b>Engine Torque (Nm) @ Max. Engine Power</b>	10.74@6500RPM
<b>Optimum Fuel Consumption (g/min)</b>	2.5@6000RPM
<b>Optimum RPM Range</b>	1000 to 6700
<b>Max. RPM</b>	8500

### 8.1.2 Engine Performance

The variation in operational altitude was considered during engine selection and the impact of altitude on engine performance was accounted for during performance analysis. Hence, the variation of altitude in which is specified by the mission profile was considered for this section of engine performance.

The core mission requirement is to provide sufficient power for take-off within the desired distance, engine power with wide open throttle (WOT) has been contoured with both RPM and altitude variations and presented in figure 8-2.

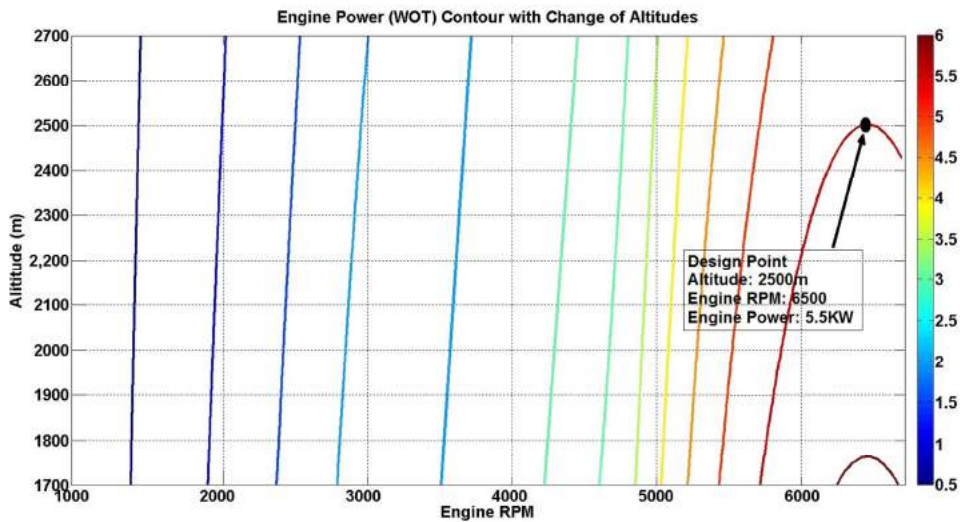


Figure 8-2 Contour of Engine Power (WOT) with variation of Altitude

Similarly, the engine torque contour with wide open throttle at operational altitude is shown in figure 6-3.

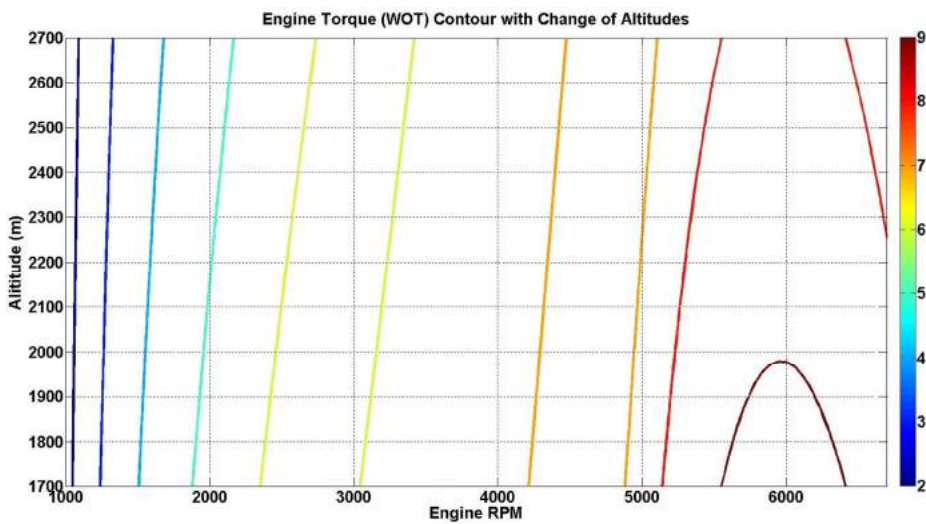


Figure 8-3 Contour of Engine Torque (WOT) with variation of Altitude

The altitude for take-off was at a design point of 2500 metres which was specified by the RFP; therefore the ADV is designed for take-off within 50 metres at this altitude. It should be noted however, that actual operational conditions are at lower altitudes as mentioned in the mission profile section of this report.

Fuel consumption of the ADV's engine has also been contoured with different throttle settings at different RPM and the resulting contour of engine performance in terms of fuel consumption is displayed in figure 8-4.

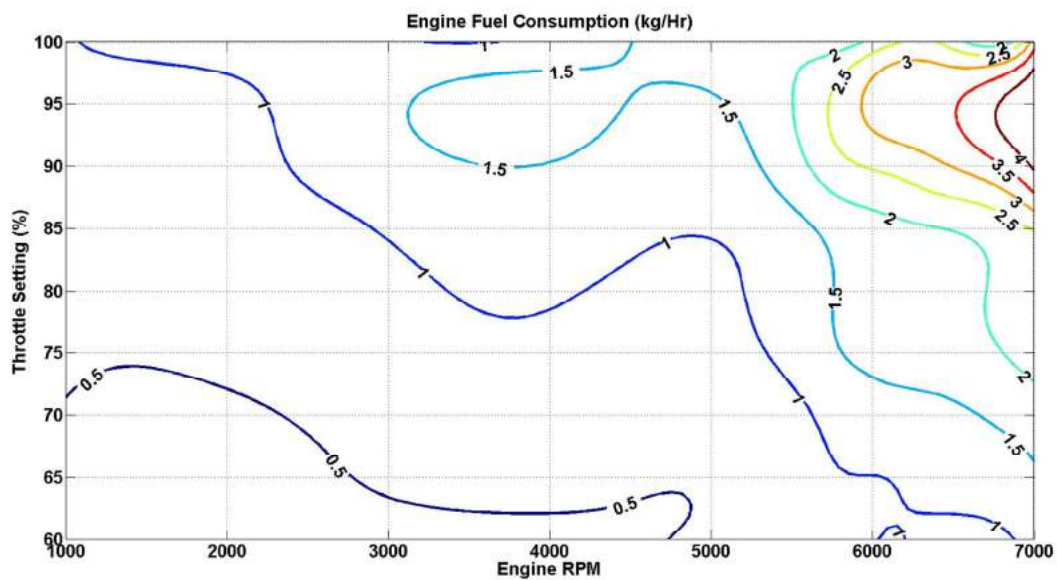


Figure 8-4 Engine Fuel Consumption

## 8.2 Propeller

### 8.2.1 ADV Propeller

The final propeller configuration has been optimised for the take-off performance of the aircraft ensuring successful take-off within 50 metres. Specifications of the ADV's propeller is summarised in table 8-2.

*Table 8-2 Propeller Specifications*

<b>Base Propeller</b>	XOAR 27x10 Sport Prop Type A
<b>Diameter (inch)</b>	31
<b>Pitch (inch)</b>	12
<b>Shaft Diameter (mm)</b>	10
<b>Material</b>	Beech Wood
<b>Weight (g)</b>	325
<b>Cost (USD)</b>	\$64.95

### 8.2.2 Propeller Design

The optimisation of the propeller for the aircraft was conducted with the purpose of producing sufficient thrust for take-off within the design criteria. The initial choice for the engine propeller was the recommended size 27x10, specified by the engine manufacturer. Measurements of the XOAR '27x10' Type A propeller were taken and scaled to a final design size of '31x12' whilst still retaining the same aerofoil characteristics to the original. Various propeller characteristics have been simulated including the thrust, propeller efficiency and torque. To satisfy take-off requirements, a 30 degrees flaps setting is required at 15.1 m/s during the take-off run. This condition paved the design optimisation required by the ADV's propeller to cover the drag that is induced by the flap settings. Figure 8-5 shows the thrust of the '31x12' propeller with drag induced by the flaps settings during take-off. From the plot, it can be seen that the thrust produced is in excess of the drag that needs to be overcome for take-off.

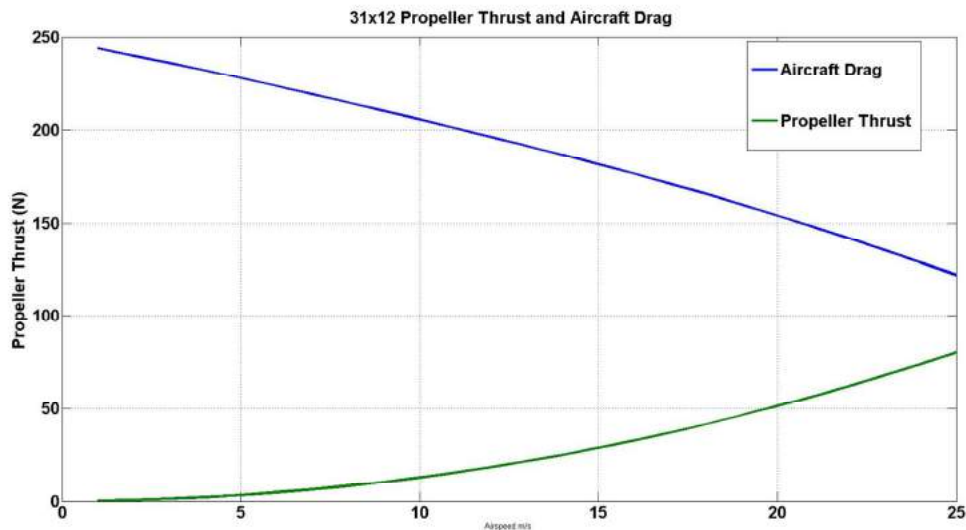


Figure 8-5 Propeller Thrust and Aircraft Drag

Propeller performance in terms of thrust, torque and efficiency were explored with a wide range of propellers, figure 8-6 shows the comparison of the propellers that were considered alongside the base “27x10” propeller.

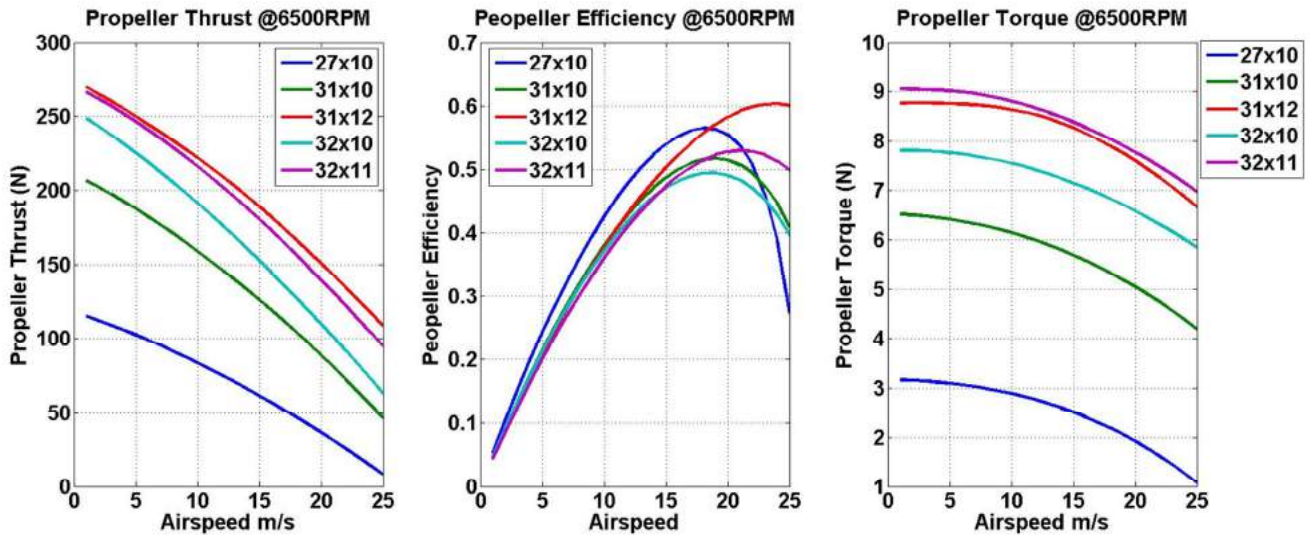


Figure 8-6 Evaluation of Performance of Various Propellers

Propeller diameter and pitch was determined based on an analysis of a wide range of propellers, the details of analysis is included in the propulsion section of the Appendix. As shown by figure 8-6, when comparing the ‘31x12’ and ‘32x11’ propeller, although thrust of the ‘32x11’ propeller is higher than the other, such increase in thrust is to a minor scale at the expense of significantly lower propeller efficiency in cruise condition. Hence, given that both the ‘31x12’ and ‘32x11’ propeller produces sufficient thrust for take-off requirement, the ‘31x12’ propeller is the more suitable choice for the entire mission.

Suitability of the ‘31x12’ propeller to the current engine has also been explored and is determined by whether the engine torque is sufficient enough to drive the propeller for optimum thrust. For such reason, engine torque has been plotted with propeller torque at the speed range of take-off condition. The results are presented in Figure 8-7.

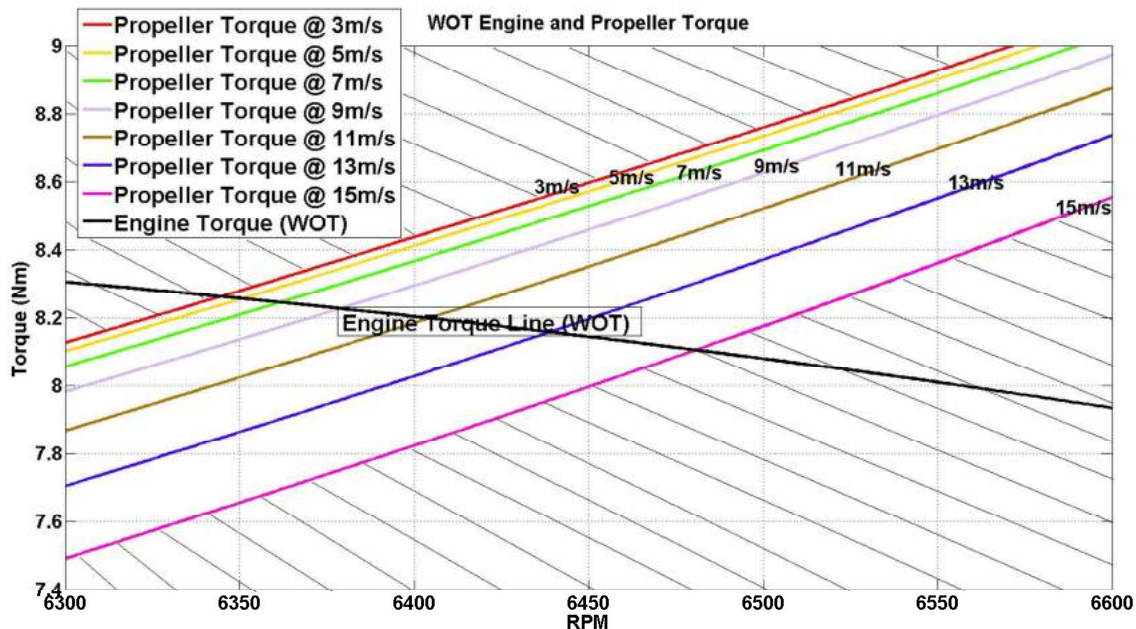


Figure 8-7 Engine Torque (WOT) Condition with ‘31x12’ Propeller

In Figure 8-7, propeller torque at different airspeeds are plotted with the full throttle engine torque where the shaded area represents the condition in which engine is inoperative. As results suggest, the selected engines produces enough Torque to drive the ‘31x12’ propeller. Correspondingly, actual thrust produced by the ‘31x12’ propeller at a specified engine RPM and the ideal thrust condition are been compared and shown in figure 8-8.

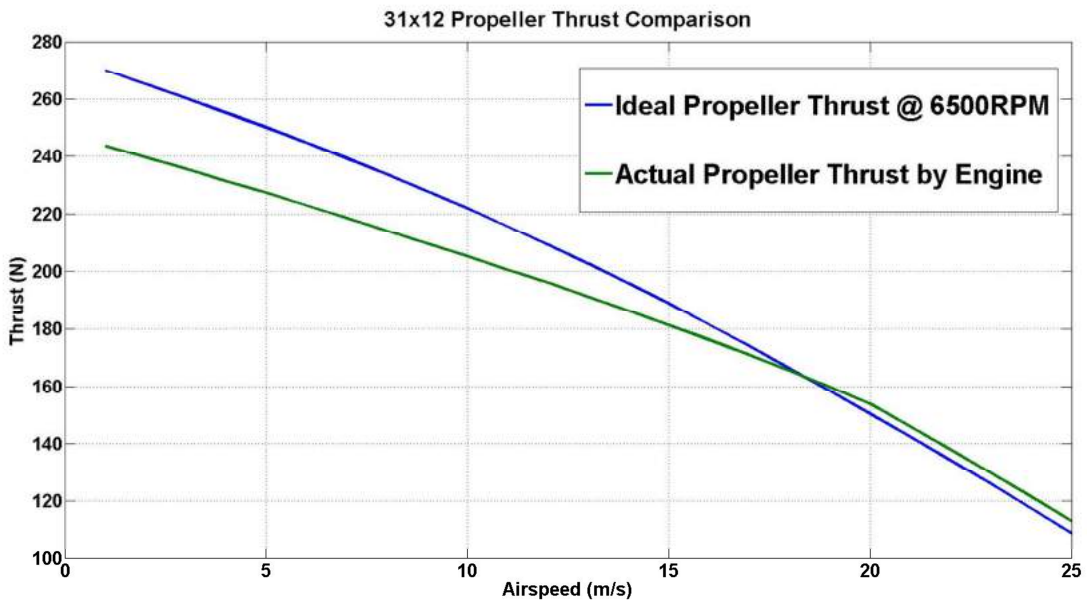


Figure 8-8 Comparison of Propeller Thrust in WOT Take-off

The results suggest that the actual propeller driven by the current engine produces less thrust than the ideal propeller operating at 6500 RPM before airspeed builds up to 17m/s. This is due to the reason that the engine does not produce the required torque for optimum propeller thrust at lower speeds, however shortly after lift-off, as RPM increases, actual propeller performance in terms of thrust is slightly better than the ideal propeller.

### 8.2.3 Propeller Characteristics

Thrust coefficient, power coefficient and propeller efficiency for the ‘31x12’ propeller have been determined by the optimum engine RPM of 6500 across the flight speed spectrum. Resulting propeller characteristics are presented in figure 8-9.

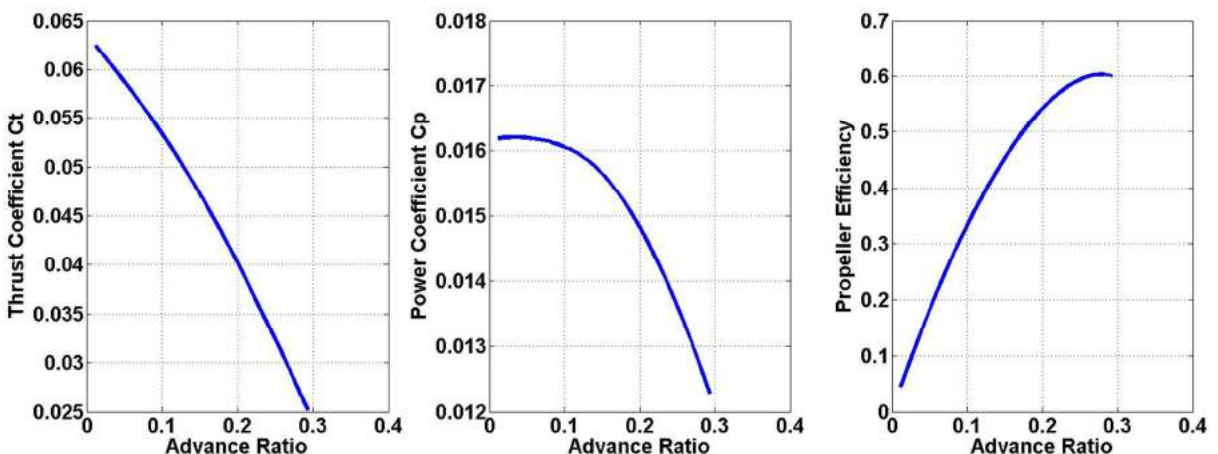


Figure 8-9 a) Propeller Power Coefficient b) Propeller Thrust Coefficient c) Propeller Efficiency

## 8.3 Propulsion System Performance

This section aims to provide a summary of the propulsion system performance of the ADV during the mission in Mount Kenya. Performance in critical flight phases (take-off/Climb, Cruise) at design altitudes are summarised and presented in section 8.3.1. Detailed engine operating conditions are also determined at different operational altitudes during the flight profile of the ADV, and a variation in throttle and corresponding engine performance is summarised in section 8.3.2. Full engine conditions in operation are included in the Appendix.

### 8.3.1 Take-Off, Climb and Cruise

Propulsion performance presented in table 2 of in take-off/Climb is summarised is determined at the lift-off speed of 15.1m/s and cruise speed of 25 m/s results at required critical elevation are given by performance of per engine.

*Table 8-3 Propulsive performance under different flight phases*

Condition	Altitude	Throttle	RPM	Thrust	Power	Torque	Eff.	SFC
Take-off	2500m	100%	6500	121.8N	5.5 kW	8.1 Nm	0.33	2.18 kg/hr
Cruise	2800m	89%	5300	36.1N	1.5 kW	2.9 Nm	0.60	1.45 kg/hr

### 8.3.2 Operational Engine Conditions

Operating condition of engine at required mission location of 2500m is by defined throttle position across the airspeed spectrum from 1m/s to the cruise speed of 25m/s, presented in Table 3. Engine condition in all critical 9 critical elevation variations have been determined by the performance department to be 2150 meters, 2085 meters, 2003 meters, 1981 meters, 1970 meters, 1831 meters, 1770 meters, 1621 meters and 2500 meters. Results are included in Appendix.

*Table 8-4 2500 meters Elevation: Engine Condition in Operation by Throttle Position*

Throttle Position (%)	RPM Range	Power (kW)	Torque (Nm)	Fuel Con. (kg/Hr)
60 (Idle)	2500 - 4400	0.25 – 0.26	0.58 - 0.95	0.45
70	3000 - 4700	0.55 – 0.67	1.26 – 1.73	0.66
80	3700 - 5300	1.06 – 1.52	2.75 – 2.69	1.05
90	3900 - 5500	1.26 – 1.86	3.01 - 3.26	1.49 – 1.76
92	4400 - 6000	1.77 – 2.90	3.78 – 4.63	1.43 – 2.90
94	4800 - 6300	2.22 – 3.84	4.44 – 5.88	1.38 – 3.31
96	5700 - 6400	3.88 – 4.29	6.51 – 6.71	2.46 – 3.23
98	6200 - 6500	4.54 – 5.03	6.66 – 7.54	3.12 – 2.99
100	6300 - 6700	5.44 – 5.50	7.71 – 8.28	2.60 – 1.70

## 9 Structures

This section is broken down into the structural sizing of the ADV wing, tail booms followed by a detailed component analysis on the landing gear system. An insight into the structural design of the payload bay is also explored. Major components of aircraft are designed to meet the requirements specified by the Federal Aviation Regulations from sections 23.321 to 23.373. The undercarriage design accounts for Federal aviation regulations sections 23.473 to 23.493.

### 9.1 V-N Diagram

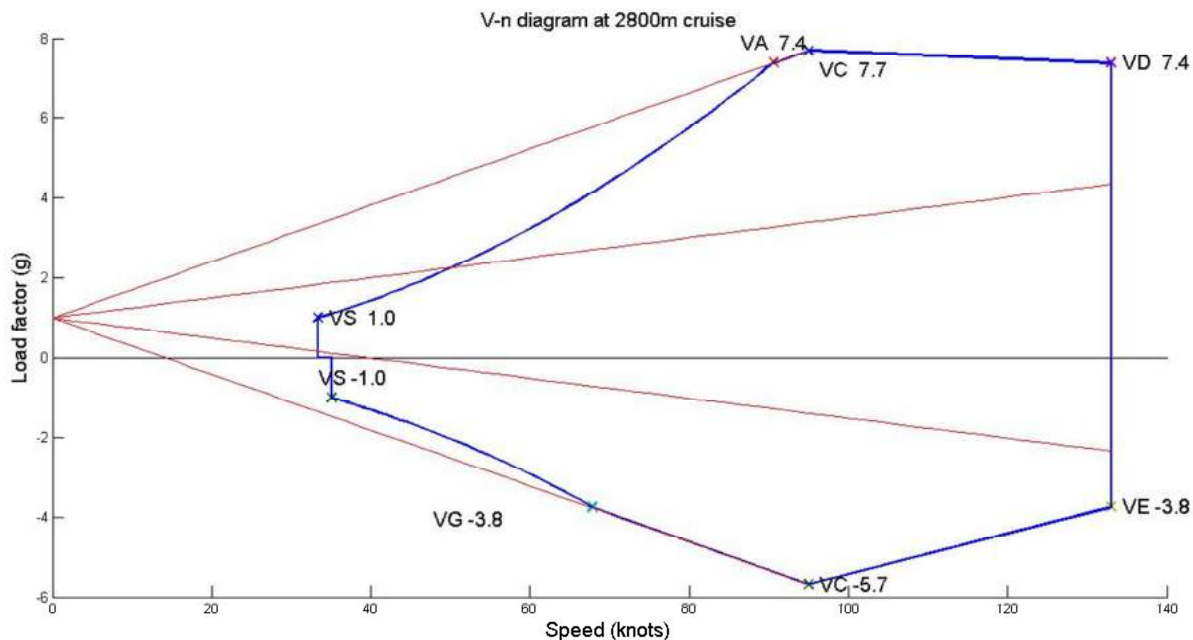


Figure 9-1 V-N Diagram

Figure 9-1 details the V-N diagram for the ADV based on Federal Aviation Regulations however the design load factor would result in overdesign of components to satisfy speeds in which the ADV will never reach. As such, the sizing procedure was carried out at a lower design cruise speed of 80 knots (39 m/s).

Table 9-1 summarises the design load cases that are considered for the ADV. The maximum load factors are  $n_g^+ = 4.52 g$  and  $n_g^- = -2.52 g$ , which are gust load factors during cruise at 2800m. These two load factors will be used to size components. The aircraft is vulnerable to gust and the result confirms with fact that low wing loading aircraft suffer greatly from gust loads.

*Table 9-1 Load Case Summary*

+ Load Case	- Load Case	Condition
<b>4.52</b>	<b>-2.52</b>	Gust at cruising at 2800 m, no flap
4.00	-2.00	Gust cruising zero fuel at 2800m, no flap
3.46	-1.46	Gust at diving at 2800 m, no flap
3.42	-1.41	Gust at stall 2500m, flap 20 degree
3.09	-1.09	Gust diving zero fuel at 2800m, no flap
2.00	-0.80	Manoeuvring at 2500m, flap 20 degree
1.44	0.58	Manoeuvring at 2800 m, no flap
1.30	-0.52	Manoeuvring zero fuel at 2800 m, no flap

## 9.2 Load Cases for Structural Design

Load cases for the sizing of boom and wings are outlined in table 9-2. Typical load cases are created by control surface deflections, resulting in either symmetrical or unsymmetrical loading condition.

*Table 9-2 Structural Design - Load Cases*

Case	Max Load factor	Condition	Load type
Right aileron down -25 degree	4.52	Cruise	Unsymmetrical
Elevator up -25 degree	4.52	Cruise	Symmetrical
Elevator down 25 degree	4.52	Cruise	Symmetrical
Positive rudder 30 degree	4.52	Cruise	Unsymmetrical
No deflection	3.46	Dive	Symmetrical
Flap deflection 50 degree	3.40	Approach	Symmetrical

These control surface deflections are simulated in AVL in order to obtain the lift distribution of forces on the wing. The results of this simulation are provided in the Appendix under the Structures section. The control surface deflections based on the conditions above are combined with the weight of individual components in order to be applied on parts which were to be sized for the ADV, namely the tail booms and the cantilever wing. Details of the loads due to the component weights are available in the Appendix.

### 9.3 Sizing of Tail Booms

The sizing of tail booms during structural design required an assumption in which these booms were tubes and thus, are subjected to bending rupture failure mode, resulting in bending moments. Lift distributions are converted into point loads and sum of moment is taken about the boom to find the reacting moment. Moments about all relative planes were calculated utilising this procedure. The highest moment is considered critical and is taken into consideration for sizing.

The ultimate loads corresponding to surface deflections as well as the moments acting on the boom are included in the Appendix. The critical bending moment case to which the boom is subjected is 9327 Nm. Critical load cases were used to test the strength of various material diameters and sheet thicknesses in order to size the component.

#### 9.3.1 Boom Material and Final Sizing

Table 9-3 summarises the results of the sizing of the tail booms. The ADV's tail booms carry high moment and thus requiring a material with high bending modulus strength  $F_b$  and high ultimate tensile strength  $F_{tu}$ . Shortlisted materials included Aluminium 7075-T6, Aluminium 2024-T3, Aluminium 6061-T6 and Aluminium 2014-T6.

Due to a thin aerofoil profile in the wing, the outer diameter size of the boom had to be minimised to fit within the structure. Additionally, weight was a major concern due to requirements of a 60 kg GTOW by the RFP. From the table below, it was decided that the material to be selected for the tail boom was Aluminium 7075-T6, this yielded a final mass of 2.51 kg.

*Table 9-3 Boom Sizing Results*

Material	Mass (kg)	M.S	Outer diameter (cm)	Inner diameter (cm)
6061-T6	2.92	0.07	10.16	9.96
2024-T3	3.17	0.14	4.45	3.81
2014-T6	2.51	0.07	5.08	4.66
7075-T6	2.51	0.07	5.08	4.66

## 9.4 Sizing of Wing

Cantilever wings are designed to withstand maximum shear force and moment generated at root. For the ADV, wing sizing was crucial as optimisation was needed in order to reduce the weight of the aircraft down to the required design criteria of 60kg GTOW.

Sizing of the wing of the ADV required lift distribution along the wing span, results of which are available in the Appendix. Additionally, shear force diagrams and bending moment diagrams along the wing span were generated for analysis based on the load cases for structural design. These diagrams are shown in figures 9-2 to 9-7.

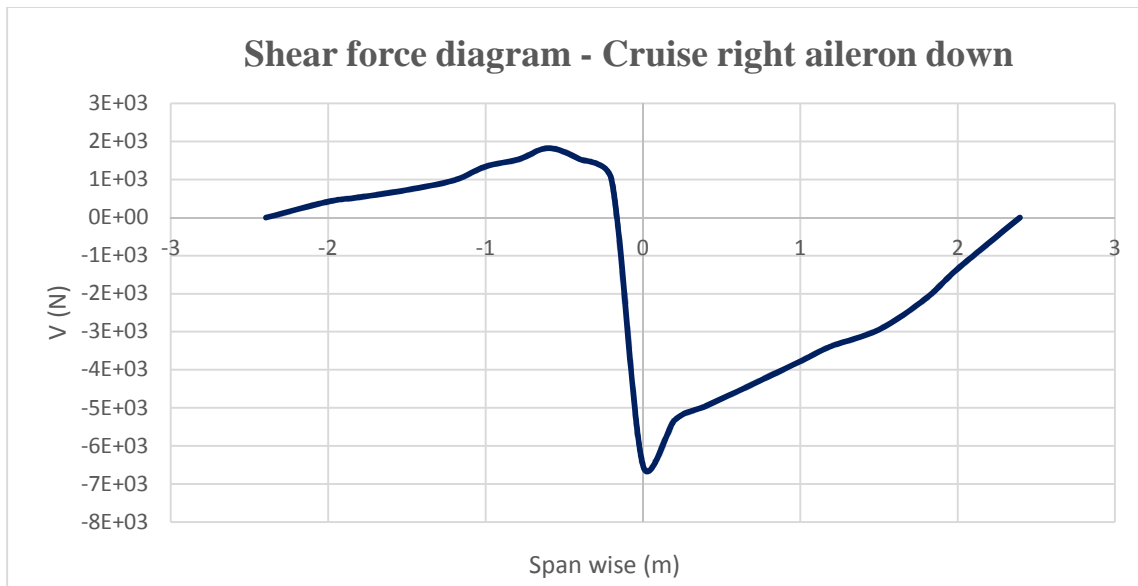


Figure 9-2 Shear Force - Cruise Aileron Down

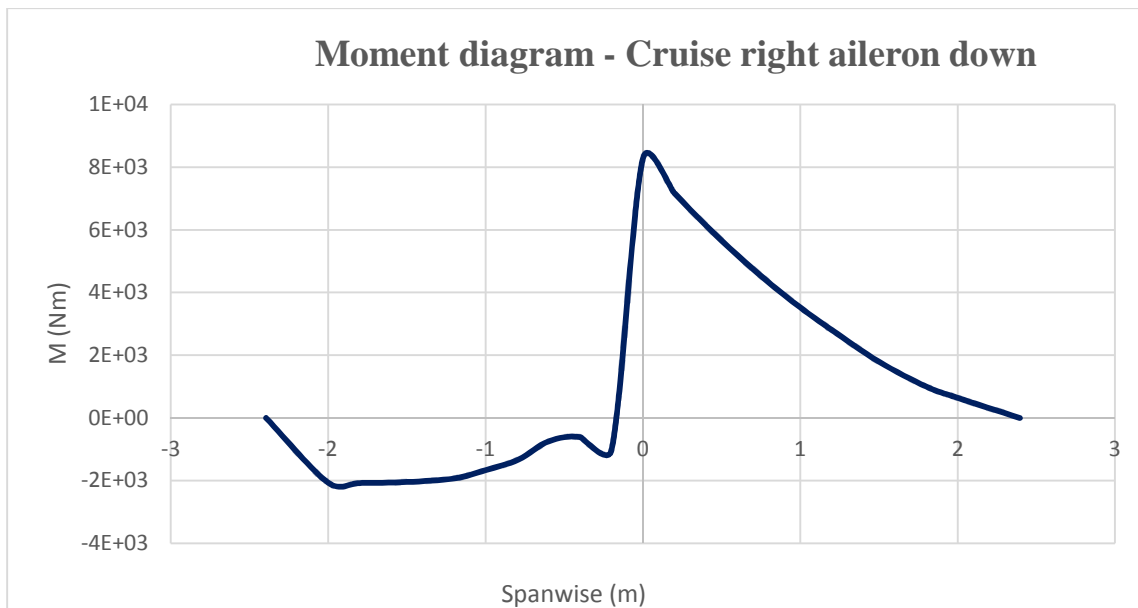


Figure 9-3 Moment Diagram - Cruise Aileron Down

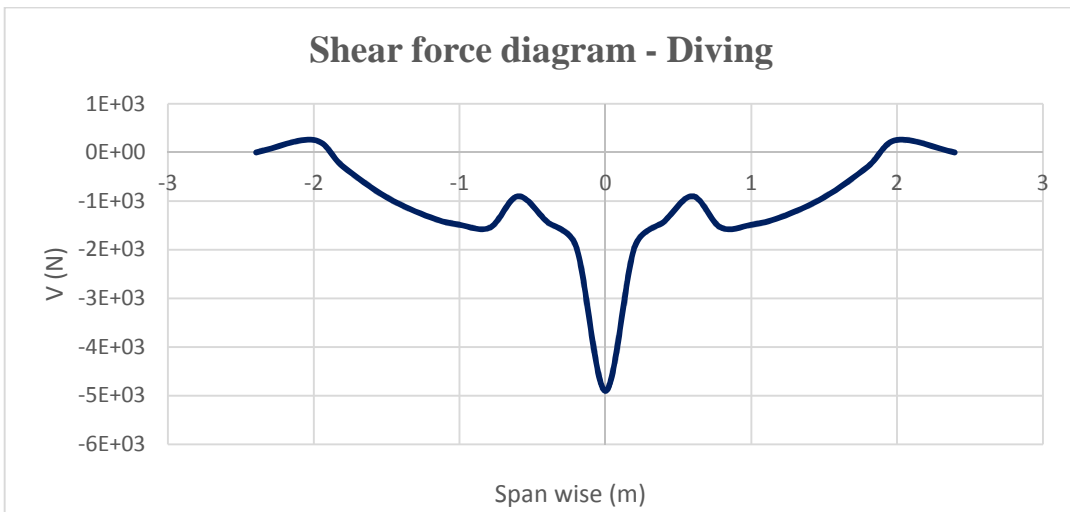


Figure 9-4 Shear Force - Diving

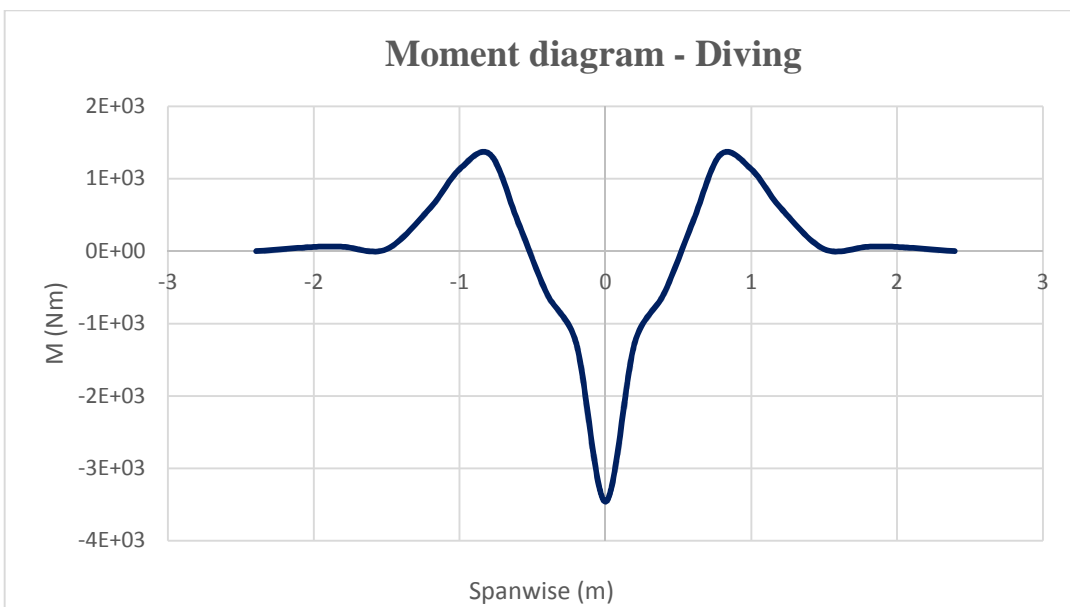


Figure 9-5 Moment Diagram - Diving

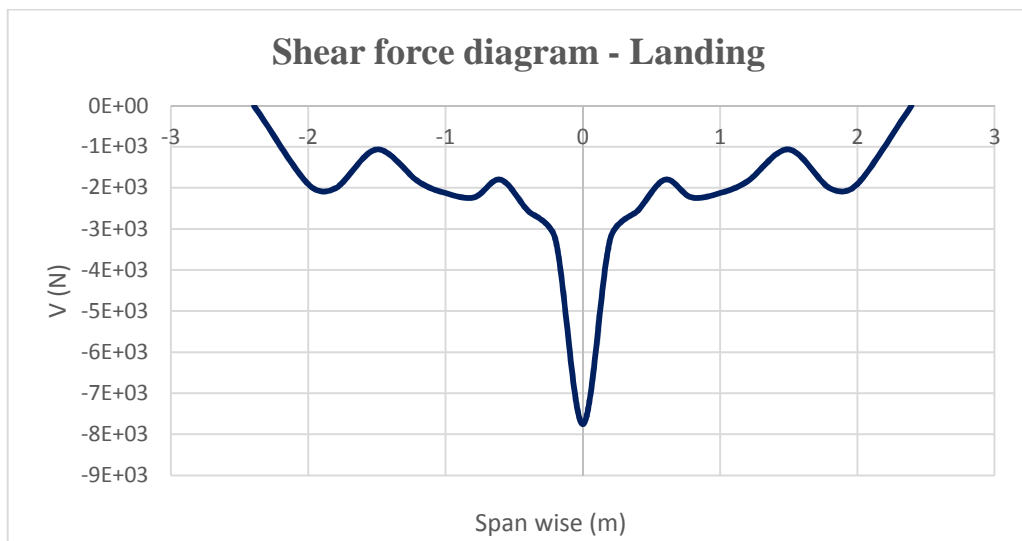


Figure 9-6 Shear Force - Landing

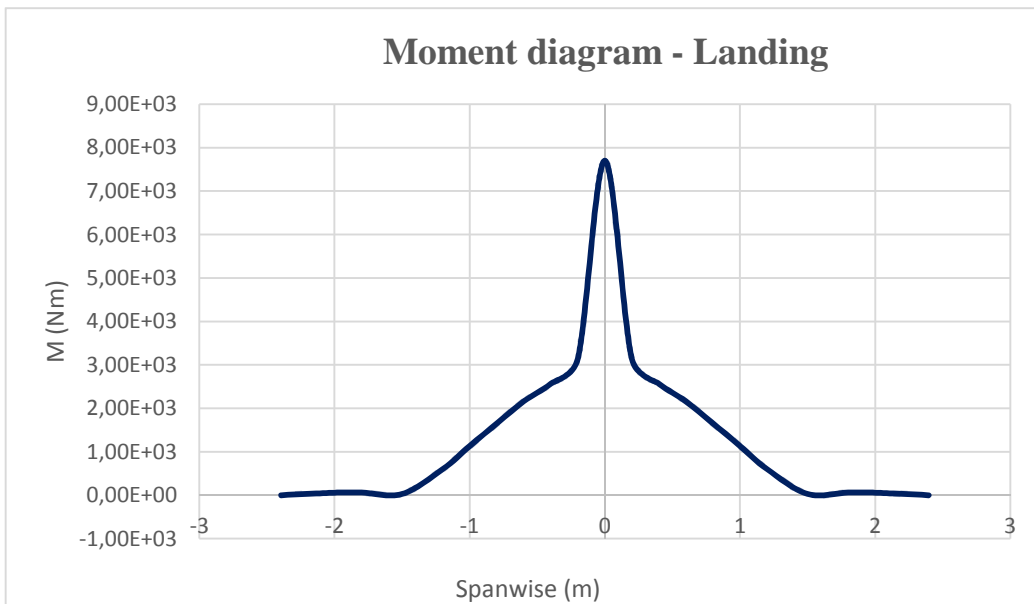


Figure 9-7 Moment Diagram - Landing

Table 9-4 Max shear and bending moment from load cases

<b>Vmax (N)</b>	<b>Mmax (Nm)</b>	<b>Location</b>	<b>Load case</b>
-6507.6	<b>8275.4</b>	Wing root (0,0)	Aileron deflection
-4902.4	-3458.8	Wing root (0,0)	Diving
<b>-7753.3</b>	7698.9	Wing root (0,0)	Landing

### 9.4.1 Wing Material and Final Sizing

ADV's wing consists of two main spars, with the main spar at the quarter chord line and seven ribs spaced 0.26 metres between each other. A simplified layout is presented in figure 9-8. Material is chosen for this component is based on the load carried by wing components. A high shear strength material is required for skin and shear web whereas a high compression strength material is ideal for caps and ribs.

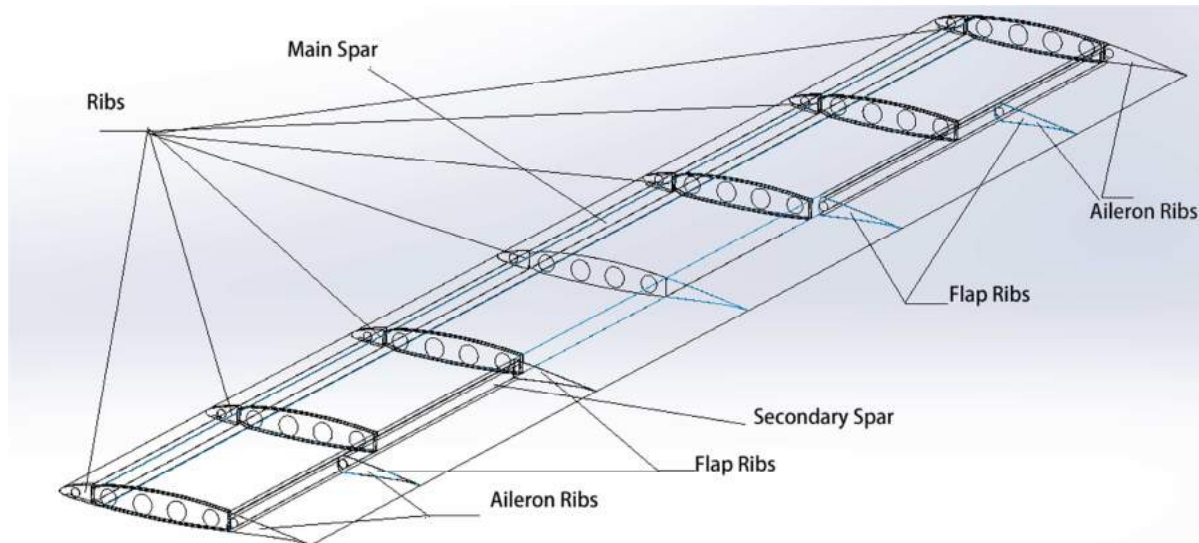


Figure 9-8 Wing Ribs and Spar Layout

Carbon fibre fabric composite is used for skin for weight optimisation due and Aluminium 2090-T83 is used for other major components.

Table 9-5 Wing Structure Summary

Component	Material	Weight (kg)	Thickness (mm)	
Skin	CF Composite Fabric	3.62	0.406	0.508
Shear web	Aluminium 2090-T83	0.86	0.406	0.508
Caps	Aluminium 2090-T83	3.18	-	-
Ribs	Aluminium 2090-T83	0.19	0.406	-
Total	-	7.85	-	-

The sheet thickness calculated for skin, web and ribs appear to be smaller than the minimum available size 0.016 in (4mm). Therefore two options 0.016 in (0.4mm) for the tip and 0.020in (5mm) for the root are chosen to minimise weight impact and they are also recommended sheet thickness to avoid buckling [2]. Sizing for the

Finally, table 9-6 shows the dimensions of the wing caps for the ADC wing. Figure 9-9 shows the material summary of the boom and wing structure.

*Table 9-6 Wing Caps Summary*

<b>Parts</b>	<b>Area (mm<sup>2</sup>)</b>
Caps at root (x2)	243.01
Caps at boom (x2)	128.03
Caps at tip (x2)	12.15

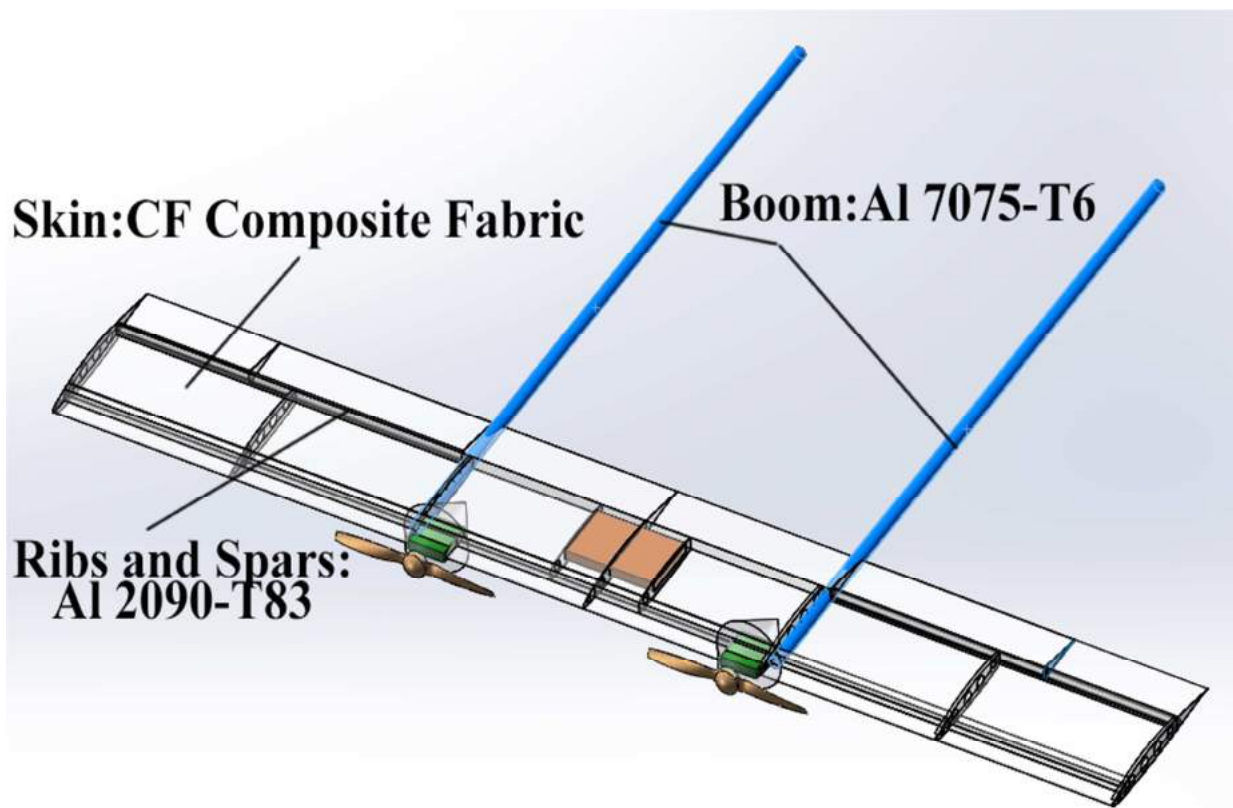


*Figure 9-9 Wing and Tail Boom Materials Summary*

## 9.5 Payload Bay

This section outlines the payload bay loading mechanism and how the cargo is secured during flight between stations around Mount Kenya. Figure 9-10 illustrates the cargo tray and loading door on the ADV. Cargo is loaded into the aircraft from the front and secured by straps (not depicted) to prevent movement during flight. The fuselage nose is separated into two sections, upper section and lower section. The upper section can be treated as a door to load the cargo into the aircraft. And the lower section is connected with the nose landing gear through a front bulkhead to ensure that landing loads are transferred into the fuselage frame. The structure of the lower section is designed to hold the weight of cargo and also supports the nose landing gear.

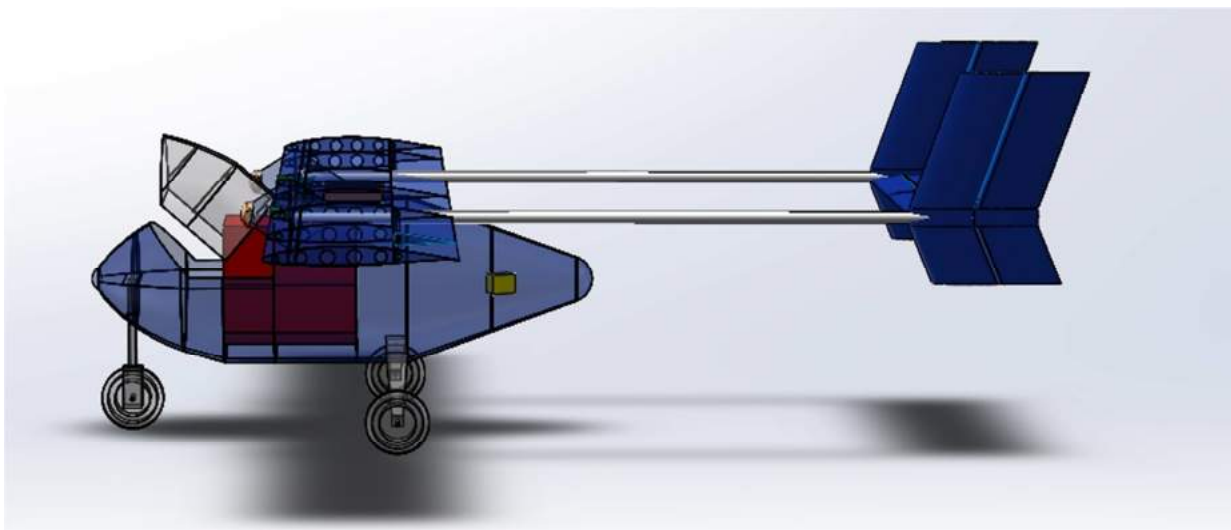
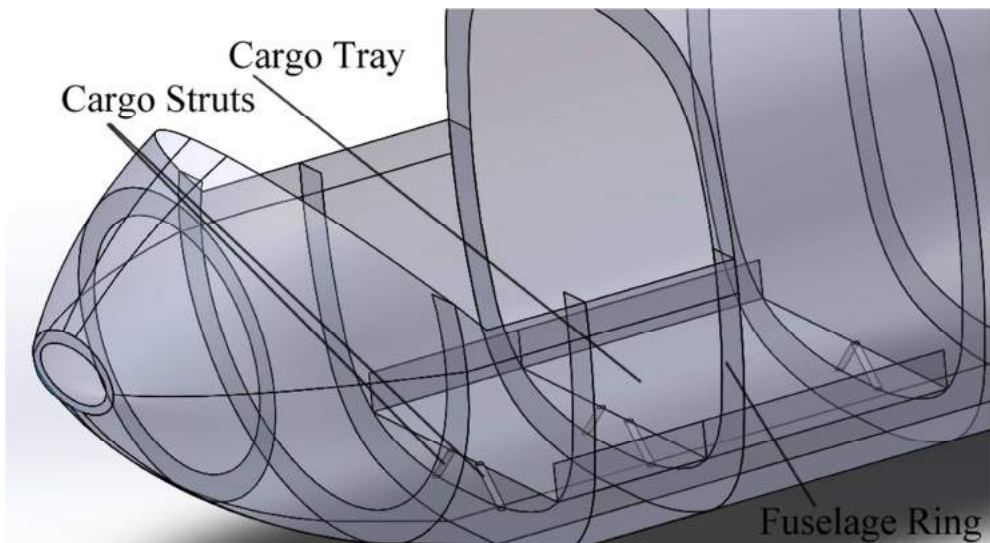


*Figure 9-10 a) Cargo Tray Design b) Fuselage Structure accommodating landing gear*

## 9.6 Undercarriage

This section focuses on the landing gear design for the ADV. Specifications of the undercarriage systems and its compliance with Federal Aviation Regulations will be discussed.

### 9.6.1 Landing Gear

The ADV integrates a tricycle landing gear configuration allowing for the aircraft to be at level height with the operator, ensuring the ease in loading cargo. The layout of the undercarriage system is shown in figure 9-2. The operation of the aircraft is intended for the region surrounding Mount Kenya therefore maintenance must be minimised for the reduced cost and ease of repairs. Thus, a non-retractable system comprising of a leaf spring cantilever main gear and a bungee cord nose gear is employed for the aircraft. The main gear has a two wheel configuration and the nose gear has one single wheel. The undercarriage system utilises three Type III 5.00-5 tyres, ideal for cleared dirt runways.

The ADV has a tip back angle of 15 degrees, placing the main leaf spring 1.33 metres aft of the centre of gravity at gross take-off weight. The design of the undercarriage aimed for a 90-10 load distribution however, a compromise was made at 83-17 in order to place the nose gear at a desirable position under the fuselage for support with the front bulkhead. Although the weight distribution is less than desired, elevator authority was tested and ensured to provide enough force for rotation during flight mechanics testing under section 11.5.1. The wheel track of the main landing gear is 1.4 metres, providing an overturn angle of 60.3°. Table 9-1 summarises the undercarriage system for the ADV.

*Table 9-7 Summary of Undercarriage System*

	Nose Gear	Main Gear
<b>Landing Gear System</b>	Bungee Cord	Leaf Spring
<b>Tyre Properties</b>	Type III 5.00-4 Nylon	Type III 5.00-4 Nylon
<b>Stroke Length</b>	0.2 m	0.24 m
<b>Strut Length</b>	0.51 m	0.51 m
<b>Location</b>	0.17 m	1.32 m
<b>Weight Supported</b>	17% MTOW	83% MTOW
<b>Design Loading</b>	FAR23.473 - FAR23.493	FAR23.473 - FAR23.493
<b>Material</b>	Aluminium 7075-T6	Aluminium 7075-T6
<b>Weight</b>	1 kg	2.49 kg
<b>Tip Back Angle</b>	15.0°	-
<b>Overturn Angle</b>	60.3°	-

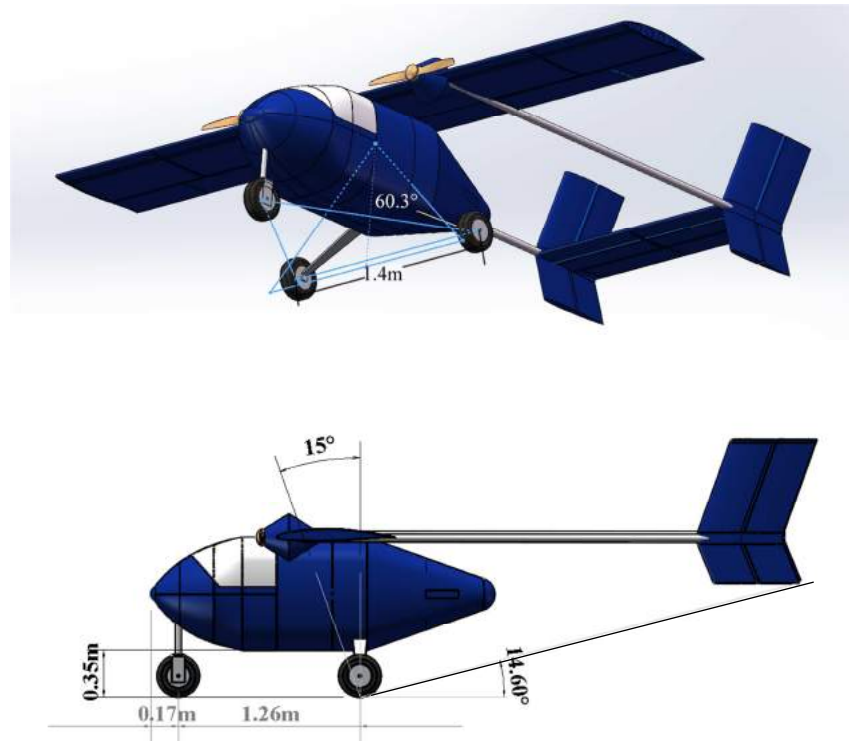


Figure 9-11 a) ADV Landing Gear Geometry- Overturn Angle and Wheel Track b) Positioning and clearances

The undercarriage system of the ADV is supported within the structure of the aircraft. The rear leaf spring is mounted on the aft section bulkhead and will be fixed during installation. The nose gear is supported by a front section bulkhead and plate to which the bungee cord is attached internally to the aircraft. The nose section is forward of the payload access. The design took inspiration from short take-off and landing systems developed by Zenith Air [7]. Figure 9-3 illustrates the structural placement of the bungee cord nose system and the leaf spring main undercarriage.

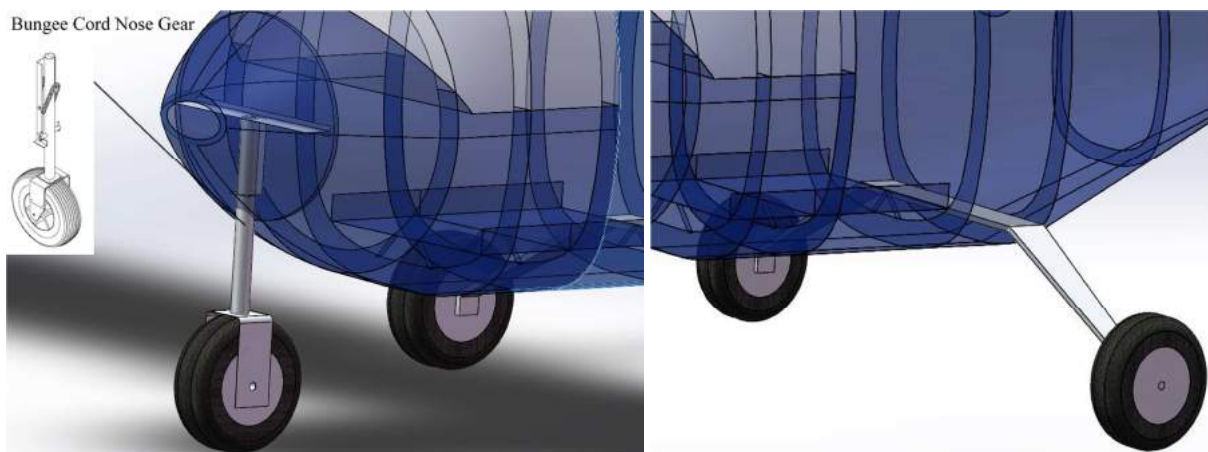


Figure 9-12 a) Nose Gear System b) Main Gear System

### 9.6.2 Detailed Undercarriage Structural Analysis

Load cases that were considered for the design of the undercarriage were specified by Federal Aviation Regulations which are summarised in table 9-2. The table indicates the load cases and the compliance of the undercarriage to each regulation. A landing load of 2.67g on the aircraft translated to a maximum load of 2 g's when lift force was considered. The most critical load case for landing gear design was the one wheel landing condition and was the driver for the landing gear geometry. The leaf spring is designed to withstand a total of 2g, which is transferred onto one leg during touch down in addition to the drag that is produced at the tyre. This was followed by the side load conditions and finally the braked roll condition. This section of the report will detail structural analysis of the main landing gear for the most critical case. The remaining load cases in addition to the detailed analysis of forces to which the undercarriage is subjected are covered in the Appendix.

*Table 9-8 Undercarriage Load Cases (tick indicates compliance)*

	Level Landing (i) ✓FAR 23.479	Level Landing (ii) ✓FAR 23.479	Tail Down ✓FAR 23.481
<b>Vertical Load at cg</b>	2.67	2.67	2.67
<b>Fore/Aft Load at cg</b>	0.67	0.67	0.67
<b>Lateral Load</b>	0.00	0.00	0.00
<b>Undercarriage Load (vertical)</b>	2.00	2.00	2.00
One Wheel Landing ✓FAR 23.483	Braked Roll ✓FAR 23.485	Side Load ✓FAR 23.493	
<b>Vertical Load at cg</b>	2.67	2.67	1.33
<b>Fore/Aft Load at cg</b>	0.67	2.14	0.33
<b>Lateral Load</b>	0.00	0.00	0.50
<b>Undercarriage Load (vertical)</b>	2.00	2.00	1.33

The leaf spring system was modelled in SolidWorks and meshed in ANSYS to conduct a finite element analysis. Equivalent stress, shear stress and displacement values were calculated and were reinforced by running the same case in SolidWorks simulator. Figures show the results from the ANSYS simulation. The remaining critical load cases that were considered are summarised in the Appendix of this report. The material selected for the undercarriage was Aluminium 7076-T6, which is a common undercarriage material able to withstand high compressive loads [8].

Since weight was a major design concern for the ADV, optimisation of the undercarriage had to be carried out to slim down the component where stresses are not as significant. For the landing cases, these regions are closer towards the wheel, as the stresses experienced by the leaf spring

are primarily the shear of the cantilever occurring at the fuselage connection (see figure 9-5). A taper is introduced and the thickness of the leaf spring is reduced to an acceptable value where the margin of safety is still significant. Weight optimisation of the leaf spring reduced the weight of the main undercarriage component to 2.49 kg.

From the analysis, the most critical case generates an equivalent stress of 405 MPa, yielding a margin of safety of 0.29 for the design. Total deflection of the aircraft for this case is 0.17 cm which is an acceptable range preventing any collision of the ADV components with the ground.

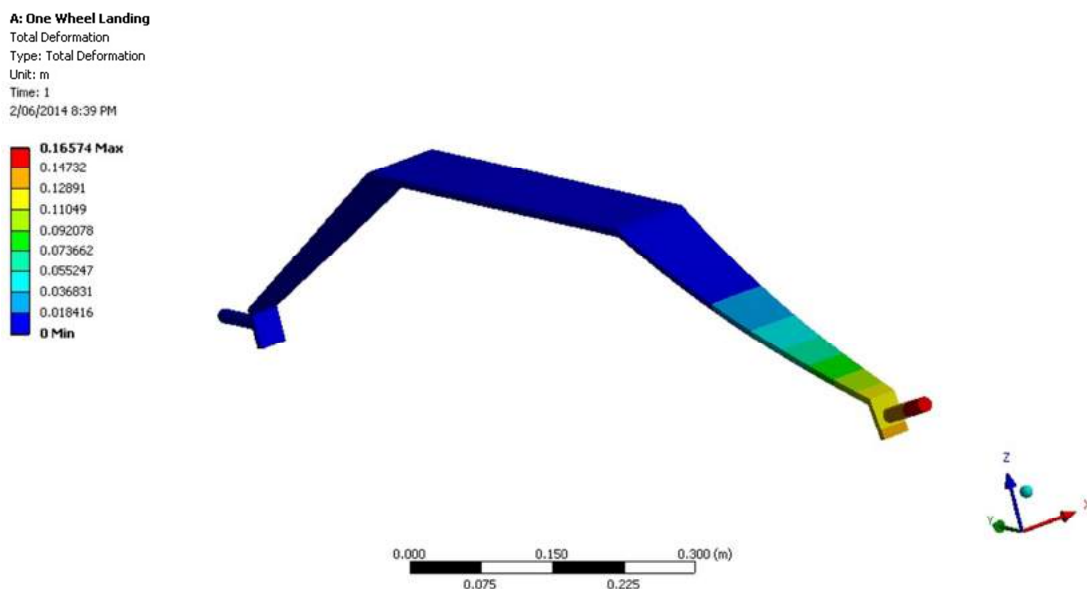


Figure 9-13 Leaf Spring FEA - Total Deformation

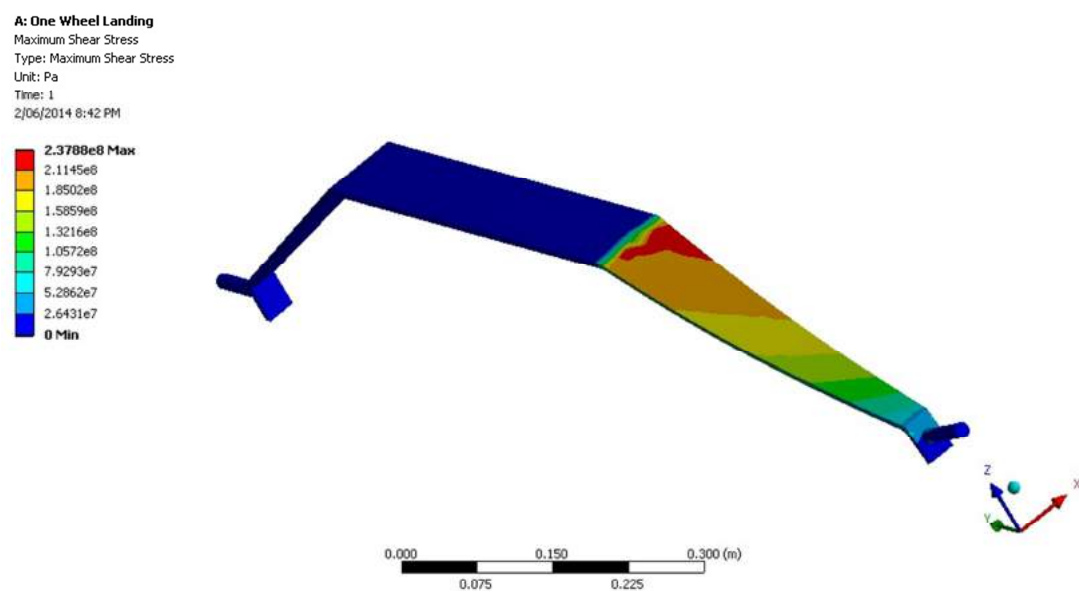


Figure 9-14 Leaf Spring FEA - Maximum Shear Stress

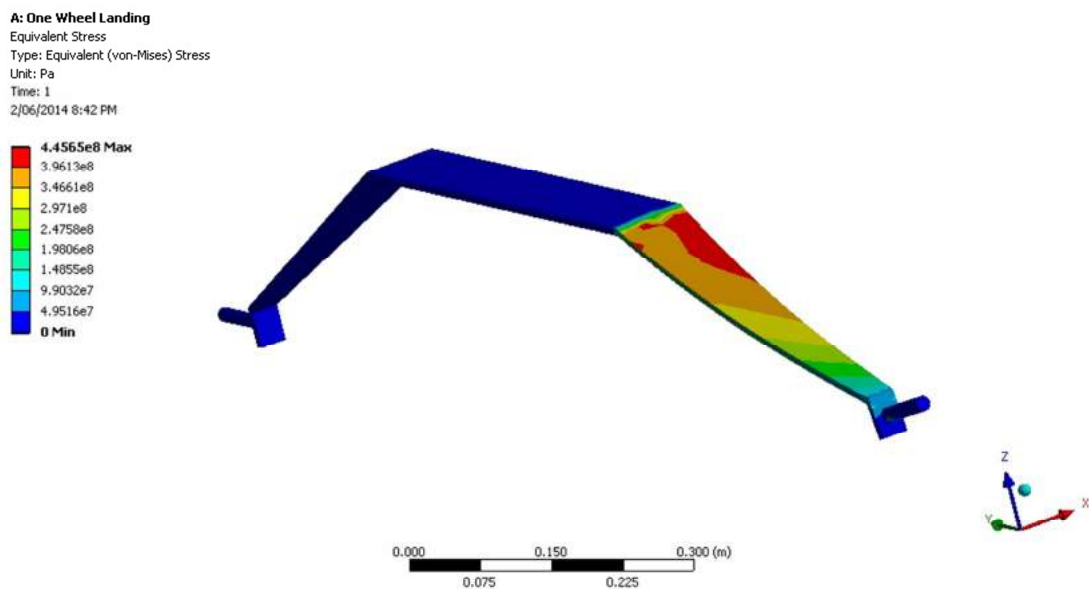
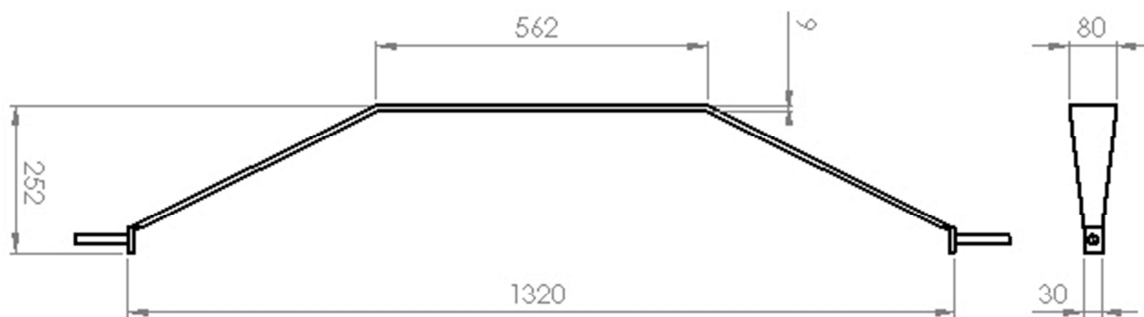
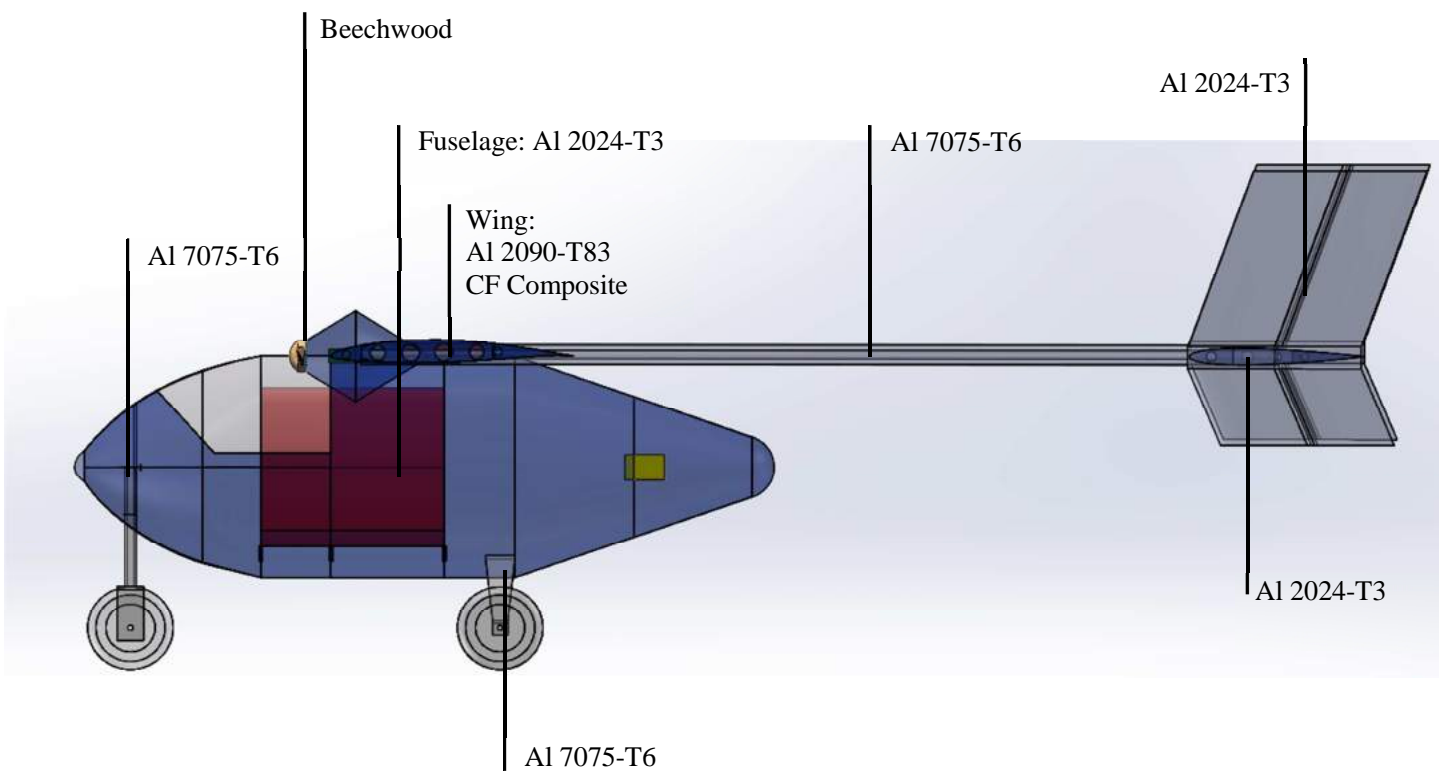


Figure 9-15 Leaf Spring FEA - Equivalent Stress

The final dimensions of the leaf spring can be viewed in figure 9-7. This is the optimised geometry is characterised by the taper. The wheel axle is sized at 5/8 inch which for the desired tyre and also modelled onto the landing gear.



## 9.7 Materials Summary



*Figure 9-16 Materials Summary*

Figure 9-15 breaks down the materials used in the ADV. Majority of the UAV's construction is Aluminium due to its resistance to corrosion and relatively high strength. Aluminium 7075-T6 is used in components where compressive stresses and high bending moments are present such as the tail booms and the landing gear. The aircraft also uses Aluminium 2024-T3 alloy which is an abundant and relatively cheap material for aircraft construction. During the design process however, weight optimisation was required due to the limit of a 60kg gross take-off weight, thus the wing's skin was to incorporate a composite structure, a decision that will impact upon the cost of the aircraft.

## 10 Weights and Balance

This section summarises the build-up of component weights of the ADV. The centre of gravity positions aft and forward of the aircraft are determined in this section followed by a summary of the range of centre of gravity travel. Details of the centre of gravity travel are expanded under the flight mechanics section of this report (Chapter 11).

### 10.1 Component Weight Summary

Components making up the ADV consist of the structural weights, the propulsive system, fixed equipment and the operational weight categories. A statistical estimate is performed to determine component weight build up based on correlations with existing aircraft [9]. Known masses from calculations include the wing weight, tail boom weight, avionics, fuel masses and the cargo which are obtained from their respective departments.

Figure 10-1 illustrates all major components of the ADV and their respective positions. Table 10-1 details the component weight build-up of the UAV.

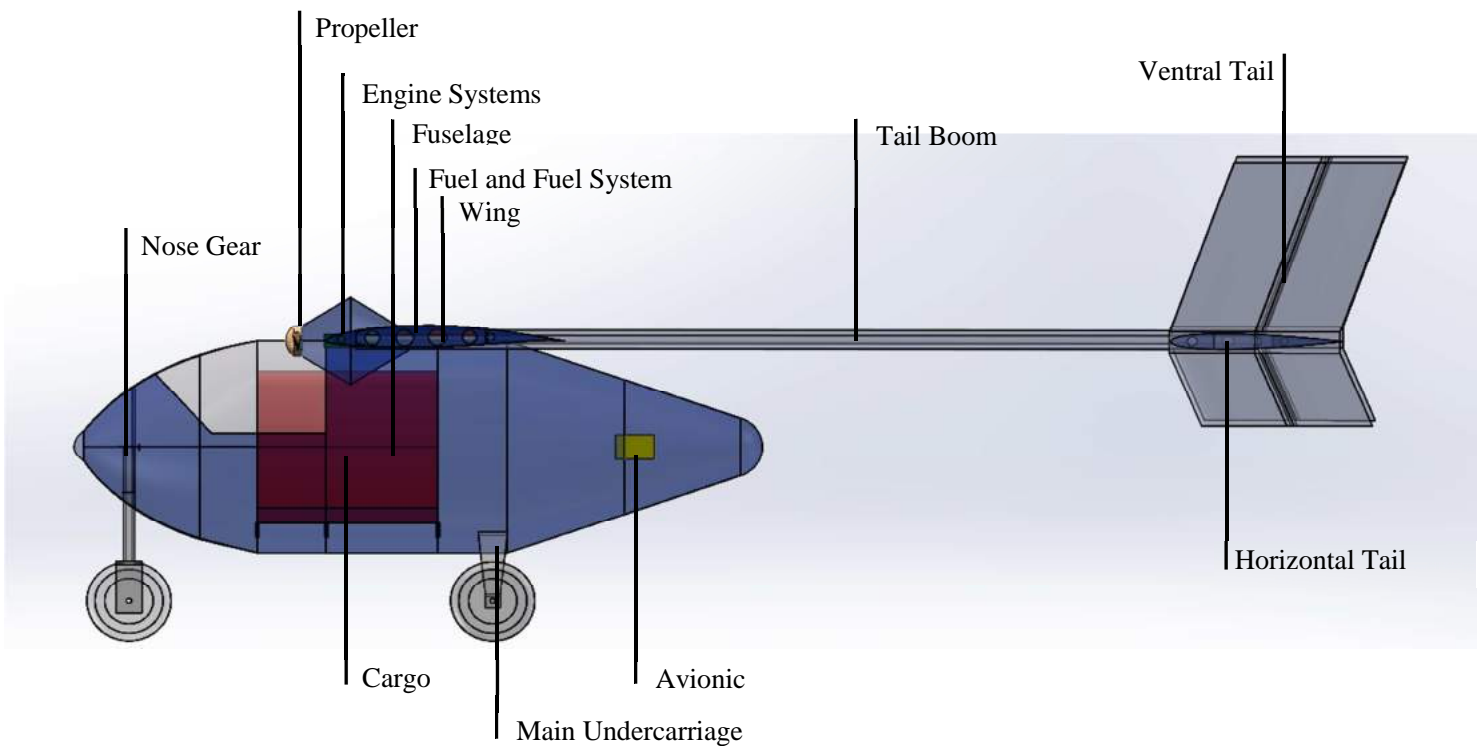


*Figure 10-1 Component Layout*

Table 10-1 Component Weight Summary

Component	Weight (kg)	X (m)	Z (m)		Weight (kg)	X (m)	Z (m)	
<b>STRUCTURE</b>				<b>PROPULSION SYSTEM</b>				
1 Wing	7.88	1.15	1.05	13	Engine + Engine System L	2.53	0.79	0.95
2 Fuselage	5.70	1.05	0.70	14	Engine + Engine System R	2.53	0.79	0.95
3 Tail Boom L	2.51	2.13	1.05	15	Fuel System	0.51	0.99	1.04
4 Tail Boom R	2.51	2.13	1.05	16	Propeller L	0.26	0.71	0.98
5 Horizontal Tail	2.42	3.54	1.05	17	Propeller R	0.26	0.71	0.98
6 Ventral Tail L	1.26	3.54	1.20		<b>Total</b>	6.09		
7 Ventral Tail R	1.26	3.54	1.20					
8 Main Landing Gear	4.00	1.50	0.16		<b>Empty Weight</b>	<b>37.13</b>		
9 Nose Landing Gear	1.83	0.17	0.21					
<b>Total</b>	<b>29.37</b>			18	Trapped Fuel/Oil	0.16	0.99	1.04
<b>FIXED EQUIPMENT</b>					<b>Operational Weight</b>	<b>37.29</b>		
10 Control System	0.97	1.52	0.83					
11 Avionics	0.20	1.95	0.89	19	Fuel	2.66	0.99	1.04
12 Power Unit	0.50	1.75	0.83	20	Cargo	20.00	0.40	0.70
<b>Total</b>	<b>1.67</b>				<b>GTOW</b>	<b>59.95</b>		

## 10.2 Centre of Gravity

The ADV has a centre of gravity range of 1.01 metres to 1.11 metres. This translates to 30% MAC to 43% MAC respectively. These values are within the stability range and the travel of centre of gravity is summarised in figure 10-2. At the forward CG, a static margin of 18% is achieved whereas the aft CG results in a 7% static margin. Detailed analysis into the travel and controllability of the aircraft will be explored in Chapter 11 which focuses on Flight Mechanics.

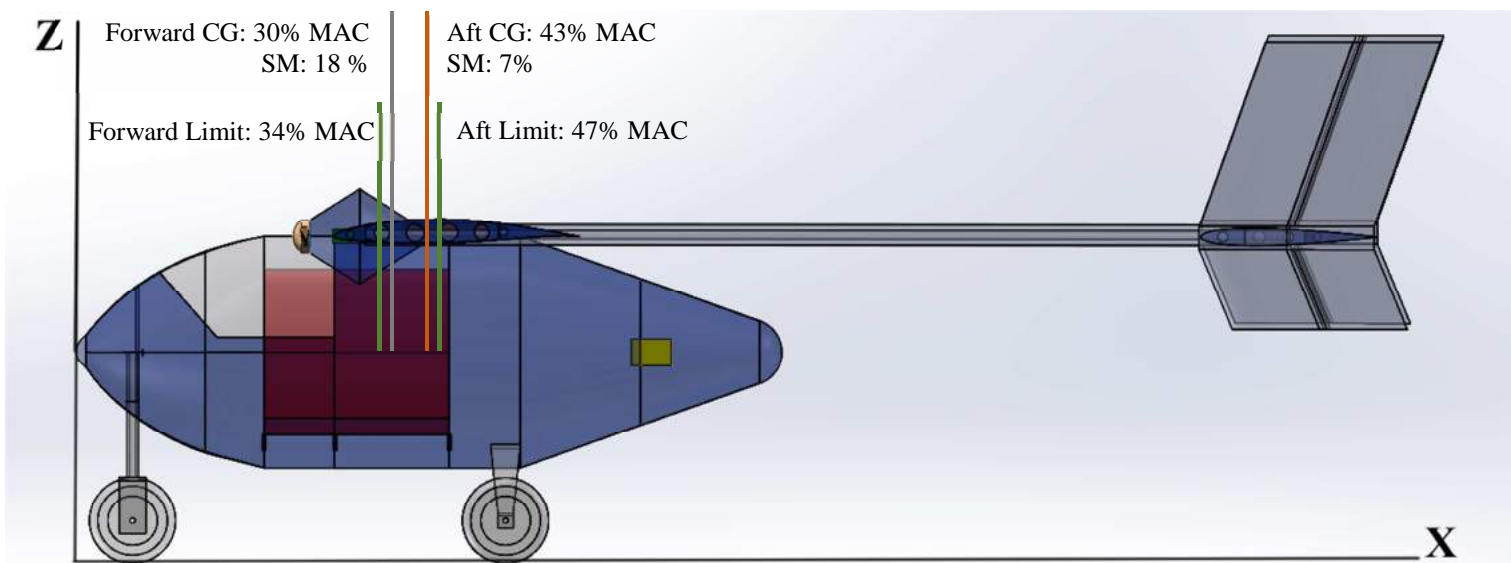


Figure 10-2 CG Travel

## 11 Flight Mechanics

The control surfaces of ADV have been designed to provide sufficient stability for both longitudinal and lateral flight operations. This design part is mainly based on the control surface methodology outlined in Raymer [4] and results are produced by the software AVL. Outputted results are iteratively dependent on the aerodynamic and propulsion values to achieve the desired flight stability and control during entire flight operation. In addition, a validation has been made to determine the reliability of the results which is available in the Appendix.

Hence, this chapter will mainly focus on:

- The finalised control surface dimensions and maximum deflections.
- The CG travel limit of the design and the actual CG travel for both full cargo load and no cargo load cases during flight operation, plus the static margin illustration.
- Longitudinal stability check by viewing the stability derivatives, elevator deflection in terms of airspeed variation and longitudinal state responses in terms of elevator control input.
- Lateral stability check by viewing the stability derivatives, one engine inoperative lateral control recovery and lateral state responses in terms of rudder control input.
- Control authority check includes: Takeoff rotation elevator authority, one engine inoperative operation and cross wind landing capability plus roll authority.
- Handling quality complying with regulations.

## 11.1 Control Surface Sizing

The finalised control surface information has been illustrated in Figure 11.1. Aileron is designed to have sufficient roll ability. Flap is designed to maximise the lift generation during take-off and landing. Elevator is designed to rotate the aircraft before lift-off speed and stalling ability. Rudder is designed to laterally trim the aircraft during one engine inoperative situation. In addition, the sweep design on the vertical tail is to avoid the downwash zone produced by the wing at high angle of attack and low speed operation to reduce the effectiveness of the rudder.

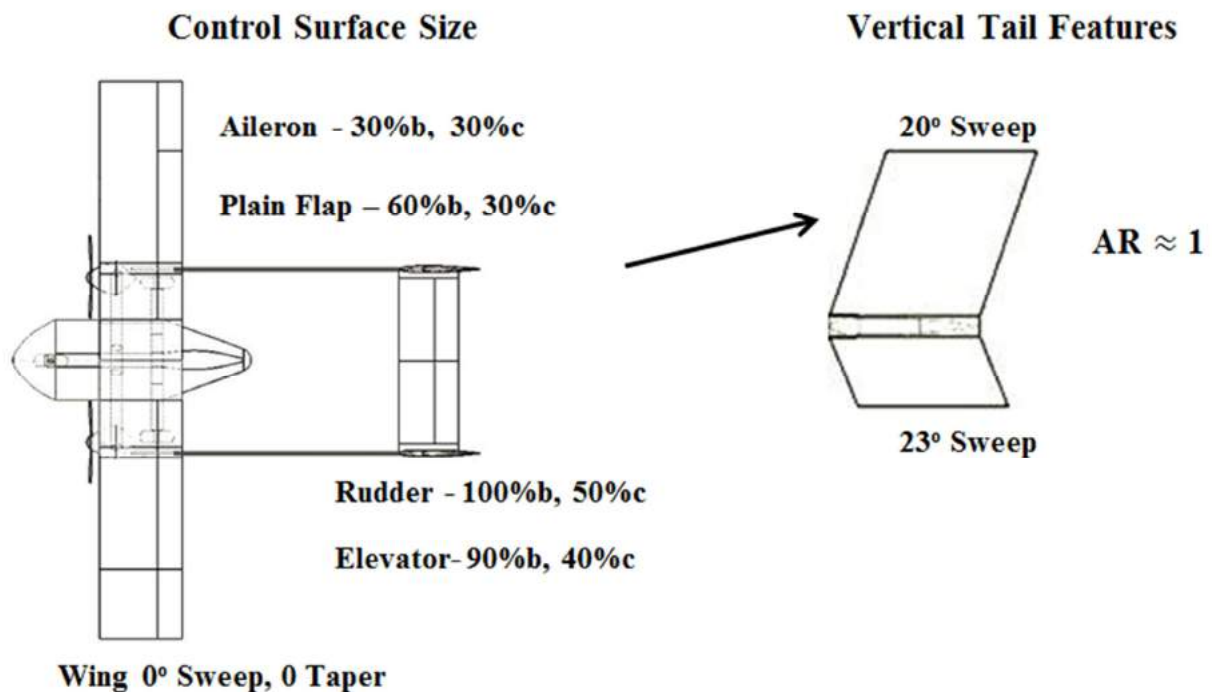


Figure 11-1 Control Surface Size and Vertical Tail Features

The detailed dimensions and maximum deflections are listed in Table 11.1. Flap deflections reach a value of 60 degrees to maximise the lift generation. Aileron and elevator have been limited to 25 degrees to avoid additional drag generation if it exceeds this value. The rudder is crucial for lateral trim when aircraft has one engine failure case so it has been set to 30 degrees maximum.

Table 11-1 Control Surface Dimensions

Control Surface	Spanwise (m)	Chordwise (m)	Deflection( $^{\circ}$ )
Aileron (each side)	0.72 m	0.22 m	$\pm 25^{\circ}$
Flap (each side)	1.44 m	0.22 m	$+60^{\circ}$
Elevator	1.42 m	0.21 m	$\pm 25^{\circ}$
Rudder – Upper	0.56 m	0.26 m	$\pm 30^{\circ}$
Rudder – Lower	0.24 m	0.26 m	$\pm 30^{\circ}$

## 11.2 CG Travel Limit and Static Margin

A ‘Scissor Plot’ in Figure 11.2 has been constructed to study the CG travel limit of the ADV. The designed horizontal tail accounts for 22% of the wing area and limit the longitudinal control CG limit from 24% at front to 46% at the back. The most aft CG limit also has a static margin of 3%, which is quite low, so the actual CG at most aft condition during flight is expected to have a static margin greater than 5%.

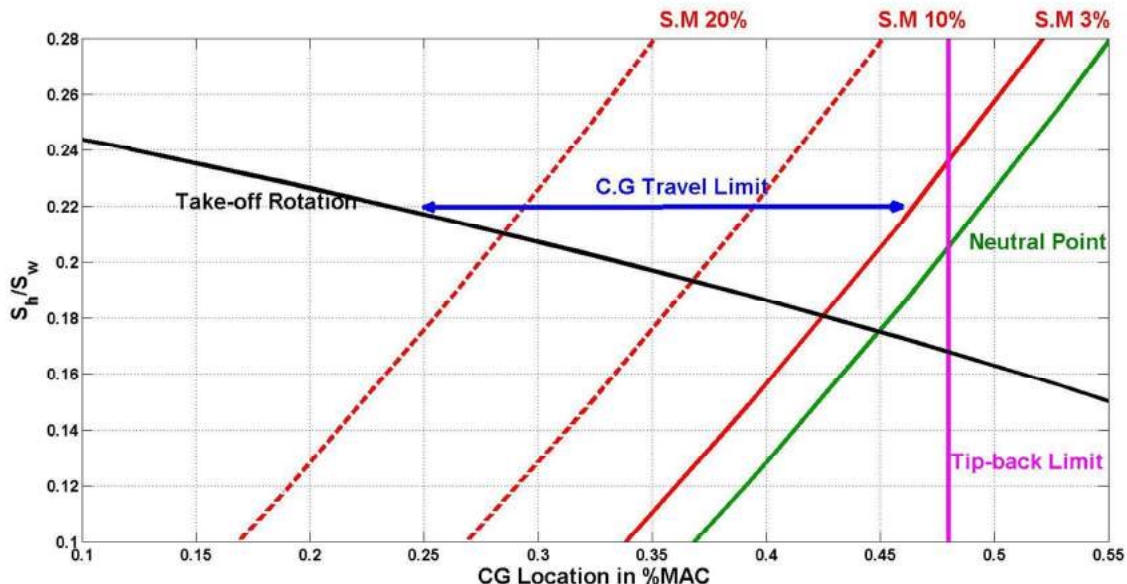


Figure 11-2 Horizontal Tail Sizing for CG Travel Limit – Scissor Plot

Regarding the size and fuel consumption for the ADV, this is quite small, and the fuel tank is located below and close to the centre of the wing. When the ADV is operating with full load, the CG travel due to fuel burn is negligible. Therefore, in Table 11.2, it can be seen that the actual CG travel at front without any cargo is 30% and at back with full cargo 43% of the MAC, which are both within the CG travel limit illustrated in ‘Scissor Plot’ study.

The static margin can also be estimated from the Figure 11.2 by using the 3%, 10% and 20% static margin lines. So the most aft static margin is 7% and most forward CG is 18%, which are both within tolerated range.

*Table 11-2 CG Travel Limit vs. CG Travel in Flight and Static Margin*

<b>CG Location</b>	Most Forward (% MAC)	Most Afterward (% MAC)
CG Travel Limit	24%	47%
CG Travel in Flight	30% (No Cargo)	43% (Full Cargo)
Static Margin in Flight	<b>18%</b>	<b>7%</b>

## 11.3 Longitudinal Stability

### 11.3.1 Longitudinal Stability Derivatives

Table 11-3 Longitudinal Stability at Most Forward CG Location

Longitudinal Stability Derivatives	Initial Climb	Cruise	Approach
$C_{m\alpha}$ (< 0 to be stable)	-1.42	-1.41	-1.40
$C_{mq}$ (< 0 to be stable)	-17.4	-18.2	-15.1
Elevator Trim	-7.1°	-3.8°	-8.4°
Angle of Attack	7.7°	2.7°	8.5°

Table 11-4 Longitudinal Stability at Most Aft CG Location

Longitudinal Stability Derivatives	Initial Climb	Cruise	Approach
$C_{m\alpha}$ (< 0 for stability)	-0.120	-0.130	-0.125
$C_{mq}$ (< 0 for stability)	-15.1	-15.8	-13.4
Elevator Trim	-2.7°	-2.4°	-3.1°
Angle of Attack	7.2°	2.6°	7.9°

### 11.3.2 Longitudinal Elevator Trim with Speed Variation

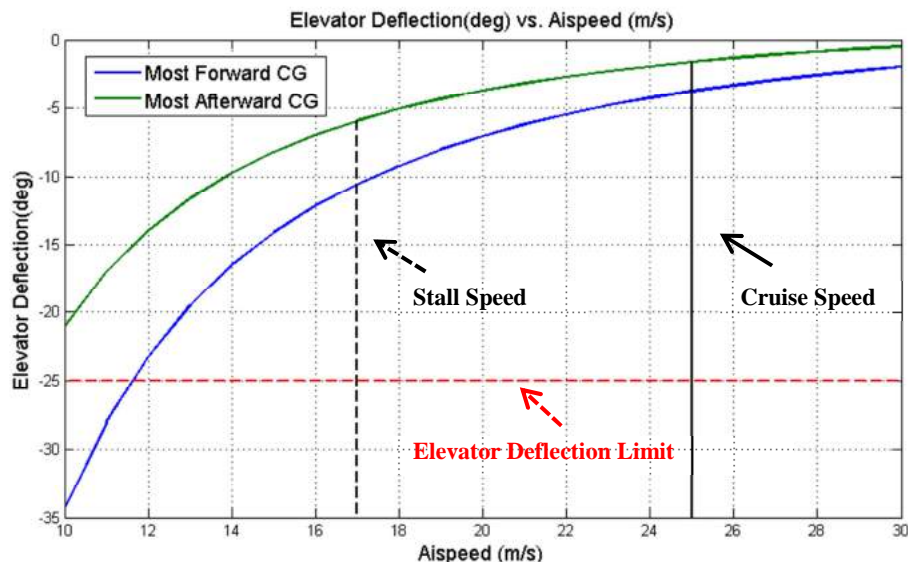


Figure 11-3 Longitudinal Elevator Trim with Speed Variation for two CG cases

By examining the stability derivatives in Table 11.3-11.4, it can be seen that the aircraft is longitudinally stable for both most forward and aft CG conditions. Also, additional check on elevator trim for both CGs is shown in Figure 11.3; the maximum elevator deflection is set at 25 degrees. With the variation of airspeed, the aircraft requires more elevator deflections to trim at low speed however still provides sufficient elevator control even aircraft reaches stall speed. This figure can reflect to the result in Table 11.3-11.4, which are consistent.

### 11.3.3 Longitudinal State Responses to Elevator Input (Most Forward CG)

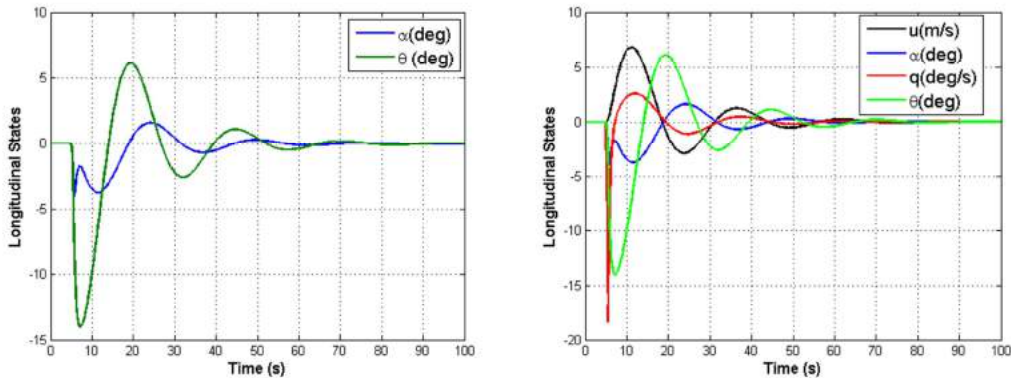


Figure 11-4 Longitudinal State Responses at Initial Climb with 5o Elevator Input for 5 seconds

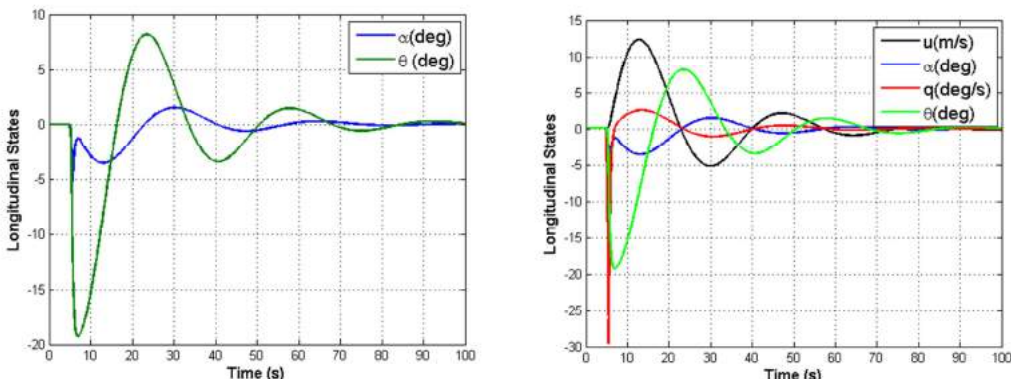


Figure 11-5 Longitudinal State Responses at Cruise with 5o Elevator Input for 5 seconds

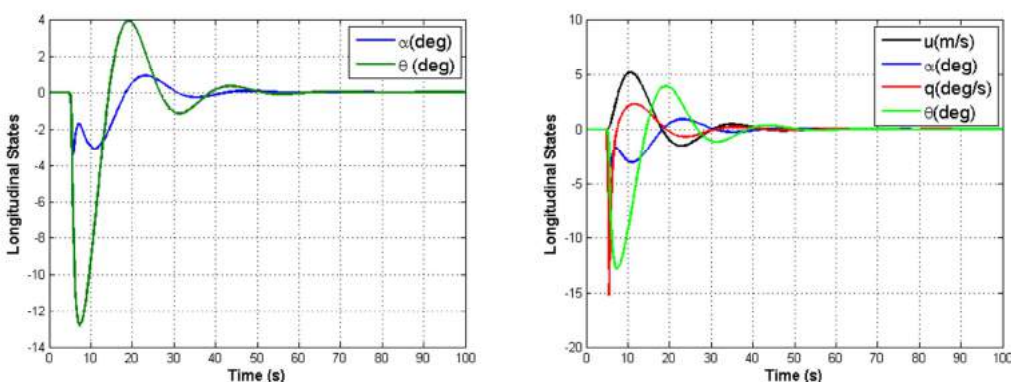


Figure 11-6 Longitudinal State Responses at Approach with 5o Elevator Input for 5 seconds

The longitudinal state responses due to elevator deflection have been studied for initial climb, cruise and approach at the most adverse CG location, i.e. most forward CG location. The elevator input is set to  $5^\circ$  and lasting 5 seconds, then the state response is observed. In Figure 11.4-11.6, they all feature oscillatory convergent responses (Regardless of the long convergent time due to the natural of the system which does not have any compensator implemented).

## 11.4 Lateral Stability

### 11.4.1 Lateral Static Stability

*Table 11-5 Lateral Stability at Most Forward CG Location*

Lateral stability derivatives	Initial Climb	Cruise	Approach
Directional stability, $C_{n_\beta}$ ( $> 0$ to be stable)	0.097	0.101	0.074
Dihedral effect, $C_{l_\beta}$ ( $< 0$ to be stable)	-0.158	-0.106	-0.171
Sideslip to side-force, $C_{y_\beta}$ ( $< 0$ to be stable)	-0.468	-0.435	-0.568
Yaw damping, $C_{n_r}$ ( $< 0$ to be stable)	-0.220	-0.215	-0.204
Roll damping, $C_{l_p}$ ( $< 0$ to be stable)	-0.511	-0.506	-0.563
$\frac{C_{l_\beta} C_{n_r}}{C_{n_\beta} C_{l_r}}$ ( $> 1$ to be spirally stable)	<b>1.57</b>	<b>1.46</b>	<b>2.35</b>

*Table 11-6 Lateral Stability at Most Afterward CG Location*

Lateral stability derivatives	Initial Climb	Cruise	Approach
Directional stability, $C_{n_\beta}$ ( $> 0$ to be stable)	0.083	0.089	0.0608
Dihedral effect, $C_{l_\beta}$ ( $< 0$ to be stable)	-0.158	-0.106	-0.167
Sideslip to side-force, $C_{y_\beta}$ ( $< 0$ to be stable)	-0.470	-0.436	-0.569
Yaw damping, $C_{n_r}$ ( $< 0$ to be stable)	-0.204	-0.200	-0.188
Roll damping, $C_{l_p}$ ( $< 0$ to be stable)	-0.514	-0.507	-0.564
$\frac{C_{l_\beta} C_{n_r}}{C_{n_\beta} C_{l_r}}$ ( $> 1$ to be spirally stable)	<b>1.79</b>	<b>1.63</b>	<b>2.85</b>

Similar to the longitudinal case, the lateral stability derivatives have been checked for both CG locations at all flight conditions. It can be proved that aircraft is laterally stable for all flight conditions from Table 11.5-11.6 where all derivatives satisfy requirement.

### 11.4.2 Lateral State Responses to Rudder Input (Most Forward CG)

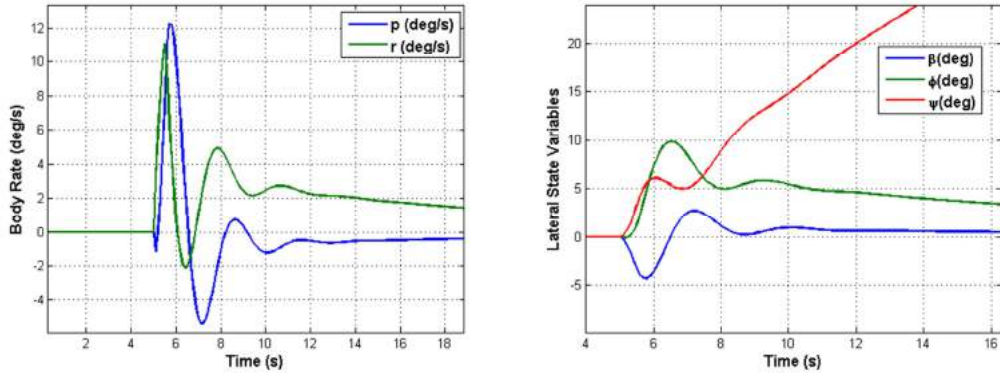


Figure 11-7 Lateral State Responses at Initial Climb with 5° Rudder Input for 5 seconds

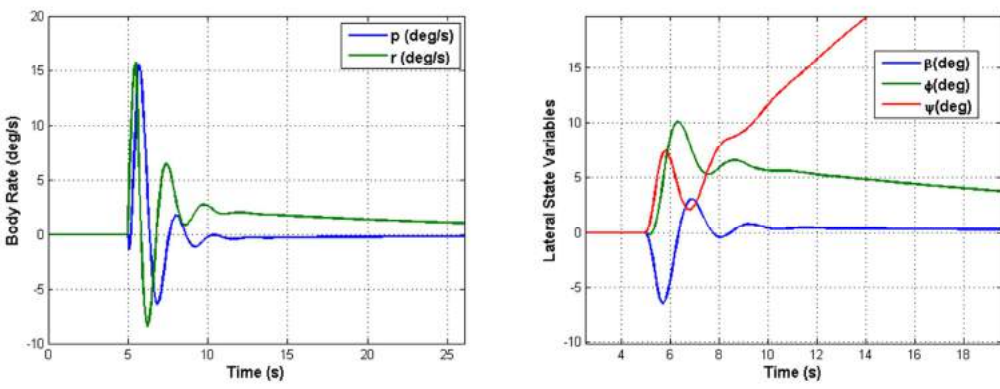


Figure 11-8 Lateral State Responses at Cruise with 5° Rudder Input for 5 seconds

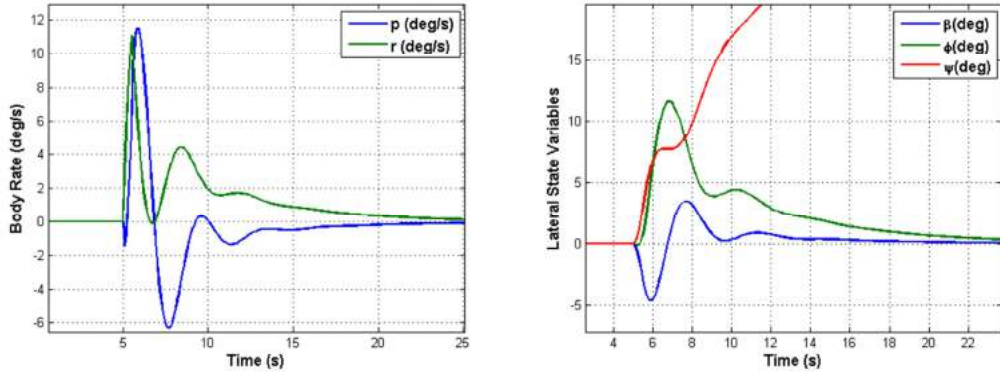


Figure 11-9 Lateral State Responses at Approach with 5° Rudder Input for 5 seconds

Similar to longitudinal case, the lateral state responses due to rudder deflection have been studied for initial climb, cruise and approach at most forward CG location. Through Figure 11.7-11.9, it is evident that the ADV maintains excellent damping quality for all conditions and settles most quickly at the initial climb, which is less than 20 seconds. Also, due to fact that ADV is spirally stable for all conditions, bank angle and sideslip angle can quickly return to

equilibrium where the yaw angle is delaying to converge and require more time to return equilibrium.

## 11.5 Control Authority

Apart from the stability analysis in previous sections, the authority check of control surfaces needs to be made to examine the control capability of the ADV at extreme flight conditions. The check list is based on Gudmunsson [2].

### 11.5.1 Take-off Rotation Elevator Control Authority (Most Forward CG)

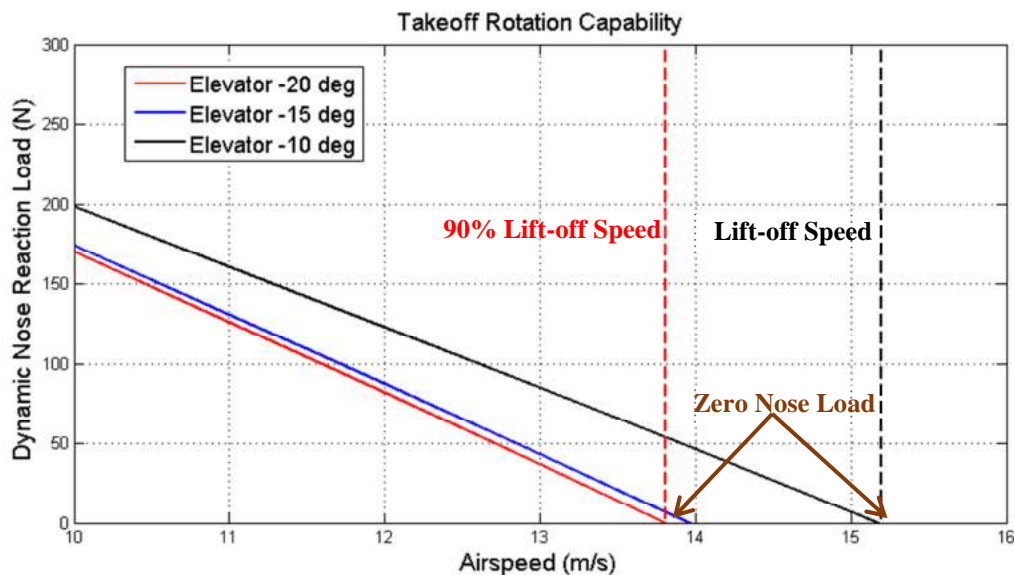


Figure 11-10 Take-off Rotation Elevator Control Authority

The take-off capability is made by checking if elevator is sufficient to produce the rotation before the ADV reaches the lift-off speed. That means it needs to bring the dynamic load at the nose to zero. In Figure 11.10, it can be seen that the ADV can be lifted off at design lift off speed with -10 degrees of elevator deflection. Additionally, -15 degrees and -20 degrees elevator deflections have been attempted and it can be found that elevator loses authority quickly from -15 to -20 (remain 5 degree margin, so it will not go beyond -20) . Finally, at -20 degree deflection, the ADV can lift off about at 90% of lift off speed. Therefore, the elevator control authority is confirmed for the aircraft.

### 11.5.2 One Engine Inoperative (Most Forward CG, $\beta = 0^\circ$ )

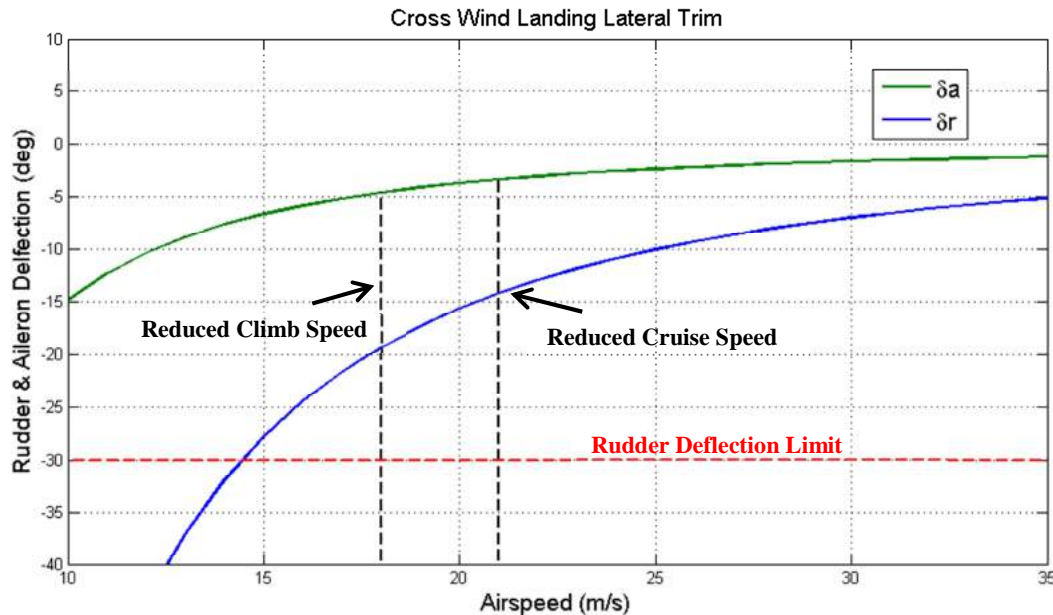


Figure 11-11 One Engine Inoperative Lateral Trim

ADV is designed to be able to laterally trim at both climb and cruise for one engine inoperative situation. However, the one engine operation does not allow ADV to maintain original cruise speed, so it must be reduced. From propulsion department, the thrust contour gives the new cruise speed is approximately 21 m/s at one engine throttle setting of 92% to provide enough propeller thrust to balance the drag. So, in Figure 11.11, at this speed, it requires -15 degrees rudder and -3.5 degrees aileron input to trim the aircraft to maintain zero sideslip angle (No additional drag increase after trim).

Also, one engine inoperative has been applied to climb just after take-off (30 degrees flaps on). From the thrust contour, the single engine propeller will provide sufficient thrust to climb at 15 degrees to clear the obstacle if the climb speed is reduced to 17m/s (speed lower than 17m/s with flaps on) with throttle setting at 98%. From Figure 11.11, it requires -20 degrees rudder and - 4.5 degrees aileron to trim the aircraft. At -20 degrees rudder deflection, it is less than 75% of maximum rudder deflection (-22.5 degrees). Therefore, ADV's ability to fly at one engine condition is confirmed.

Apart from one engine failure case, ADV needs to laterally trim for crosswind landing. So, in Figure 11-12, it simulates a 15 degree sideslip angle and it requires -11.5 degrees rudder and 3.5 degrees of aileron to trim a steady sideslip level approach flight.

### 11.5.3 Cross Wind Landing (Most Forward CG, $\beta = 15^\circ$ )

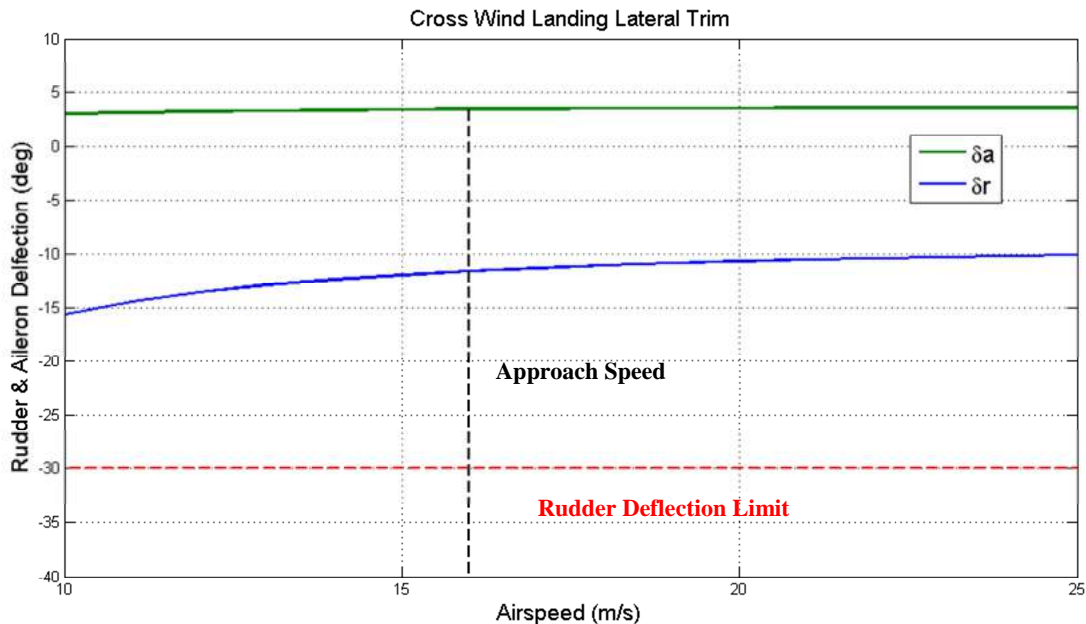


Figure 11-12 Cross Wing Landing Lateral Trim

### 11.5.4 Roll Authority Check

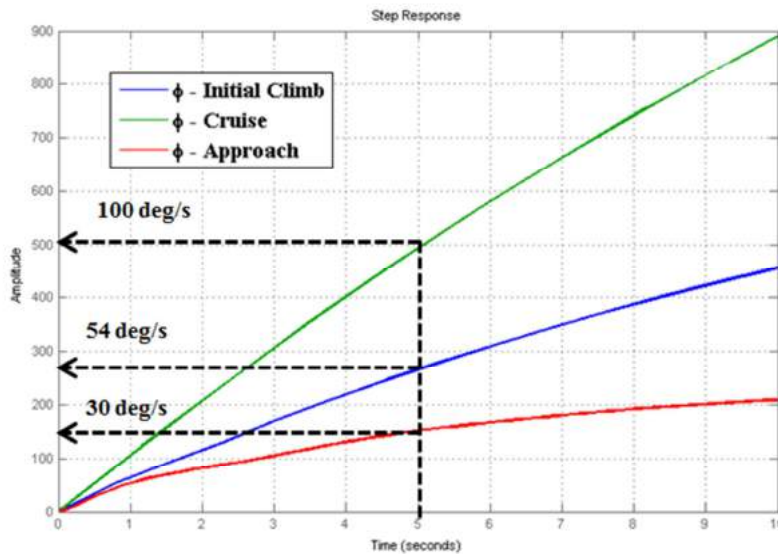


Figure 11-13 Roll Authority Check

ADV is expected to have a roll authority that can roll from -30 to 30 degrees (60 degrees magnitude) in less than 5 seconds at all flight conditions. In Figure 9.13, a 20 degrees aileron step response has been made to examine the roll angle change. It can be seen that all three flight conditions can achieve this requirement, and at cruise the roll rate can go as high as 100 degrees/s, which meets the responsive general aviation aircraft standard.

## 11.6 Handling Quality and Regulations

The dynamic handling qualities were assessed against the requirement specified in regulation MIL-HDBK-8785C for initial climb, cruise and approach conditions. ADV operating at most adverse CG (Most forward), is specified to meet the Level 1 – Category C – Class I handling quality. From Table 11.7, it can be seen that all the damping and frequency of all critical longitudinal and lateral dynamic mode are satisfying the Level 1 handling quality.

*Table 11-7 Handling Quality Check with Regulations*

Modes of Motion	MIL-HDBK Level 1	Initial Climb	Cruise	Approach
Short Period	$0.9 < \omega_{SP} < 5.5$	3.57	4.86	2.86
Mode	$0.35 < \xi_{SP} < 1.30$	0.70	0.69	0.814
Phugoid Mode	$\xi_{PM} \geq 0.04$	0.085	0.24	0.14
Dutch Roll	$\omega_{n_{DR}} \geq 0.4$	2.38	2.38	1.88
Mode	$\xi_{DR} \geq 0.08$	0.34	0.290	0.292
Roll Mode	$\tau_R \leq 1.4$	1.11	1.31	1.19

## 11.7 Summary

It can be finally summarised that:

- Control surfaces of ADV have been designed to provide sufficient control authority to trim the flight, plus dealing with extreme cases such as low speed lift off, responsive roll and one engine inoperative trim.
- Both longitudinal and lateral state can return to equilibrium after implementing a short period of control input which proves that ADV is both longitudinally and laterally stable.
- For the one engine inoperative situation, ADV has to fly at reduced speed to laterally trim to level and straight flight.
- ADV is satisfying Level 1 – Category C – Class I handling quality based on regulation MIL-HDBK-8785C.

## 12 Aircraft Systems

This section of the report summarises the Avionics system of the UAV, actuation of autopilot loop as well as the control system for the aircraft.

### 12.1 Avionics

ADV adopts a commonly used avionics architecture system and the schematic is shown in figure 12-1 [10]. The flight computer is used to handle the data received from GPS, inertia measurement unit and pressure sensors, which include latitude, longitude, altitude, velocity, track angle, time, roll, pitch, and yaw, etc. After collecting the data, flight computer outputs OWM servo commands, and sends information to the ground station via a data modem. A switch is presented to switch the control mode of the aircraft between manual and automatic control.

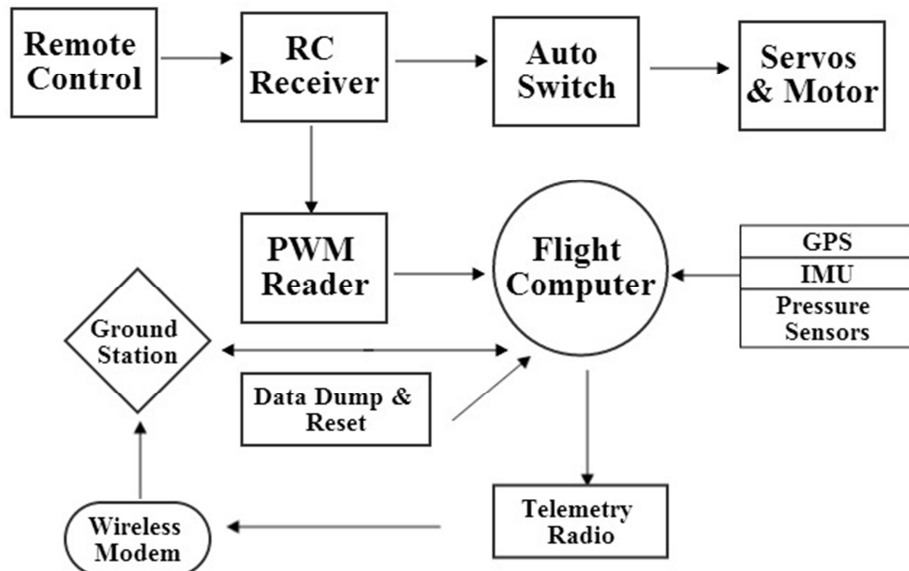


Figure 12-1 Avionics System Architecture

For the ADV, the avionics system components are summarised under table 12-1. The remote control is only used for ground action, take-off, and landing.

*Table 12-1 Avionics Components*

<b>Component</b>	<b>Name</b>	<b>Price (\$)</b>	<b>Weight (g)</b>
<b>Flight Computer</b>	SPC5200CBV400B	20.77	3
<b>IMU</b>	ADIS16405BMLZ	623.94	50
<b>GPS</b>	Hemisphere GPS Crescent Board + GPS Outfitters Titan 3 Antenna	370.00	20
<b>Dynamic Pressure</b>	AMS 5812 0003-D	60.00	3
<b>Static Pressure</b>	AMS 5812 0150-B	60.00	3
<b>Telemetry Radio</b>	FreeWave MM2-P-T 900 MHz	670.00	14
<b>Manual Control</b>	Spektrum DX7 2.4GHz	249.95	113
<b>Failsafe Switch</b>	Acroname RxMux	19.00	
<b>Total</b>		<b>\$ 2073.66</b>	<b>196 g</b>

## 12.2 Actuation

The actuation of ADV's flight loop is based on autopilot. Autopilot is the default setting for all flight paths between mission stages and is only active when the flight path is clear with adequate GPS signal. When the flight path is diverging to an unwanted path, the autopilot system will override to let the aircraft fly back the last recorded location. During this process, GPS will keep record the location of the aircraft to ensure that ADV is under control.

In addition, manual control is used when the aircraft is taking-off and landing to ensure that ADV arrives at the appropriate location within the airfield for cargo unloading and loading.

## 12.3 Control System

### 12.3.1 GPS

The primary function of the GPS is used to locate the aircraft to ensure that it is on the right flight path. One other purpose of using GPS is to treat it as a guide to help the aircraft relocate to last recorded location, when the signal of radio is missing, and the ground station loses direct control of the ADV.

### 12.3.2 Fuel Systems

The fuel used for selected DA-100 engine is normal petrol fuel, which has a density of 719.7 kg/m<sup>3</sup>. According to the analysis of performance, the fuel needed for the longest flight distance 50 km is 2.66kg. Hence, the minimum volume needed is 3756 cm<sup>3</sup>. The designed fuel tank has a dimension of 25cm × 40cm × 4cm, which provides 4000 cm<sup>3</sup> volume for the fuel. The fuel is stored in one designed fuel tank which location inside of the middle of the wing, this is shown in figure 12-2. The fuel tank is supported by three wing ribs, and is located between two engines to provide both with fuel through direct lines.

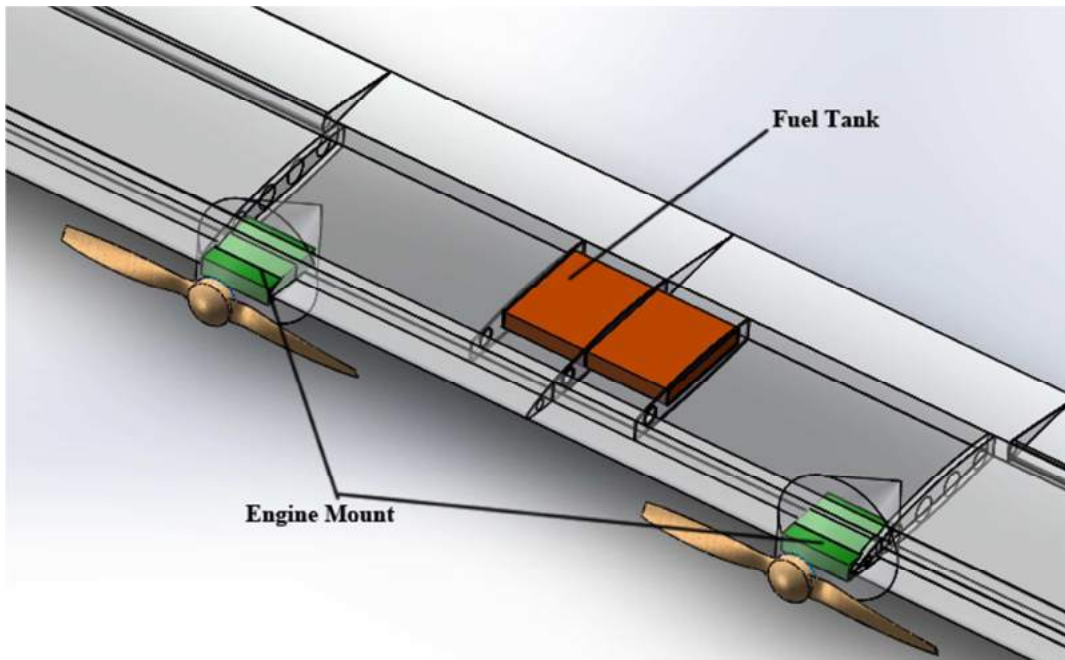


Figure 12-2 Fuel System

### 12.3.3 Ground Control

The required ground station operators include:

- Manual control operator responsible for supervising the ADV at take-off, landing and ground operations
- Cargo operator monitors the condition of the cargo as well as the loading and unloading
- Communications manager is responsible for all SATCOM communications with the aircraft and the air traffic control.

The human system interface within the ground control station is designed with high levels of automation to reduce human error effects in the system. The interface provides a summary of the critical data. Critical information such as the aircraft attitude, position, velocity, payload and weather conditions will be provided so the operator has sufficient situational awareness to monitor the aircraft and effect changes if necessary.

## 13 Cost and Development

This section presents the cost estimation for the UAV.

Nowadays, winning a contract not only means satisfying the proposal requirements but also requires doing so at the lowest possible cost. ADV was designed with the mission requirements set as priority. Lowering cost is always a mission requirement, but the fact that this UAV is intended to operate in areas with limited resources makes the aim for low cost especially important.

The aircraft's total cost and details on the contributing elements will be described. Roskam's *Airplane Design* [11] was used to estimate the cost of the Avicargo adapted for the particular characteristics and operation conditions of the UAV. The total aircraft cost is composed of Research Development Testing and Evaluation cost (RDTE) and acquisition cost. The total life cycle cost is made up of RDTE cost, acquisition cost, operation and maintenance cost and disposal cost.

The production run of 43 UAV includes 3 for RDTE purposes, a target of 15 for service in Mount Kenya, and 25 for available sell to other rural areas for missions which require large payload. The operational life of the aircrafts is assumed to be 30 years. The summary of the results are outlined in table 13-1.

*Table 13-1 Cost analysis summary*

CATEGORY	COST (thousand)*
RDTE (per aircraft)	\$11.31
Acquisition (per aircraft)	\$50.36
Operation and Maintenance (per aircraft flight)	\$0.0731
Total Life Cycle Cost (per aircraft)	\$752.23

\* All Costs in 2014 dollars

### 13.1 Airplane Cost: Development and Acquisition Cost

The RDTE (development) costs include:

- Airframe engineering and design cost.
- Development support and testing cost.
- Flight test airplane cost.
- Flight test operation cost.
- Cost to finance the flight test airplane.

*The TOGW, empty weight, maximum velocity, engine and avionics costs and assumed technological factors were utilised to determine the RDTE cost. Each engine was estimated to be \$901 each and the avionics system was \$2,070. The RDTE cost breakdown is summarised in*

Table 13-2. The overall RDTE is found to be approximately \$452,000, assuming no profit is desired by the enterprise for this stage of the design cost.

*Table 13-2 Breakdown for RDTE cost*

CATEGORY	COST (thousand)*
Airframe Engineering and Design Cost	\$83.8
Development Support and Test Cost	\$0.78
Flight Test Airplane Cost	\$315.07
Flight Test Operation Cost	\$0.413
Cost to Finance the Flight Test Airplanes	\$45.2
<b>Total</b>	<b>\$452.42</b>

\* All Costs in 2014 dollars

The expenses contributing to the total acquisition cost include:

- Manufacturing cost.
  - Airframe engineering and design cost.
  - Airplane production cost: engines and avionics: engine and avionics, manufacturing, materials, tooling and quality control.
  - Production flight test operations cost.
  - Cost of financing the manufacturing program.
- Profit made by the manufacturer.

The manufacturing cost is a function of the variables previously cited. As opposed to the RDTE cost, it also depends on the number of aircrafts produced. The effect of the number of aircrafts produced over the total cost is shown in Figure 13-1. This is known as the learning curve.

Figure 13-1 compares the learning curve for two labour costs: China labour cost, assumed to be \$3.5 per hour [12], and USA labour cost, assumed be \$30 as suggested by Roskam. It is notable the outstanding effect of labour cost on the total cost: the cost is increased around 320% if the UAV's are manufacture in USA. AviCargo assumed Chinese labour cost values in estimation of the aircraft cost and plans to utilise Chinese factories if cost is a concern for the customer.

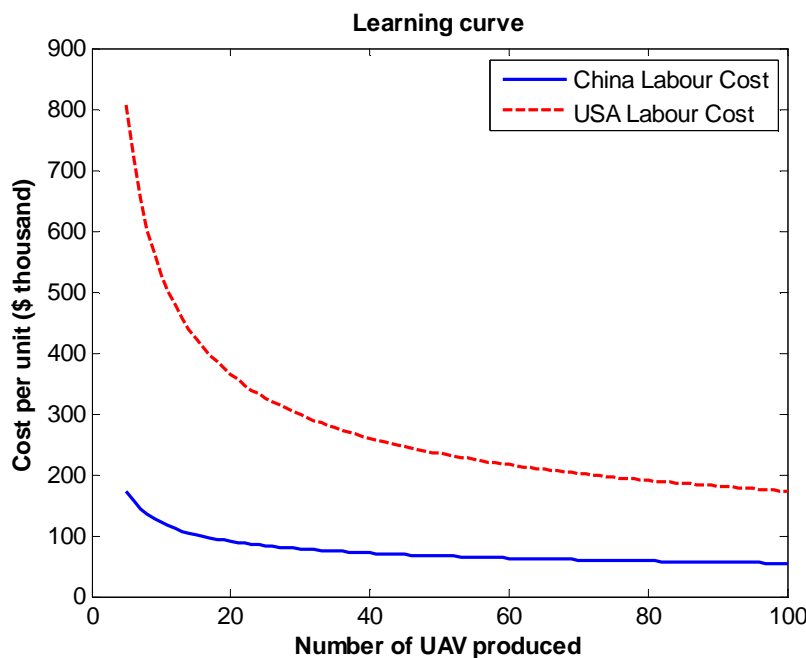


Figure 13-1 Comparison of cost per unit (RDTE + acquisition) produced (USA vs. China)

Figure 13-2 shows the actual learning curve assuming Chinese labour cost. The significant result is that at least 20 airplanes should be produced for final cost to be worthwhile for the customer. Doubling the number of airplanes from 20 to 40, the manufacturing cost is reduced by 22%. This is the expected amount that AviCargo team plans to manufacture and sell.

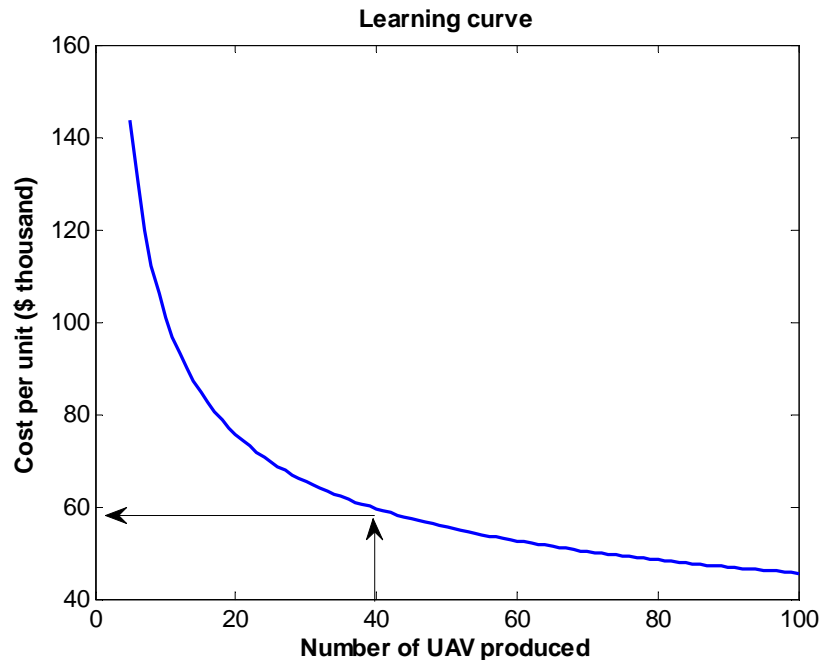


Figure 13-2 Cost per unit (RDTE + acquisition) over aircraft quantity produced China Labour Cost

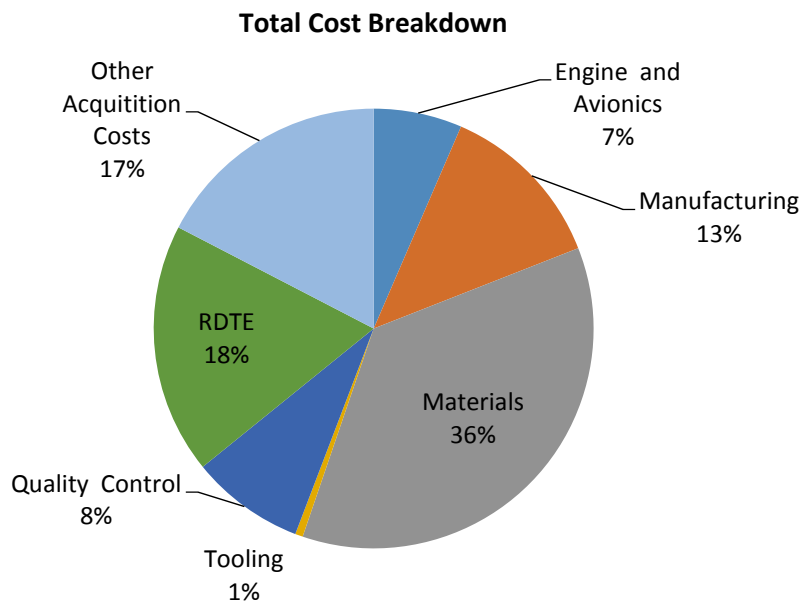
Through two years of manufacturing, 40 ADV's will be produced, 15 for service in Mount Kenya and 25 for distribution for other purposes. The breakdown acquisition cost for the whole production run is presented in Table 13-3. The highest contribution to the total acquisition cost comes from the production cost.

Table 13-3 Breakdown for acquisition cost

CATEGORY	COST (thousand)
Airframe Engineering and Design Cost	\$35.09
Airplane Production Cost	\$1,586.7
Production Flight Test Operations Cost	\$164.8
Financing Cost	\$183.12
Manufacturer Profit	\$183.12
<b>Total</b>	<b>\$2,014.3</b>

\* All Costs in 2014 dollars

Finally, a summary of the contribution of all the components in the production cost together with the rest of cost components is shown in Figure 13-3. It is notable that the highest contribution comes from the materials cost. Because of its penalty on the final cost, lighter advanced materials, such as composites, that would reduce the GTOW have been utilised to a minimal.



*Figure 13-3 Contribution of elements to total airplane cost*

The final sale price of each of the 40 UAV produced during the two years production program is **\$86,335** including a 40% profit for the company.

## 13.2 Operational and Maintenance Cost and Life Cycle Cost

The operational and maintenance costs include:

- Fuel and oil cost.
- Insurance cost.
- Maintenance cost.
- Depreciation cost.
- Ground station and navigation cost.

The operational and maintenance cost is proportional to the operational lifetime of the aircraft. A 30 years lifetime has been assumed for the calculations. Another factor influencing this cost is the annual distance travelled, or number of flights. Its relation is linear with all the costs except depreciation. The behaviour of the operational and maintenance cost with the number of flights per year is presented in Figure 13-4. It can be observed that the depreciation cost becomes stable after around two hundred flights per year. Therefore, the customer may be aware that the results presented here in after are valid for this minimum number of operations per year. Over 100 number of operations the operational and maintenance cost will be around the values that are presented.

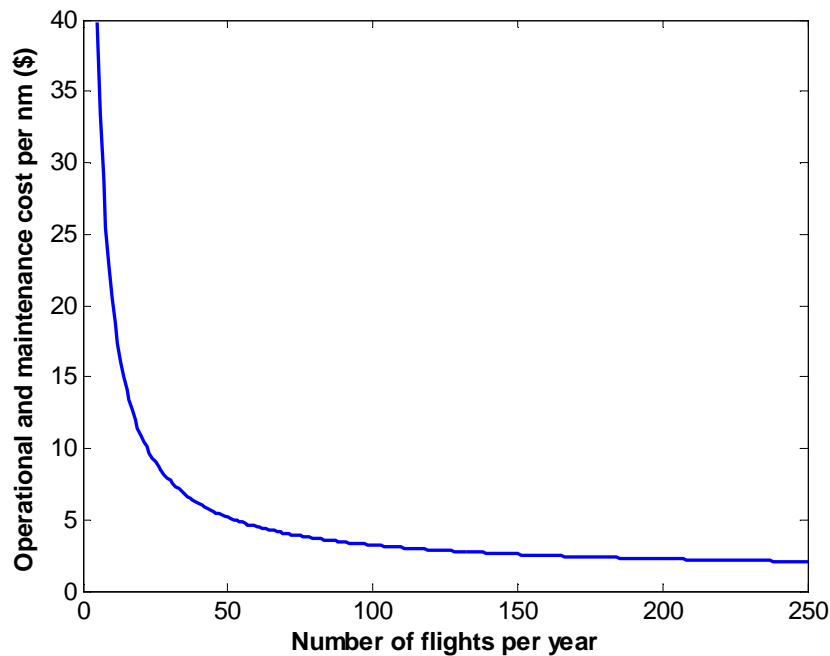


Figure 13-4 Variation of operational and maintenance cost with number of flights

The operational and maintenance cost breakdown component over the entire lifetime of each aircraft is outlined in Table 13-4.

*Table 13-4 Breakdown for operational and maintenance cost*

CATEGORY	COST (thousand)
Engine and Oil Cost	\$71.43
Insurance Cost	\$131.69
Maintenance Cost	\$329.97
Depreciation Cost	\$214.08
Ground Station and Navigation Cost	\$75.95
<b>Total</b>	<b>\$658.43</b>

\* All Costs in 2014 dollars

To determine the cost to actually operate the UAV, the operational and maintenance cost per flight was calculated. It was found to be approximately **\$73.1 per flight**.

The total Life Cycle Cost (LCC) of the UAV is composed of:

- Price of the UAV.
  - RDTE cost.
  - Acquisition cost.
  - Profit
- Operational and maintenance cost.
- Disposal cost.

The price of the UAV, operational and maintenance cost and the disposal cost are summed up together to make up the total LCC. The disposal cost was assumed to be 1% of the total LCC.

The total Life Cycle Cost of an ADV is roughly **\$752,288**.

## 14 Conclusion

The ADV that has been developed represents a unique aircraft class which is just emerging. The large payload capabilities and relatively quick turn around times to successfully complete a mission specified by the RFP indicates the potential for applications to which the ADV may be suited. The design of the ADV is a combined iterative process in which this report has covered.

Section 2 of this design report explored the RFP set by the Flying Donkey Challenge and covered the design goals and targets in which the ADV was to be designed for. A review of design was conducted in the third section of this design report, comparing the ADV to existing STOL aircraft. This section provided insight to the unique capabilities of the ADV, highlighting it as a different class in aircraft type, with design characteristics both seeking inspiration from STOL aircraft and recon UAVs.

Section 4 outlined the mission analysis, with plans on the flight path to successfully complete the Flying Donkey Challenge. An analysis into the mission types revealed the operational conditions to which the ADV was subject, reinforcing the need for certain design aspects such as reliability in design and robustness due to the conditions that the ADV will face. Section 5 explored the ADV as a final product and an assessment into its core design features revealed the design philosophy behind decisions that were made by AviCargo.

A summation of performance characteristics were detailed in Section 6, reinforcing the capability of the ADV to succeed the takeoff run condition of 50 metres as well as a minimum radius turn of 100 metres. Both criteria for performance were met by the ADV, with the take-off obstacle cleared approximately 35 metres into the phase of flight. Turn radius of 100 metres was confirmed during the cruise phase of flight through a minimum throttle input.

Section 7 further detailed the aerodynamic performance of the ADV and looked at 3-D drag characteristics and performance at crucial phases of flight. An exploration into high lift devices that were used on the ADV is also included. Furthermore, moving into section 8, propulsion system optimisation was seen as a crucial aspect, affecting the performance of the ADV. The reasoning for this was due to the high altitude operational conditions to which the propulsion system was subject towards resulting in deterioration in engine performance. Optimisation of the propulsion system was carried out in this section to tune the ADV in order to successfully meet RFP requirements.

Section 9 explored the structural sizing of the tail boom and wing of the ADV and introduced the structural concept between the payload bay design. A detailed exploration into undercarriage design was also carried out, with the optimisation of components to ensure the gross take-off limits are complied to during the design process. A summary of the component build up was also included in section 10, with a brief introduction into the centre of gravity travel, in which was confirmed to be stable (Static margin of 7% to 18%) in section 11 which looked into the static and dynamic stability of the ADV. Section 11 also explored the control authority of control surfaces to confirm the ADV's ability to operate successfully during flight, ensuring all performance criteria are met.

Finally section 12 detailed the avionics architecture of the system and section 13 looked into the cost of production and distribution. For the design of the ADV, development and manufacturing has resulted in a cost price per aircraft of \$86,400 if production was to be headed in China for development of 40 units over two years. Manufacturing of the ADV in-house within Australia or the USA would result in a higher price and would be left as an option for the consumers who decide to commission the aircraft. China was chosen as the manufacturing base for the ADV due to the Flying Donkey's ambition to develop the cargo delivery system around Mount Kenya to a larger scale operation if deemed successful, thus reducing the manufacturing cost in combination with AviCargo's design attempts to simplify the ADV for operation and maintenance would fast track the goals of the challenge.

## A Appendix – Aerodynamics

### a) Validation of XFLR5

For XFLR5 validation the airfoil data base from Nicolai was used [1]. The aerofoil chosen for validation is the NACA 23012 and it is simulated at  $9 \times 10^6$  Reynolds number. The reported values by Nicholai are  $CL_{max} = 1.8$  and  $\alpha_{CL=0} = -1.4^\circ$ . The following figure A-1 shows the XFLR5 simulation results.

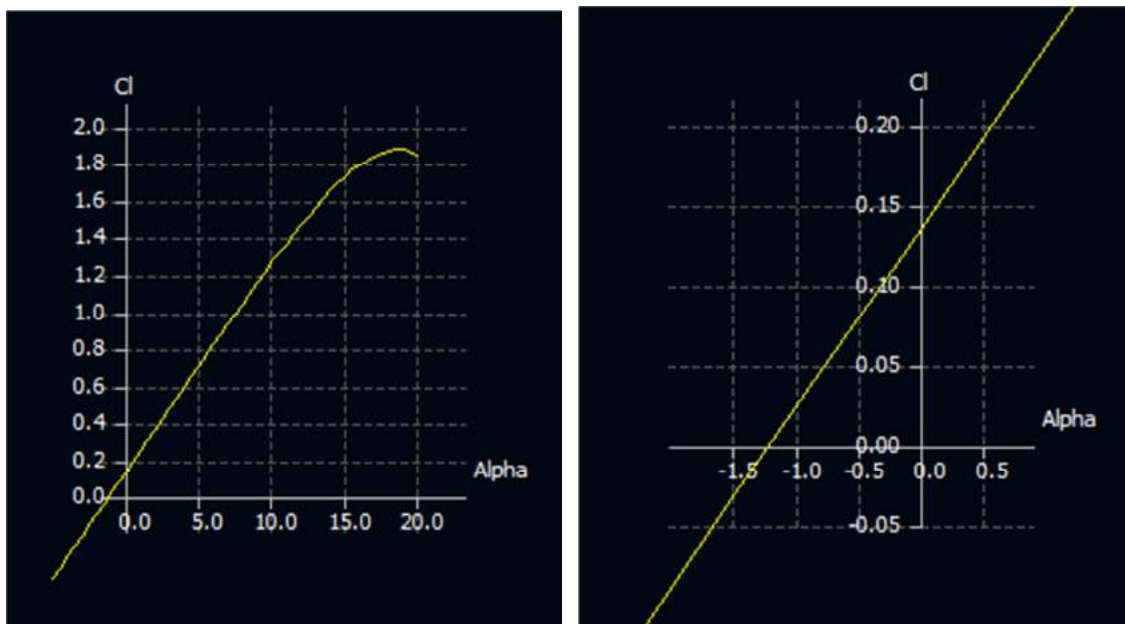
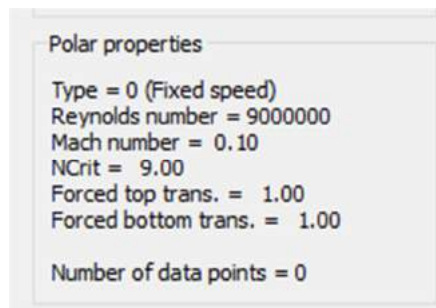


Figure A-1 Lift Coefficient vs. angle of attack XFLR5



## B Appendix – Propulsion

### b) Evolution of Engine Selection

Due to the heavy weight of the previous selected engine, a lighter engine needs to be used. The selected engine needs also to be more powerful when considering the effect of altitude elevation on engine power. As engine specifications are given at standard sea level, altitude elevation at mission location will possibly degrade engine performance. In fact as Altitude increase while air density decreases, engine power output will consequently decrease as well. Such relationship is governed by the formula:

$$BHP_h = \frac{BHP_0 \left[ \frac{\rho}{\rho_0} - \left( 1 - \frac{\rho}{\rho_0} \right) \right]}{7.55} \quad (2)$$

As a result, as air density decrease at the critical mission location of 2500m above sea level, engine power decrease by 75.27%. Accounting for such factor, power required for take-off determined previously now becomes:

$$BHP_{2500m} = \frac{13.3}{0.7527} = 17.6697 \text{ BHP} = 13.2 \text{ kW}$$

Taken such effect into consideration, each selected engine should produce more than 6.5hp of power to satisfy the take-off requirement. Hence 6 UAV engines have been selected and guided by the core requirement of engine selection, relevant specifications are summarised in Table 12.

*Table B-1 Potential Engine Choices*

Name	Power (kW)	Weight (kg)	P/W (kg/kW)	Fuel Con. (g/min)	Size ( $m^3$ )	Cost (USD)
3W-157iXB2 [13]	8.5	6.0	1.4	110	$3.04 \times 10^{-3}$	\$1822
3W-170iXB2 [14]	9.0	6.0	1.5	128	$3.41 \times 10^{-3}$	\$2022
Gobler – Hirth F41 [15]	8.9	2.6	3.4	120	$2.58 \times 10^{-2}$	\$1300
Quadra Aerrow Q1000b [16]	7.0	2.7	2.6	118	$4.38 \times 10^{-3}$	\$1350
<i>Desert Aircraft DA100L</i> [17]	7.3	2.5	2.9	71	$4.32 \times 10^{-3}$	\$999
Desert Aircraft DA-120 [18]	8.9	2.3	3.98	113	$4.52 \times 10^{-3}$	\$1199

As highlighted, the DA-100L has high power to weight ratio with lower lowest cost and comparatively smaller size, hence has been selected for the propulsion system.

### c) Operational Engine Conditions at different altitudes

As determined by the mission profile, there are 9 critical operational altitudes in which the engine performance has to account for. Results of engine condition across the flight speed spectrum from start to cruise speed have been determined by throttle position. Related engine condition in terms of RPM range, Power range, Torque range and fuel consumption are summarised and presented in table A-2 to A-9.

*Table B-2 2150 meters Elevation: Engine Condition in Operation by Throttle Position*

<b>Throttle Position (%)</b>	<b>RPM Range</b>	<b>Power (kW)</b>	<b>Torque (Nm)</b>	<b>Fuel Con. (kg/Hr)</b>
60 (Idle)	2500 - 4400	0.26 – 0.28	0.61 - 0.98	0.45
70	3000 - 4700	0.58 – 0.63	1.32 – 1.82	0.66
80	3600 - 5100	1.01 – 1.22	2.28 – 2.64	1.05
90	3900 - 5500	1.31 – 1.95	3.15 – 3.38	1.49 – 1.76
92	4400 - 6000	1.85 – 3.04	3.96 – 4.83	1.43 – 2.90
94	4800 - 6300	2.34 – 4.00	4.66 – 6.07	1.38 – 3.31
96	5700 - 6400	4.11 – 4.48	6.45 – 6.98	2.46 – 3.23
98	6200 - 6500	4.71 – 5.24	6.91 – 8.08	3.12 – 2.99
100	6300 - 6700	5.73 – 5.72	8.00 – 8.61	2.60 – 1.70

*Table B-3 2085 meters Elevation: Engine Condition in Operation by Throttle Position*

<b>Throttle Position (%)</b>	<b>RPM Range</b>	<b>Power (kW)</b>	<b>Torque (Nm)</b>	<b>Fuel Con. (kg/Hr)</b>
60 (Idle)	2500 - 4400	0.26 – 0.28	0.62 – 0.99	0.45
70	3000 - 4700	0.59 – 0.65	1.32 – 1.83	0.66
80	3600 - 5100	1.03 – 1.25	2.29 – 2.67	1.05
90	3900 - 5500	1.32 – 1.96	3.17 – 3.42	1.49 – 1.76
92	4400 - 6000	1.87 – 3.06	3.99 – 4.87	1.43 – 2.90
94	4800 - 6300	2.36 – 4.04	4.70 – 6.16	1.38 – 3.31
96	5700 - 6300	4.17 – 4.51	6.51 – 7.05	2.46 – 3.23
98	6200 - 6500	4.73 – 5.28	6.94 – 8.13	3.12 – 2.99
100	6400 - 6700	5.70 – 5.78	8.06 – 8.67	2.60 – 1.70

*Table B-4 2003 meters Elevation: Engine Condition in Operation by Throttle Position*

<b>Throttle Position (%)</b>	<b>RPM Range</b>	<b>Power (kW)</b>	<b>Torque (Nm)</b>	<b>Fuel Con. (kg/Hr)</b>
60 (Idle)	2500 - 4400	0.26 – 0.28	0.63 – 1.00	0.45
70	3000 - 4700	0.61 – 0.68	1.34 – 1.84	0.66
80	3600 - 5100	1.03 – 1.26	2.33 – 2.69	1.05
90	4000 - 5500	1.33 – 1.98	3.19 – 3.46	1.49 – 1.76
92	4500 - 6000	1.89 – 3.09	4.04 – 4.93	1.43 – 2.90
94	4800 - 6400	2.39 – 4.08	4.75 – 6.23	1.38 – 3.31
96	5800 - 6500	4.21 – 4.55	6.55 – 7.12	2.46 – 3.23
98	6200 - 6500	4.78 – 5.33	6.99 – 8.18	3.12 – 2.99
100	6400 - 6800	5.75 – 5.83	8.14 – 8.75	2.60 – 1.70

*Table B-5 1981 meters Elevation: Engine Condition in Operation by Throttle Position*

<b>Throttle Position (%)</b>	<b>RPM Range</b>	<b>Power (kW)</b>	<b>Torque (Nm)</b>	<b>Fuel Con. (kg/Hr)</b>
60 (Idle)	2500 - 4400	0.26 – 0.28	0.64 – 1.01	0.45
70	3000 - 4700	0.59 – 0.65	1.36 – 1.86	0.66
80	3600 - 5100	1.03 – 1.25	2.34 – 2.70	1.05
90	4000 - 5500	1.33 – 1.99	3.21 – 3.47	1.49 – 1.76
92	4500 - 6000	1.89 – 3.10	4.05 – 4.94	1.43 – 2.90
94	4800 - 6400	2.40 – 4.09	4.76 – 6.24	1.38 – 3.31
96	5800 - 6500	4.23 – 4.56	6.56 – 7.13	2.46 – 3.23
98	6200 - 6500	4.79 – 5.34	7.02 – 8.23	3.12 – 2.99
100	6400 - 6800	5.77 – 5.84	8.15 – 8.77	2.60 – 1.70

*Table B-6 1970 meters Elevation: Engine Condition in Operation by Throttle Position*

<b>Throttle Position (%)</b>	<b>RPM Range</b>	<b>Power (kW)</b>	<b>Torque (Nm)</b>	<b>Fuel Con. (kg/Hr)</b>
60 (Idle)	2500 - 4400	0.26 – 0.28	0.62 – 1.00	0.45
70	3000 - 4700	0.59 – 0.65	1.33 – 1.86	0.66
80	3600 - 5100	1.03 – 1.25	2.34 – 2.71	1.05
90	4000 - 5500	1.34 – 2.00	3.21 – 3.49	1.49 – 1.76
92	4500 - 6000	1.90 – 3.11	4.07 – 4.95	1.43 – 2.90
94	4800 - 6400	2.41 – 4.10	4.77 – 6.25	1.38 – 3.31
96	5800 - 6500	4.24 – 4.57	6.58 – 7.15	2.46 – 3.23
98	6200 - 6500	4.80 – 5.35	7.01 – 8.24	3.12 – 2.99
100	6500 - 6800	5.78 – 5.86	8.16 – 8.79	2.60 – 1.70

*Table B-7 1831 meters Elevation: Engine Condition in Operation by Throttle Position*

<b>Throttle Position (%)</b>	<b>RPM Range</b>	<b>Power (kW)</b>	<b>Torque (Nm)</b>	<b>Fuel Con. (kg/Hr)</b>
60 (Idle)	2500 - 4400	0.28 – 0.29	0.64 – 1.02	0.45
70	3000 - 4700	0.60 – 0.66	1.35 - 1.88	0.66
80	3600 - 5100	1.05 – 1.26	2.38 – 2.73	1.05
90	4000 - 5500	1.36 – 2.03	3.26 - 3.52	1.49 – 1.76
92	4500 - 6000	1.93 – 3.16	4.12 - 5.02	1.43 – 2.90
94	4800 - 6400	2.45 – 4.16	4.85 - 6.34	1.38 – 3.31
96	5800 - 6500	4.32 – 4.64	6.67 - 7.26	2.46 – 3.23
98	6200 - 6500	4.86 – 5.43	7.10 – 8.36	3.12 – 2.99
100	6500 - 6800	5.87 – 5.95	8.27 – 8.92	2.60 – 1.70

*Table B-8 1770 meters Elevation: Engine Condition in Operation by Throttle Position*

<b>Throttle Position (%)</b>	<b>RPM Range</b>	<b>Power (kW)</b>	<b>Torque (Nm)</b>	<b>Fuel Con. (kg/Hr)</b>
60 (Idle)	2500 - 4400	0.28 - 0.29	0.62 – 1.03	0.45
70	3000 - 4700	0.6 - 0.66	1.35 – 1.89	0.66
80	3600 - 5100	1.06 - 1.28	2.38 – 2.77	1.05
90	4000 - 5500	1.37 - 2.04	3.27 - 3.54	1.49 – 1.76
92	4500 - 6000	1.94 - 3.18	4.15 - 5.05	1.43 – 2.90
94	4800 - 6400	2.47 - 4.19	4.89 - 6.39	1.38 – 3.31
96	5800 – 6500	4.36 - 4.67	6.71 - 7.30	2.46 – 3.23
98	6200 - 6500	4.89 – 5.47	7.16 – 8.41	3.12 – 2.99
100	6500 - 6800	5.91 – 5.99	8.33 – 8.98	2.60 – 1.70

*Table B-9 1621 meters Elevation: Engine Condition in Operation by Throttle Position*

<b>Throttle Position (%)</b>	<b>RPM Range</b>	<b>Power (kW)</b>	<b>Torque (Nm)</b>	<b>Fuel Con. (kg/Hr)</b>
60 (Idle)	2500 - 4400	0.28 - 0.29	0.65 – 1.05	0.45
70	3000 - 4700	0.61 - 0.68	1.42 – 1.95	0.66
80	3600 - 5100	1.08 - 1.33	2.51 – 2.76	1.05
90	4000 - 5500	1.39 - 2.08	2.44 – 2.81	1.49 – 1.76
92	4500 - 6000	1.98 - 3.24	4.22 - 5.13	1.43 – 2.90
94	4800 - 6400	2.53 - 4.27	4.96 - 6.51	1.38 – 3.31
96	5800 – 6500	4.45 - 4.76	7.33 - 7.44	2.46 – 3.23
98	6200 - 6500	4.96 – 5.56	7.25 – 8.54	3.12 – 2.99
100	6500 - 6800	6.00 – 6.10	8.47 – 9.13	2.60 – 1.70

#### d) Estimation of Propeller Diameter and Pitch

Initially, as recommended by engine manufacture, a propeller of brand XOAR and size of 27x10 has been selected for the propulsion system. However to satisfy the take-off requirement of the mission, propeller needs to be designed and optimised at the take-off speed. Hence, for a Two-bladed propeller initial estimation of propeller diameter and pitch are determined by:

$$D = 1000 \sqrt[4]{\frac{P_{HP}}{53.5 \times RPM^2 \times V_{KTAS}}} = 33 \text{ inch} [2]$$

$$P_D = 1251 \left( \frac{V_{KTAS}}{RPM} \right) \left( \frac{1}{\eta_p} \right) = 9 \text{ inch} [2]$$

D: Propeller Diameter (inch)

$P_D$ : Propeller Pitch (inch)

$V_{KTAS}$ : True airspeed at Lift-off (Knots)

RPM: Engine RPM at maximum engine power

$P_{BHP}$ : Maximum engine power (HP)

$\eta_p$ : Propeller efficiency [19]

As result suggests, the required size of propeller to satisfy the take-off speed of 15m/s has been estimated to be 33x10. Assuming the same aerofoil characteristics to the XOAR 27x10 Sport Prop Type A, which the aerofoil has been measured and summarised in Table 13.

Table B-10 Measurement of 27x10 Sport Prop Type A

27x10 XOAR Propeller		
r/R	c/R	beta
0.1	0.1202	32.5418
0.2	0.1161	28.5039
0.3	0.1137	26.8849
0.4	0.1283	18.2305
0.5	0.1420	15.4122
0.6	0.1379	12.5978
0.7	0.1382	9.0658
0.8	0.1274	6.2934
0.9	0.0849	5.7099
1.0	0.0475	6.3271

Simulated by Xrotor, performance of both propellers at fixed RPM in terms of thrust has been compared along with the actual drag profile of the aircraft and presented in Figure A-1.

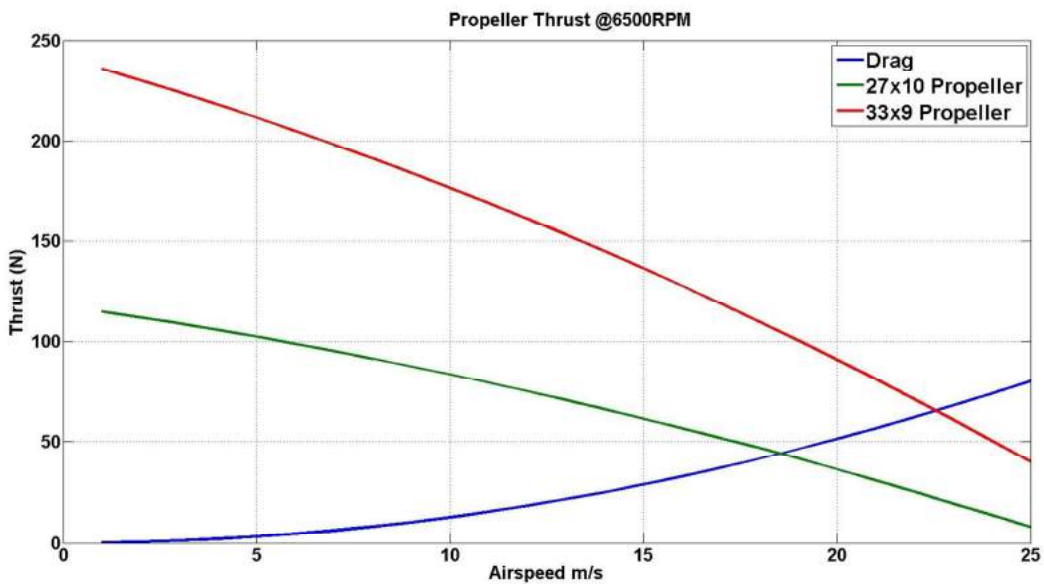


Figure B-1 33x9 and 27x10 Ideal Propeller Thrust Comparison

As result suggests, although the 27x10 propeller is able to produce more thrust for lift-off, it does not produce enough thrust for the aircraft to reach the desired cruise condition of 25 m/s. Similar conclusion also applies to the 33x9 propeller, this means either an even larger diameter propeller or a propeller with larger pitch or a propeller with the right combination of diameter and pitch is required. Intuitively, the pitch of the desired should be larger than 9 inch for to satisfy the required thrust for both take-off and cruise. Hence ideal thrust and required torque of propellers with 10 in pitch and variation of diameters have been compared with the drag profile and maximum engine torque at 6500 RPM and presented in Figure A-2:

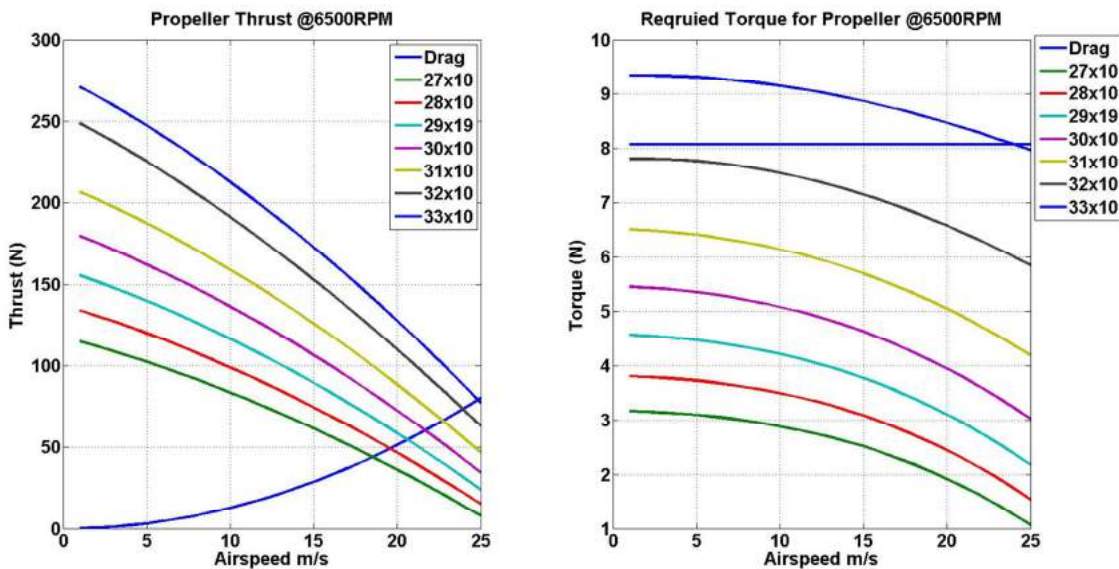


Figure B-2 Ideal Thrust and Required Torque for Propellers with varying geometry

As shown by the figure, maximum engine torque at 6500RPM sets out the boundary for propeller diameter, with the current selected engine, propellers with diameter larger than 32inch cannot be driven by the limited engine torque. Moreover, as increase in diameter increases the thrust produced by propeller and thrust needs to be further increased to overcome drag for the current take-off requirement, range of propeller diameter further reduced to either a 31inch or 32inch diameter with increase in propeller pitch. To determine the propeller performance in actual flight operation, propellers have been simulated with the selected DA-100L engine. Results are summarised and presented in Figure A-3.

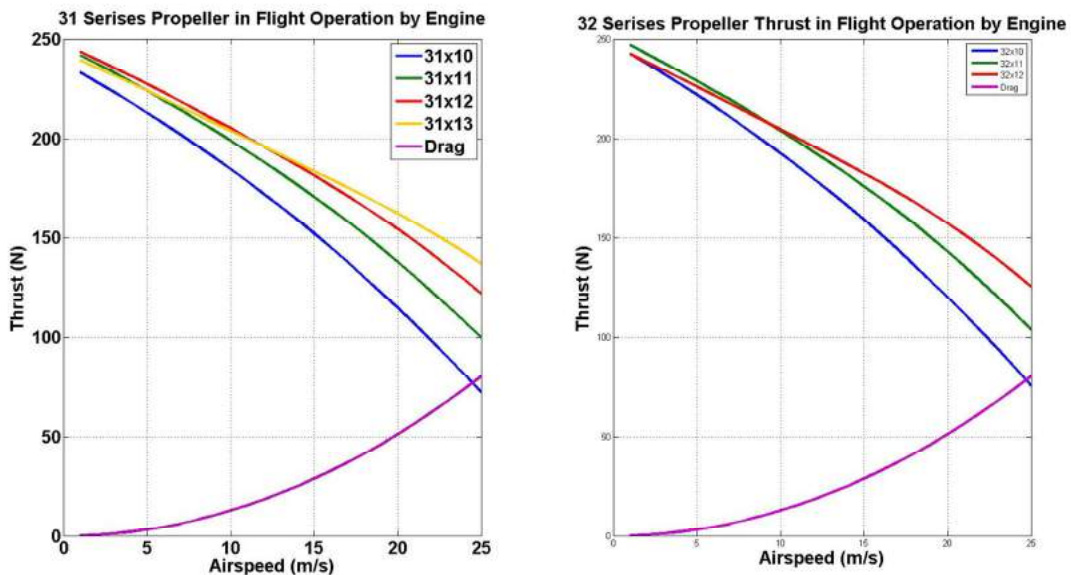


Figure B-3 Comparison of Propeller Thrust in Flight Operation by Engine

As result suggests for the propeller of diameter 31 inch, thrust decreases at from start to 12m/s when propeller pitch increased to 13inch as compared with the 12inch pitch. Similarly, for propeller of diameter 32inch, thrust decreases from start to 10 m/s when propeller pitch increases to 12inch as compare to 11inch propeller pitch. This is due to that the selected engine does not produce the torque required to drive the propeller to its optimum performance in terms of thrust. Due to the interest of propeller design is to optimise the propeller performance for shorter take-off distance, thrust at lower speed range is crucial for the aircraft to accelerate faster and consequently reducing the lift-off distance. Hence both the '31x12' and the '32x11' propeller are the better choice than other propellers of other size. However to decide which of the two propeller best suits the mission, propeller performance has been further investigated, in specific, to explore propeller efficiencies. Results plotted in Figure A-4:

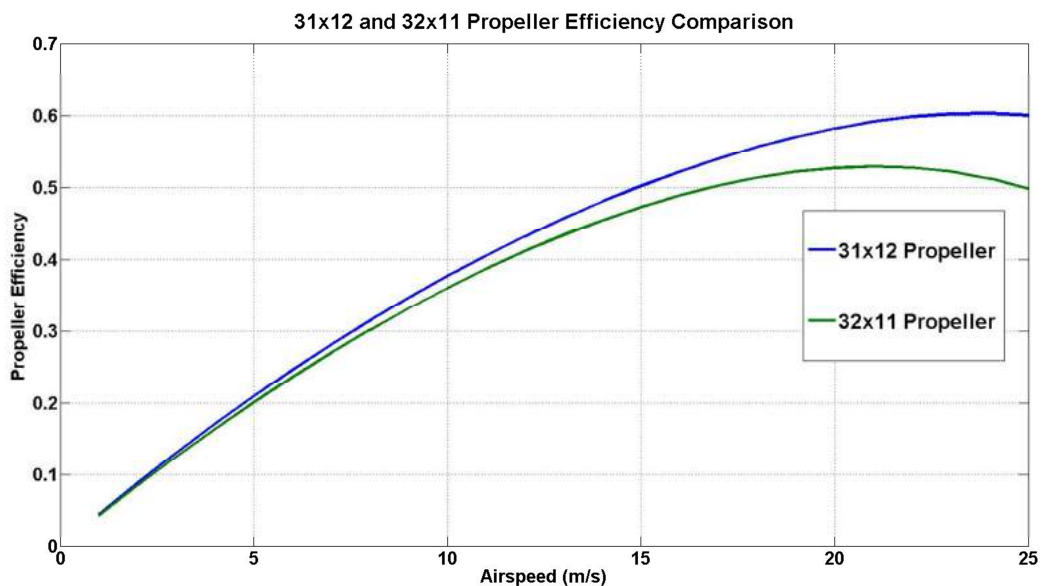


Figure B-4 31x12 and 32x11 Propeller Efficiency Comparison

As figure A-4 shows, the 31x12 propeller has higher efficiency across the flight operation, especially at cruise speed of 25m/s, efficiency of the 31x12 propeller is at 0.6 where the 32x11 propeller is only at 0.5. Hence the with the same XOAR Sport Prop Type A aerofoil characteristics, a 32x12 Propeller is determined to best suit the current mission.

### e) Validation of Xrotor

Xrotor has been used to simulate propeller performance. To validate the credibility of Xrotor, three propeller profiles have been simulated by Xrotor and resulting power coefficient and thrust coefficient across the same advance ratio range are compared with the results by UIUC Propeller Database [20]. Propeller Geometries used for validation are presented in Table A-11.

*Table B-11 Geometry of Master Airscrew Propellers*

Master Aircrew 11x8			Master Aircrew 11x7			Master Aircrew 11x6		
r/R	c/R	Beta	r/R	c/R	Beta	r/R	c/R	Beta
0.15	0.159	35.04	0.15	0.15	34.62	0.15	0.152	32.31
0.2	0.145	41.53	0.2	0.145	39.58	0.2	0.147	35.95
0.25	0.146	41.45	0.25	0.147	38.36	0.25	0.149	34.78
0.3	0.151	37.33	0.3	0.152	32.99	0.3	0.154	30.11
0.35	0.155	32.95	0.35	0.157	28.34	0.35	0.158	25.94
0.4	0.158	29.67	0.4	0.159	25.34	0.4	0.16	23.28
0.45	0.159	26.92	0.45	0.16	22.92	0.45	0.16	21.16
0.5	0.159	24.5	0.5	0.159	20.66	0.5	0.16	19.17
0.55	0.158	22.46	0.55	0.158	18.64	0.55	0.159	17.5
0.6	0.156	20.65	0.6	0.156	16.87	0.6	0.156	16.06
0.65	0.153	19	0.65	0.152	15.32	0.65	0.153	14.73
0.7	0.148	17.5	0.7	0.146	14.01	0.7	0.148	13.49
0.75	0.143	16.29	0.75	0.14	12.93	0.75	0.142	12.51
0.8	0.136	15.19	0.8	0.133	11.97	0.8	0.135	11.53
0.85	0.128	14.03	0.85	0.124	10.96	0.85	0.127	10.51
0.9	0.119	12.94	0.9	0.115	9.99	0.9	0.117	9.47
0.95	0.104	11.33	0.95	0.102	8.93	0.95	0.104	8.58
1	0.09	9.7	1	0.089	7.86	1	0.091	7.7

Geometry of the above propellers are input into Xrotor and simulated at the same RPM and speed range as to the simulation condition of UIUC. Resulting comparison of power coefficient and thrust coefficient are presented in figure A-5.

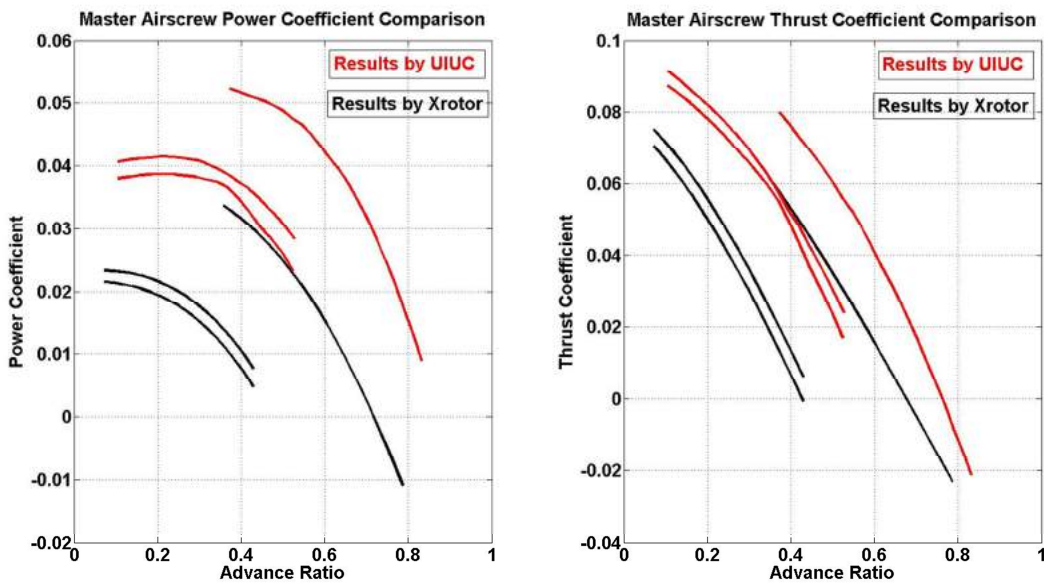


*Figure B-5 X-Rotor Validation of Airscrew Propellers*

As results suggest, power coefficient and thrust coefficient of the simulated propeller by Xrotor program appears to be less than results from the UIUC Propeller Data base. For better accuracy in analysis, correction factor needs to be applied on the power and thrust simulation. Taking into account the discrepancies of all simulated propellers, it has been determined that power coefficient by results from the UIUC propeller database is around 70% higher than the power coefficient obtained by Xrotor, and for thrust coefficient, such discrepancy is estimated to be around 20%. Hence for all propellers simulated by Xrotor, such correction factors have been applied.

## C Appendix – Flight Mechanics

### a) Initial Sizing

Initially, the control surface sizing starts with design volume rate base on reference [2] [4]. So, the initial values are:

*Table C-1 Horizontal and Vertical Tail Sizing*

Component \ Ratio	Aspect Ratio (AR)	Volume Rate (V)
Horizontal Tail	3	0.8
Vertical Tail	2	0.08

*Table C-2 Control Surface Sizing*

Horizontal Tail	Span (b)	Chord (c)
Elevator	90%	40%
Vertical Tail	Span (b)	Chord (c)
Rudder	50%	50%
Wing	Span (b)	Chord (c)
Aileron	25%	30%
Flaps	65%	30%

Table B.1-B.2 summarises the initial input values of the tail and control surface. The horizontal tail sizing can be done by using the ‘Scissor’ technique to prove that it provides sufficient longitudinal control authority, the method is shown in the equations below:

$$\frac{S_h}{S_w} = \frac{C_{L\alpha}(\bar{X}_{cg} - \bar{X}_{acw}) + C_{m\alpha fus}}{\eta C_{L\alpha h} \frac{\delta_{ah}}{\delta_a} (\bar{X}_{ach} - \bar{X}_{cg})}$$

And the final horizontal tail can be sized according to the most forward and afterward are traveling within the limit bounded by restrictions in scissor plot. Also, both stick fix and stick free static margin can be determined by Equation B.2-3 and imposed into the scissor plot.

$$N_0 \text{ Fix} = \frac{x_{ac}}{c} + \eta_t \frac{C_{L\alpha \text{ tall}}}{C_{L\alpha \text{ total}}} \bar{V} \left(1 - \frac{d\epsilon}{d\alpha}\right)$$

$$N_0 \text{ Free} = N_0 \text{ Fix} - \eta_t \frac{C_{L\alpha \text{ tall}}}{C_{L\alpha \text{ total}}} \bar{V} \tau \left(1 - \frac{d\epsilon}{d\alpha}\right)$$

## b) Vertical Tail Sizing

Due to the fact that ADV is a twin-engine configuration, there is no universal solution for vertical tail sizing if the ADV is flying with one engine inoperative. Therefore, the following procedure is taken to size the vertical tail along with rudder:

1. Run the AVL simulation with assumed tail size values and obtain the lateral derivatives.
2. Apply the lateral equilibrium equations:

$$\begin{bmatrix} C_L & 0 & C_{y\delta_r} \\ 0 & C_{l\delta_a} & C_{l\delta_r} \\ 0 & C_{n\delta_a} & C_{n\delta_r} \end{bmatrix} \begin{bmatrix} \phi \\ \delta_a \\ \delta_r \end{bmatrix} = \begin{bmatrix} -C_{y\beta} \cdot \beta \\ -C_{l\beta} \cdot \beta \\ -C_{n\beta} \cdot \beta - C_{n_0} \end{bmatrix}$$

Calculate the off-set thrust coefficient  $C_{n_0}$  and sub in all the required derivatives to obtain the rudder and aileron deflection to trim zero sideslip level flight.

3. Check whether the rudder and aileron deflection is within 75% and 25% of maximum deflection, along with checking the derivatives to be spirally stable.
4. Due to the propulsion and aerodynamic restrictions, reduce the operational speed or update drag data for one engine inoperative situation.
5. If the current vertical tail and rudder surface sizing allow the successful lateral trim of the ADV during one engine operation, then fix the design, otherwise return to step 1, select new reasonable value and iterate the process.

## c) Vertical Tail Design

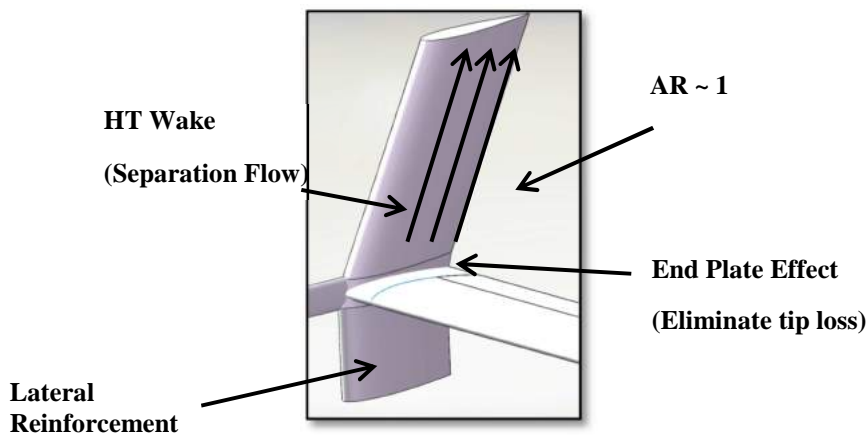


Figure C-1 Vertical Tail Design

Figure B-1 illustrates the vertical tail design of ADV. The main feature is that the vertical tail has been made into two parts, both with sweep angle. The philosophy behind this design feature is during high of attack flight, the horizontal tail may produce separated flow or wake which will be absorbed by the inner side of the vertical tail, thus the vertical tail effectiveness will be sufficiently reduced. Therefore, lateral controllability is ensured by adding a lower section to the tail so that it will not affected by the potential separated flow from the horizontal tail. The sweep is implemented to avoid the wing separation flow zone at high angle of attack [2].

#### **d) State Response – Longitudinal and Lateral Control Input**

The state response of both longitudinal and lateral cases are be simulated by inputting an elevator and rudder deflection of 5 degrees for a short time period followed by a release. This can be achieved by applying the Flight Simulation developed in subject AERO3560 – Flight Mechanics 1, University of Sydney.

The result produced from this simulation represents the natural response of aircraft without any physical compensation. And, those states are:

$$X_{\text{lon}} = [u \ \alpha \ q \ \theta] \quad X_{\text{lat}} = [v \ \beta \ p \ r \ \phi \ \psi]$$

#### **e) Elevator Take-off Control Authority and Trim with Speed Variation**

Elevator control authority at take-off can be examined by letting the dynamic load at nose to be zero, and the equations is:

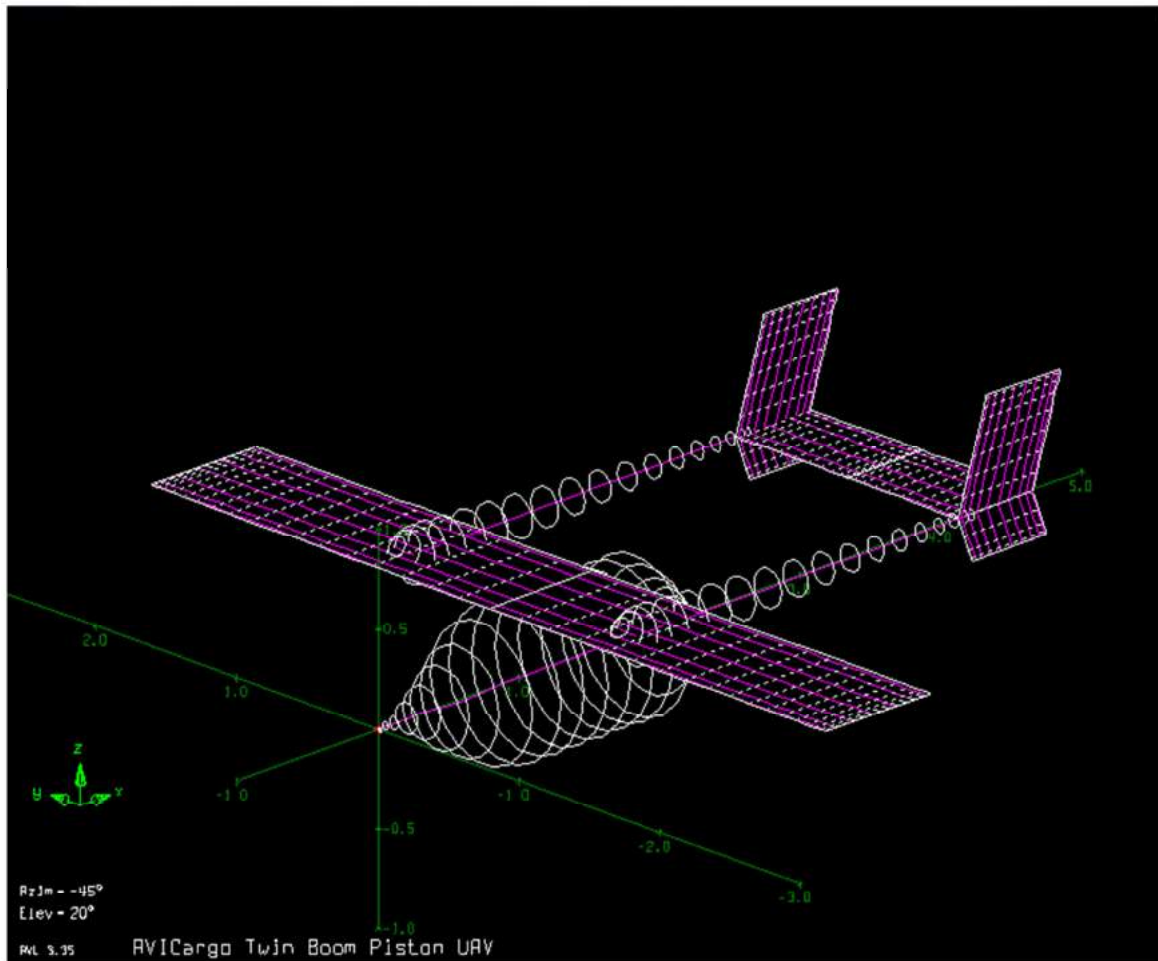
$$R_N = \frac{T \cdot y_t + (W + L_{HT} - L_W) \cdot (x_M - \mu \cdot h_{CG}) + L_W \cdot x_W - L_{HT} \cdot l_{HT} - M_W}{x_N + x_M - 2\mu \cdot h_{CG}}$$

Elevator trim with speed trim can be verified with equation:

$$\delta_e = \frac{-C_{m0} - (\frac{x_{cg}}{c} - N_0 \text{ Fix}) \cdot C_L}{C_{m\delta_e}}$$

## f) AVL Modelling

The ADV has been modelled in AVL software; which requires dimension, run case and mass files to produce the stability derivatives. In addition, it provides lift distribution for both wing and horizontal tail.



## g) Dynamic Mode and Eigen Characteristics (Most Adverse CG)

### Initial Climb

Table C-3 Initial Climb Dynamic Mode and Eigen Characteristics

Eigen value	Damping	Freq. (rad/s)	Mode
-2.50e+000 $\pm$ 2.55e+000i	7.00e-001	3.57e+000	Short Period
-5.46e-002 $\pm$ 6.43e-001i	8.46e-002	6.45e-001	Phugoid
-4.06e-004	1.00e+000	4.06e-004	Conv/Div
-1.11e+001	1.00e+000	1.11e+001	Roll
-8.18e-001 $\pm$ 2.24e+000i	3.44e-001	2.38e+000	Dutch Roll
-3.30e-002	1.00e+000	3.30e-002	Spiral

### Cruise

Table C-4 Cruise Dynamic Mode and Eigen Characteristics

Eigen value	Damping	Freq. (rad/s)	Mode
-3.38e+000 $\pm$ 3.50e+000i	6.94e-001	4.86e+000	Short Period
-8.67e-002 $\pm$ 3.49e-001i	2.41e-001	3.60e-001	Phugoid
-1.27e-003	1.00e+000	1.27e-003	Conv/Div
-1.54e+001	1.00e+000	1.54e+001	Roll
-8.53e-001 $\pm$ 2.82e+000i	2.90e-001	2.38e+000	Dutch Roll
-4.69e-002	1.00e+000	4.69e-002	Spiral

### Approach

Table C-5 Approach Dynamic Mode and Eigen Characteristics

Eigen value	Damping	Freq. (rad/s)	Mode
-2.33e+000 $\pm$ 1.66e+000i	8.14e-001	2.86e+000	Short Period
-6.63e-002 $\pm$ 4.56e-001i	1.44e-001	4.61e-001	Phugoid
-3.03e-004	1.00e+000	3.03e-004	Conv/Div
-1.19e+001	1.00e+000	1.19e+001	Roll
-5.50e-001 $\pm$ 1.80e+000i	2.92e-001	1.88e+00	Dutch Roll
-1.43e-001	1.00e+000	1.43e-001	Spiral

## **h) Validation – Cessna 172**

A full set of flight data of Cessna 172 containing stability and control derivatives is provided by Roskam (2003). These derivatives are used to trim the aircraft for 3 flight conditions and obtain the Eigen values.

*Table C-6 Cessna 172 Longitudinal Static Trim*

<b>Static Trim</b>	Initial Climb	Cruise	Approach
Elevator Trim	-0.81°	2.8°	3.5°
Angle of Attack	5.2°	-1.4°	2.5°

Table D-6 gives the elevator deflection required for longitudinal trim and the resulting angle of attack. The data provided gives angle of attack to be 5.4 degree at initial climb, 0 at cruise and 4 degree at approach. In comparison, the computation of trim produces fairly accurate trim result and lead to the generation of Eigen values.

### **Initial Climb**

*Table C-7 Initial Climb Dynamic Mode and Eigen Characteristics*

<b>Eigen value</b>	<b>Damping</b>	<b>Freq. (rad/s)</b>	<b>Mode</b>
-2.65e+000 + 2.72e+000i	6.98e-001	3.79e+000	Short Period
-2.20e-002 + 2.64e-001i	8.30e-002	2.65e-001	Phugoid
-4.84e-004	1.00e+000	4.84e-004	Conv/Div
-9.03e+000	1.00e+000	9.03e+000	Roll
-7.63e-001 + 2.66e+000i	2.76e-001	2.77e+000	Dutch Roll
4.86e-002	-1.00e+000	4.86e-002	Spiral

### **Cruise**

*Table C-8 Cruise Dynamic Mode and Eigen Characteristics*

<b>Eigen value</b>	<b>Damping</b>	<b>Freq. (rad/s)</b>	<b>Mode</b>
-3.80e+000 + 4.95e+000i	6.09e-001	6.24e+000	Short Period
-2.24e-002 + 1.46e-001i	1.51e-001	1.48e-001	Phugoid
-1.68e-003	1.00e+000	1.68e-003	Conv/Div
-1.54e+001	1.00e+000	1.54e+001	Roll
-7.63e-001 + 3.72e+000i	2.01e-001	3.79e+000	Dutch Roll
-1.83e-002	1.00e+000	1.83e-002	Spiral

## Approach

*Table C-9 Approach Dynamic Mode and Eigen Characteristics*

Eigen value	Damping	Freq. (rad/s)	Mode
-1.82e+000 + 2.30e+000i	6.19e-001	2.94e+000	Short Period
-3.64e-002 + 3.30e-001i	1.09e-001	3.32e-001	Phugoid
-6.02e-004	1.00e+000	6.02e-004	Conv/Div
-7.60e+000	1.00e+000	7.60e+000	Roll
-5.93e-001 + 2.10e+000i	2.72e-001	2.18e+000	Dutch Roll
3.00e-002	-1.00e+000	3.00e-002	Spiral

ADV has very similar Eigen characteristics to Cessna 172, except that Cessna 172 has positive Eigen value of spiral mode at initial climb and approach. So, they are divergent and spirally unstable. The ADV has similar issue if it retracts the flap at initial climb and has no flap at approach. This issue is mostly caused by the design flight conditions are having low speed operation (low stall speed) with flaps extension at initial climb and approach.

## D Appendix – Structural Design of Wing and Booms

### a) V-N Diagram Construction and Load Considerations

Based on calculations from the constraint plot, the following aircraft fundamental parameters are acquired. Also as FAR instructions are in imperial units, information is displayed in this system and the results will be converted to SI units for consistency.

*Table D-1 Major aircraft parameters*

GTOW (lbf)	S (ft <sup>2</sup> )	b (ft)	W/S
130.10	38.02	15.721	3.422

However, no material can satisfy the load condition with load factor 7.28g during the sizing procedure, demanding a lower load factor based on a lower design cruise speed. The speed is chosen to be higher than the cruise stall speed Vs and higher than the designated cruise speed 80ft/s for analysis.

*Table D-2 Load factor under new condition*

Speed (knots)		Load factor	Condition
Vcr	50	4.52	Gust
		-2.52	
VD	70	3.46	Gust
		-1.46	
VA	40	1.44	Manoeuvring
		0.58	

## b) AVL Simulation – Lift Distribution

The lift distributions are obtained from AVL from the analysis of stability and control.

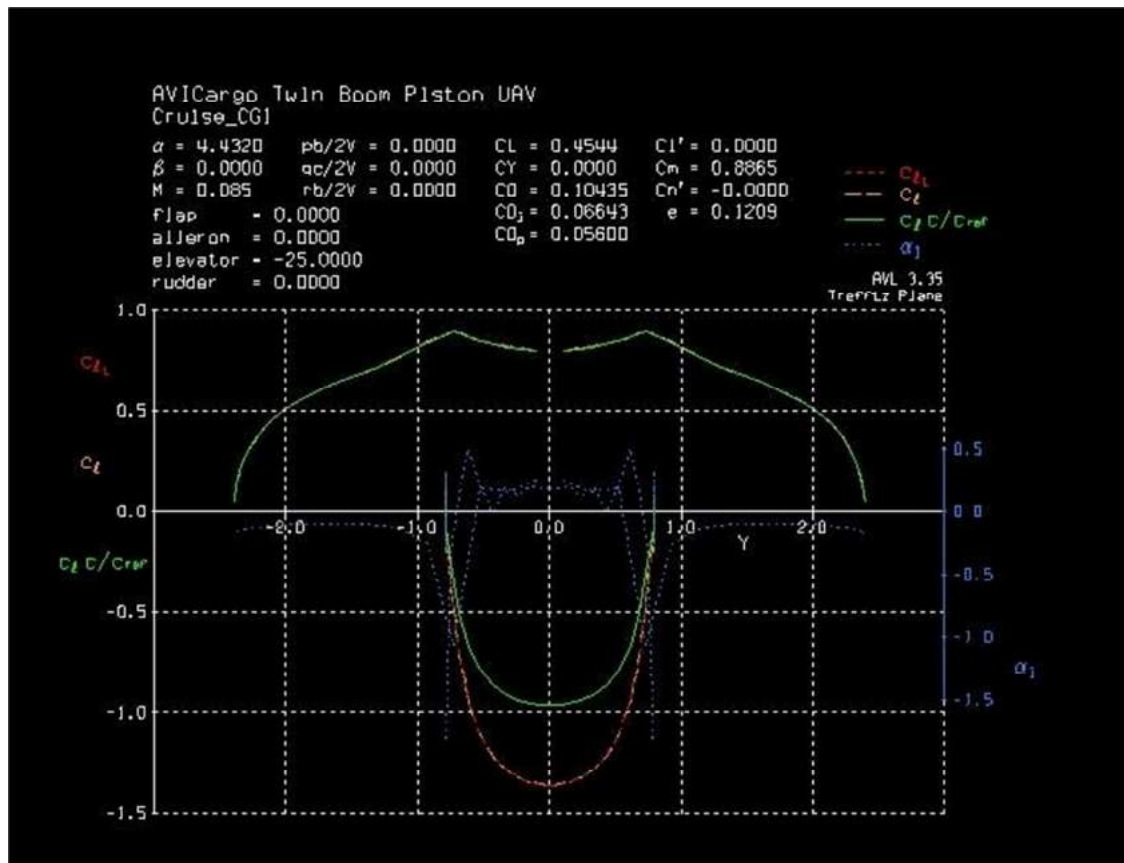


Figure D-1 Cruising maximum negative elevator deflection (elevator up 25 degree)

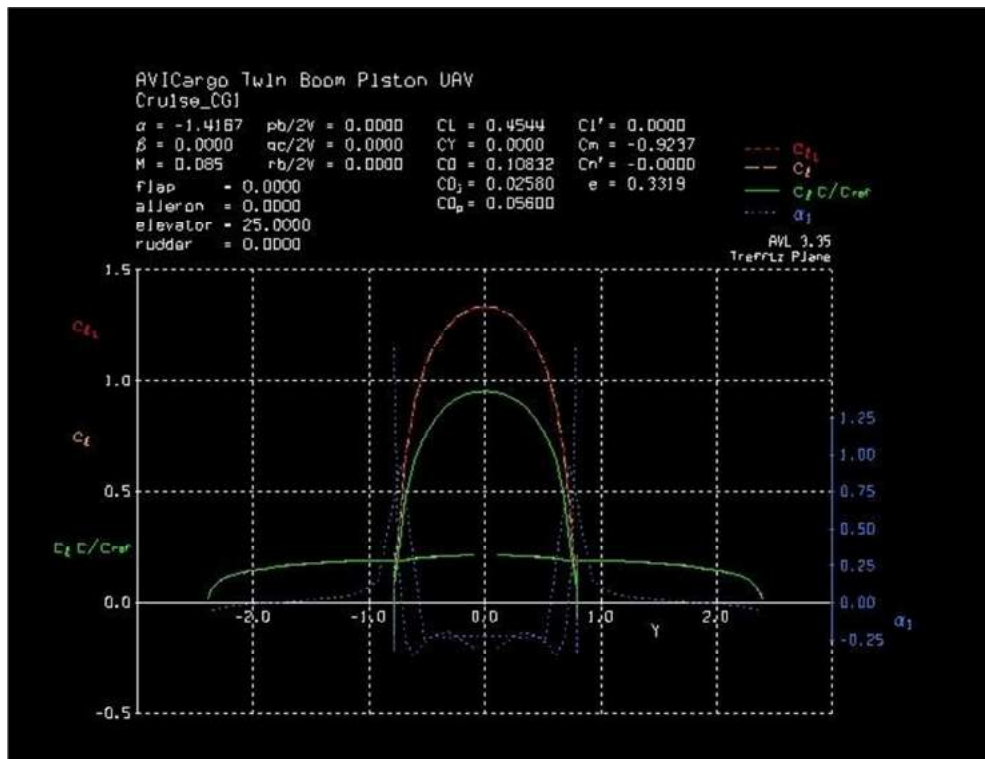


Figure D-2 Cruising maximum positive elevator deflection (elevator down 25 degree)

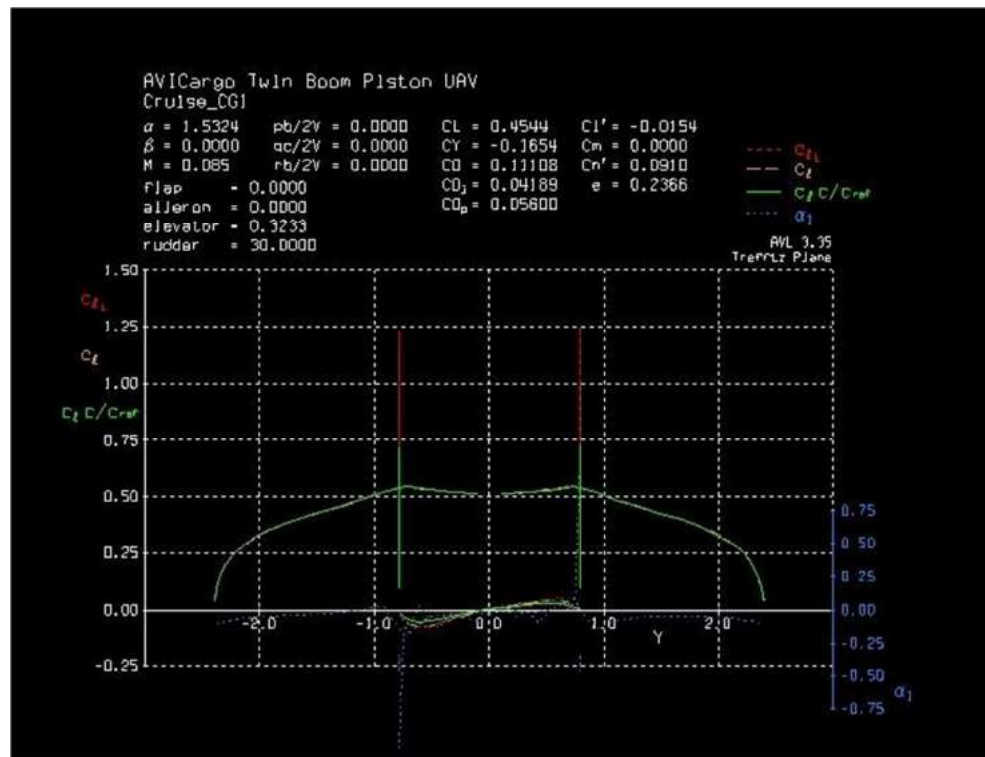


Figure D-3 Cruising maximum positive rudder deflection (30 degree)

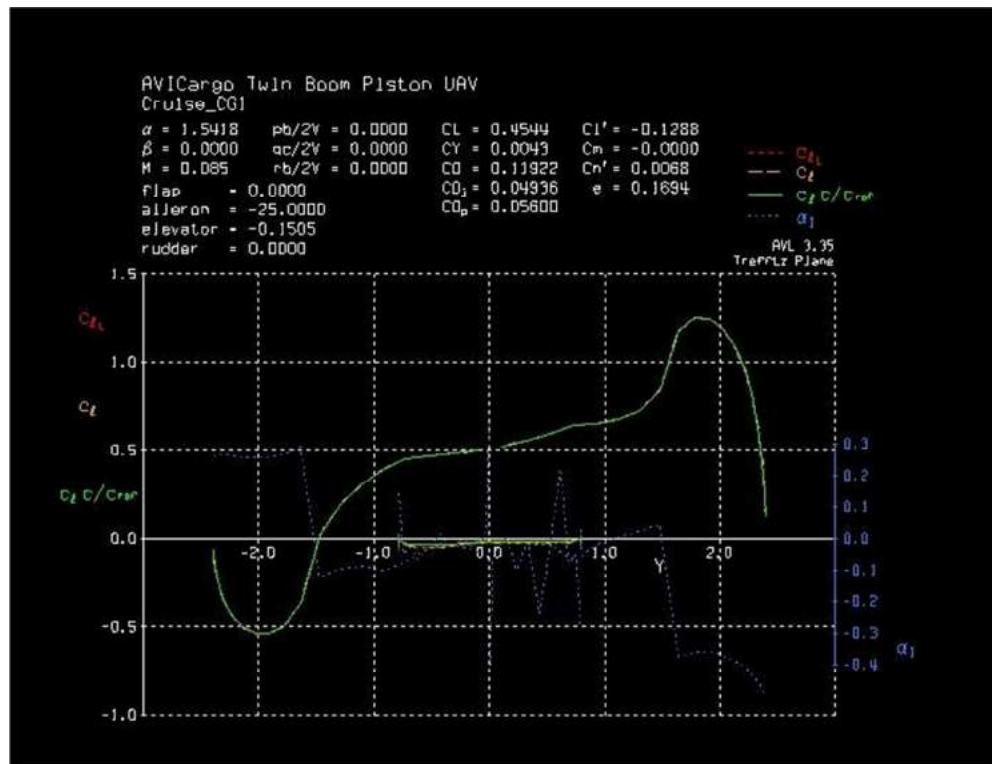


Figure D-4 Cruising right aileron maximum deflection down (-25 degree)

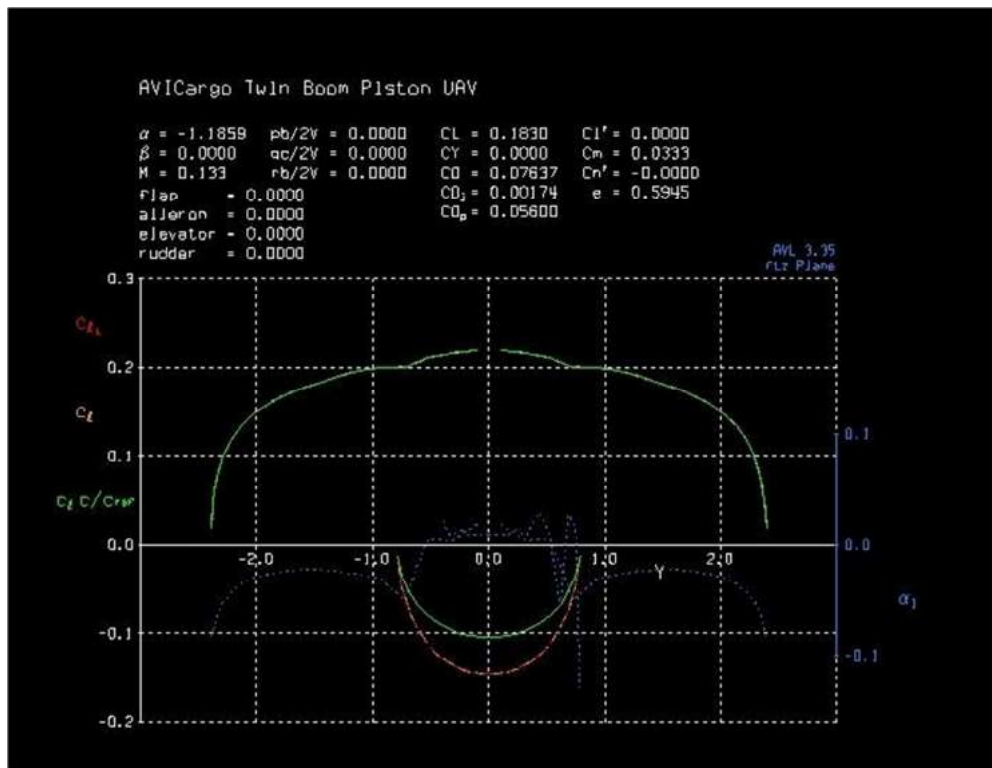


Figure D-5 Diving no control surface deflection

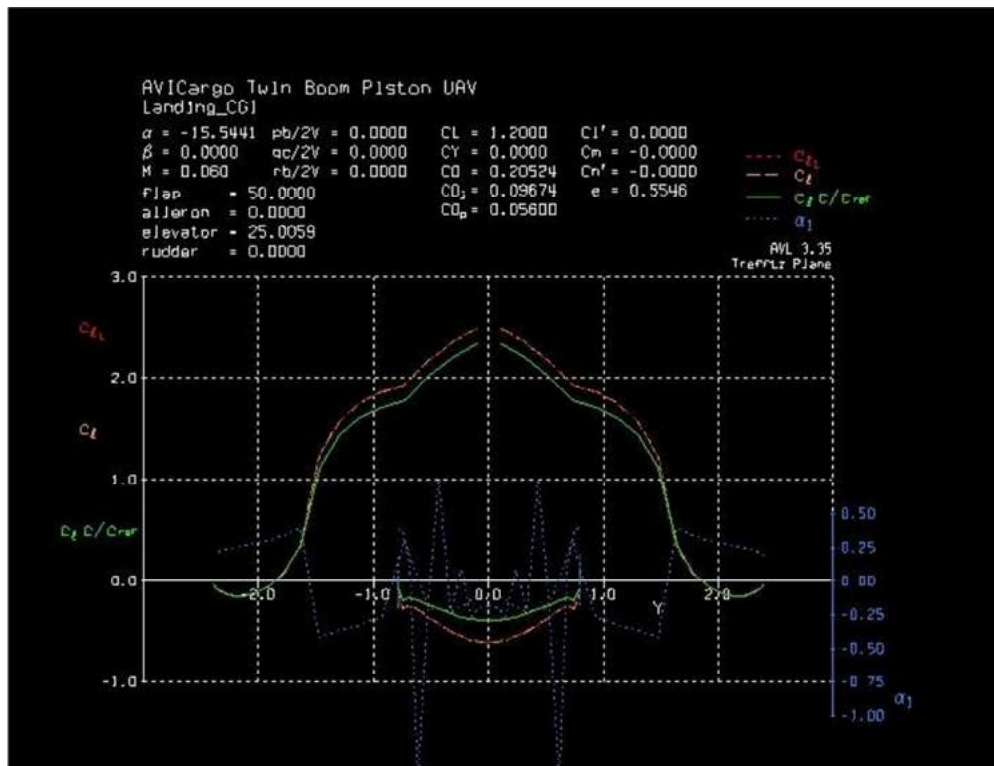


Figure D-6 Landing full flap deployed (50 degree)

### c) Component Loads due to Weight

Table D-3 Limit component weights at 1g and corresponding load factors

Engine	VT	Wing	HT	Fuselage	Boom	n	Condition
279.35	87.13	332.56	103.43	798.14	133.02	4.52	Cruise gust
213.84	66.70	254.57	79.17	610.97	101.83	3.46	Dive gust
210.13	65.54	250.16	77.80	600.37	100.06	3.4	Landing

\*\* (Weights are in Newton. Engine weight includes fuel, engine and propeller weights. VT stands for Vertical tail. HT stands for Horizontal Tail)

These weights together with lift created from control surface deflection are then applied on structural parts. These weight values will be substituted by final weight values of component for the most accurate result.

## d) Sizing of Booms – Loads and Bending Moments

*Table D-4 Ultimate loads at corresponding load factors created by control surface deflection*

Load case	Fx (N)	Fy (N)	Total Lift left surface Fz (N)	Total Lift right surface Fz (N)	Total lift surface Fz (N)
Right aileron down	0.00	0.00	2936.38	5700.02	<b>8636.40</b>
Negative elevator	0.00	0.00	-2612.72	-2612.72	<b>-5225.43</b>
Positive elevator	0.00	0.00	2612.72	2612.72	<b>5225.43</b>
Positive rudder	0.00	<b>665.12</b>	0.00	0.00	0.00
Diving	0.00	0.00	2963.67	2963.67	<b>5926.74</b>
Landing	0.00	0.00	4642.01	4642.01	<b>9284.02</b>

\*\* (The applied load on rudder is assumed to be 10 kg stick force since FAR 23-441 specification does not apply for the UAV in this case. Lift on surface indicates wing and horizontal tail).

*Table D-5 Moment acting at right boom*

Load case	Mx (Nm)	My (Nm)	Mz (Nm)
Right aileron down	0.00	-5796.16	0.00
Negative elevator	0.00	<b>9326.88</b>	0.00
Positive elevator	0.00	-5199.80	0.00
Positive rudder	0.00	0.00	1849.03
Diving	0.00	6183.04	0.00
Landing	0.00	8636.47	0.00

Max bending moment: 9326.88 Nm

Load case: Landing full flap deflection 50 degree

The maximum bending moment is then used to calculate applied bending stress and then checked again bending modulus of a material

$$M.S = \frac{n^+ \times \sigma_{allowed}}{\sigma_{applied}} = \frac{n^+ \times \left( \frac{Fb}{Ftu} \right) \times Ftu}{\frac{Mr_{out}}{0.5 * (r_{out}^4 - r_{in}^4)}}$$

## I. Boom material

Boom carries high moment and thus requiring a material with high bending modulus strength  $F_b$  and high ultimate tensile strength  $F_{tu}$ . Shortlisted materials include Aluminum 7075-T6, Aluminum 2024-T3, Aluminum 6061-T6, Aluninum 2014-T6.

*Table D-6 Listed properties of Aluminum in English units*

Material	Aluminium					
Form	Tube					
Variant	6061	2024	2014	7075		
Temper	T6	T3	T6	T6		
Thickness, in	<b>0.025-0.50</b>	<b>0.018-0.50</b>	Up to <b>1.000</b>	< 0.249	<b>0.250-0.499</b>	<b>0.50-0.749</b>
$F_{tu}$ , ksi	42	66	65	82	85	85
$F_{cy}$ , ksi	/	/	/	/	/	/
$F_{su}$ , ksi	/	/	/	/	/	/
$E$ , ksi	/	/	/	/	/	/
$\omega$ (lb/in <sup>3</sup> )	0.098	0.100	0.101	0.101		

\*\* (Adapted from MIL-HDBK-5H, Military handbook of metallic materials and elements for aerospace vehicle structures)

*Table D-7 Boom diameters and mass*

Material	Mass (kg)	M.S	Outer diameter (cm)	Inner diameter (cm)
6061-T6	2.92	0.07	10.16	9.96
2024-T3	3.17	0.14	4.45	3.81
2014-T6	2.51	0.07	5.08	4.66
7075-T6	2.51	0.07	5.08	4.66

For minimum mass, either 2014-T6 or 7075-T6 is selected for boom construction. The final mass is 2.51 kg.

## E Appendix - Undercarriage

### a) Landing Gear Geometric Layout

The geometric layout of the tricycle landing gear system is sized based on the centre of gravity of the aircraft. The ADV has a forward CG of 1.01 metres and an aft cg of 1.11 metres. A tip back angle of  $15^\circ$  was used to position the main landing gear from the aft CG [2]. The position of the nose landing gear was determined with the purpose of achieving an ideally 90-10 load distribution to allow for ease of rotation during take-off. There was a compromise between the position of the nose gear and the load it supported due to the limited space in the front section of the ADV due to a lack of structural support in the front section of the fuselage. As a compromise, a load distribution of 83-17 which is still within the ideal 6-20% range specified by Currey which constitutes a wheel base of 1.16 metres [8].

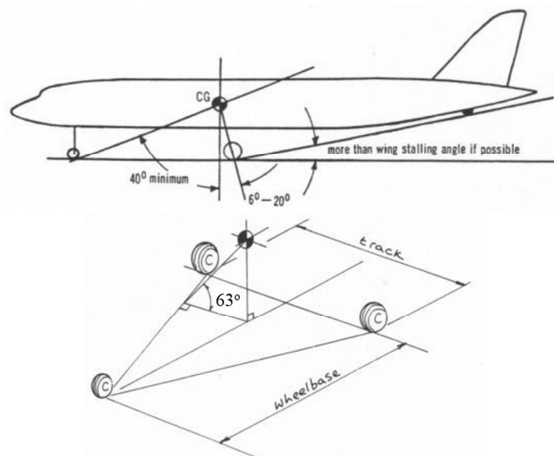


Figure E-1 Tricycle Landing Gear Layout [21]

The lateral position of the landing gear is defined by the wheel track and was determined to be 1.4 metres. Lateral stability was a design criterion when positioning the undercarriage and an overturn angle requirement of  $<63^\circ$  was required [2]. The trade off in this case was that the reduction in wheel track would decrease the strut weight due to a reduced strut length however increase the overturn angle. Weight is of particular importance in the design of the ADV and as such a wheel track of 1.4 m was decided resulting in an overturn angle of  $60.3^\circ$  which lies in the acceptable limits outlined in figure E-1.

## b) Tyre Selection

The ADV is designed to take-off and land on cleared dirt runways, a surface in which is typically suited for Type III tyres [2]. These tyres typically offer low-pressure for cushioning and floatation and are readily available which would be beneficial when considering the operating conditions and location in which the ADV is intended. Type III tyres are ideally implemented for piston aircraft with a ground speed of less than 140 knots.

Both the nose wheel and the main wheels are subject to landing forces however the main landing gear is subjected to higher static loads and the nose wheel is subject to greater dynamic loads and therefore is typically 60-100% the tyre size of the main undercarriage. In order to determine a suitable tyre size, Raymer's statistical approach in tyre sizing was implemented to determine the minimum wheel diameter which is defined by the equation below [4].

$$\text{Diameter (in.)} = A \cdot W_w^B$$

where

$A = 1.51, B = 0.349$  (general aviation)

$W_w$  = weight on wheel

The maximum weight on one wheel is determined by the FAR23 load cases, which yields a minimum tyre diameter of 9.9 inches. In accounting for the possibility of future growth in weight of the aircraft a 25% addition to the load may be incorporated, however in the case of the ADV, this isn't ideal due to the GTOW constraint of 60kg.

The selected tyre for the undercarriage ADV is the Type III 5.00-4 Nylon Tube Type which is the smallest commercially available type III tyre. Its properties are summarised under table E-1.

Table E-1 Tyre Type

Nose Gear and Main Gear Tyre	
<b>Type</b>	Type III 5.00-4 Nylon
<b>Diameter</b>	13.25 in (33.66 cm)
<b>Width</b>	4.30 in (10.90 cm)
<b>Max deflection</b>	3.20 in (8.130 cm)
<b>Weight</b>	4.30 lb (1.95 kg)

### c) Shock Absorber Types

Shock absorber selection for the ADV was based on the criteria of reducing cost and minimising the need for maintenance and repairs. As such, simple systems were employed which consists of a leaf-spring cantilever main gear and a bungee cord shock absorber for the nose gear. Both systems have minimal moving parts and a simplistic in design, thus more suited for the operational conditions of the design mission.

### d) Stroke Length Calculation

The stroke length of a landing gear system is determined by a combination of the stroke provided by the tyre and the stroke by the strut. Both tyre deflection and shock absorber deflection depends on the kinetic energy that is resultant during landing and is determined by:

$$\Delta KE = \frac{-WV^2}{2g} = -S \cdot n_s \cdot NW - S_t \cdot n_t \cdot NW + (W - L)(S + S_t)$$

where

$W$  = aircraft weight, lb = 132.16 lb

$V$  = sink speed,  $fts^{-1}$  ( $10fts^{-1}$ ) according to FAR 23.473

$S_t$  = tyre deflection, ft = 0.27 ft

$S$  = strut deflection, ft

$N$  = landing gear load factor = 3

$n_t$  = tyre efficiency = 0.47

$n_s$  = shock absorber efficiency = 0.5 (spring leaf), 0.6 (rubber bungee)

The equation above describes kinetic energy and is summarised to approximate the stroke length as follows:

$$\frac{V^2}{2g} = N(S \cdot n_s + S_t \cdot n_t)$$

From the relationship above, the defined stroke length for the cantilever spring is 0.24 metres (9.58 inches) and for the bungee cord shock absorber it is 0.2 metres (8 inches). These deflection values are less than the clearance length of the ADV and so the spring leaf system for the main gear and the bungee cord design for the nose gear were used for the ADV.

### e) Design Approach

For the ADV's main landing gear, the design of the system carried out by satisfying regulations specified by authorities. The landing gear system is modelled using SolidWorks, then a finite element analysis with SolidWorks simulator and ANSYS to test for stresses and potential failures. Since weight was a primary concern of the design of this UAV, optimisation in the landing gear system needed to be carried out to reduce the weight. This was iteratively performed through varying the leaf spring geometry and rerunning FEA to ensure compliance with regulations.

Table E-2 shows the loads that are applied to the landing gear during finite element analysis.

*Table E-2 Load Cases for Undercarriage Design*

	<b>Level Landing (i) FAR 23.479</b>	<b>Level Landing (ii) FAR 23.479</b>	<b>Tail Down Landing FAR 23.481</b>	
Vertical Load at Wheel	487.91 N	587.84 N	587.84 N	
Fore/Aft Load at Wheel	392.38 N	392.38 N	196.19N	
Lateral Load at Wheel	0.00 N	0.00 N	0.00 N	
	<b>One Wheel Landing FAR 23.483</b>		<b>Braked Roll FAR 23.485</b>	<b>Side Load Conditions FAR 23.493</b>
Vertical Load at Wheel	975.82 N	487.91 N	324.46 N	
Fore/Aft Load at Wheel	392.38 N	521.09 N	195.46 N	
Lateral Load at Wheel	0.00 N	0.00 N	293.92 N	

### f) Stress Analysis

The results from FEA for the critical load cases are displayed in this section. The smallest margin of safety for the main undercarriage is 0.29 for the one wheel landing condition. The remaining conditions have a higher margin of safety. Figures E- to E- summarises the FEA results.

## One Wheel Landing

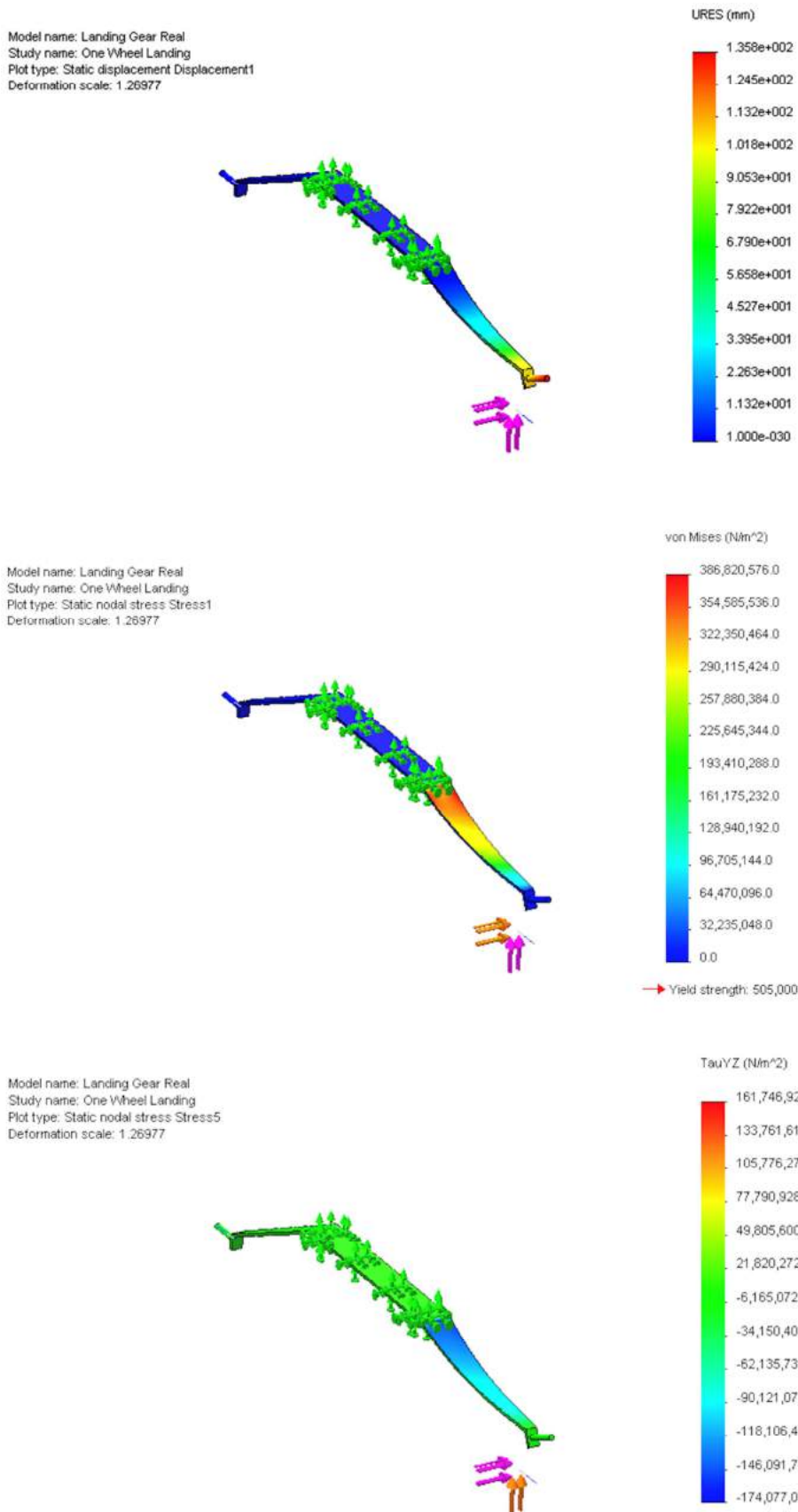
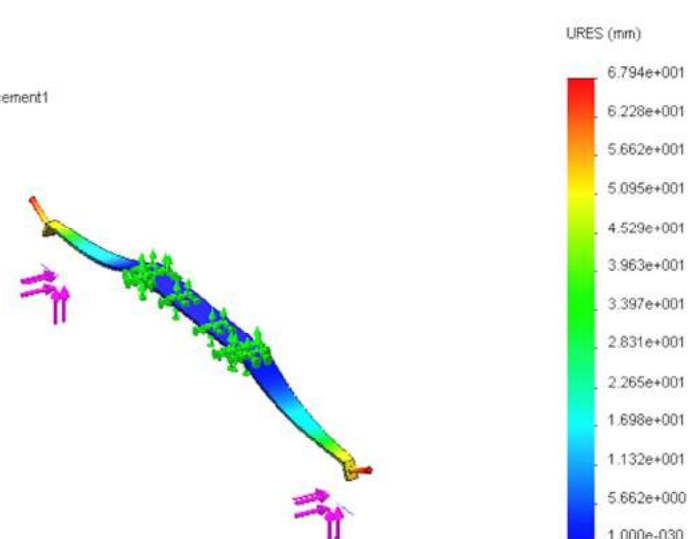


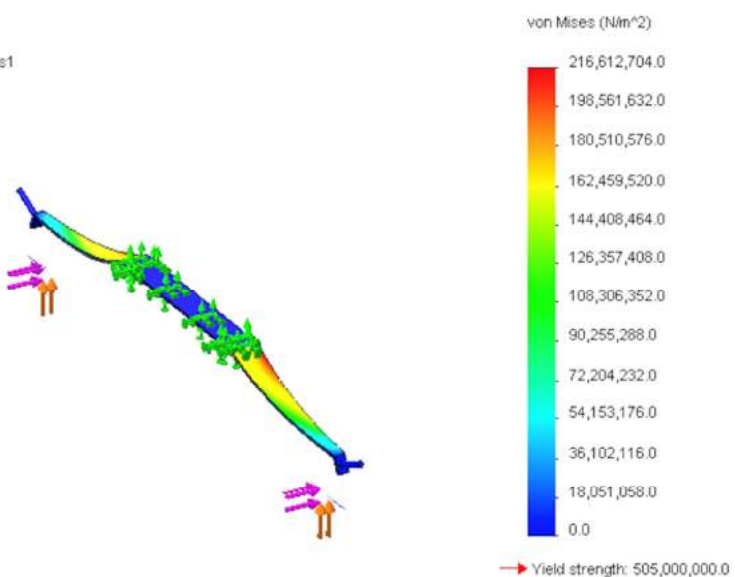
Figure E-1 One Wheel Landing - SolidWorks

## Braked Roll Condition

Model name: Landing Gear Real  
 Study name: Braked Roll Condition  
 Plot type: Static displacement Displacement1  
 Deformation scale: 2.53506



Model name: Landing Gear Real  
 Study name: Braked Roll Condition  
 Plot type: Static nodal stress Stress1  
 Deformation scale: 2.53506



Model name: Landing Gear Real  
 Study name: Braked Roll Condition  
 Plot type: Static nodal stress Stress2  
 Deformation scale: 2.53506

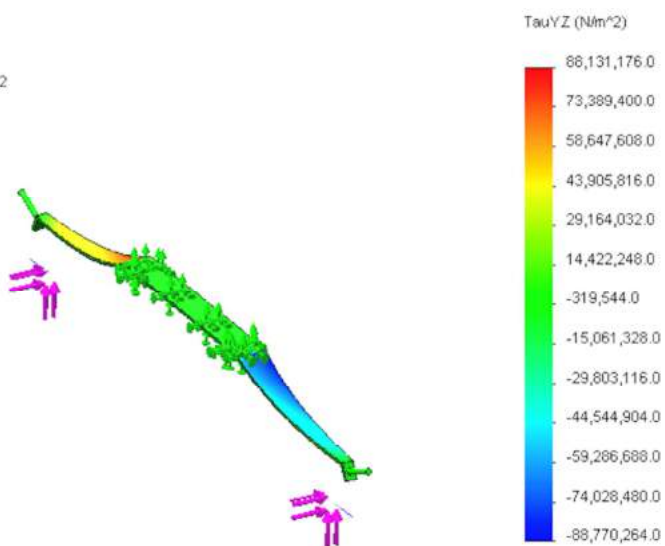


Figure E-2 Braked Roll - SolidWorks

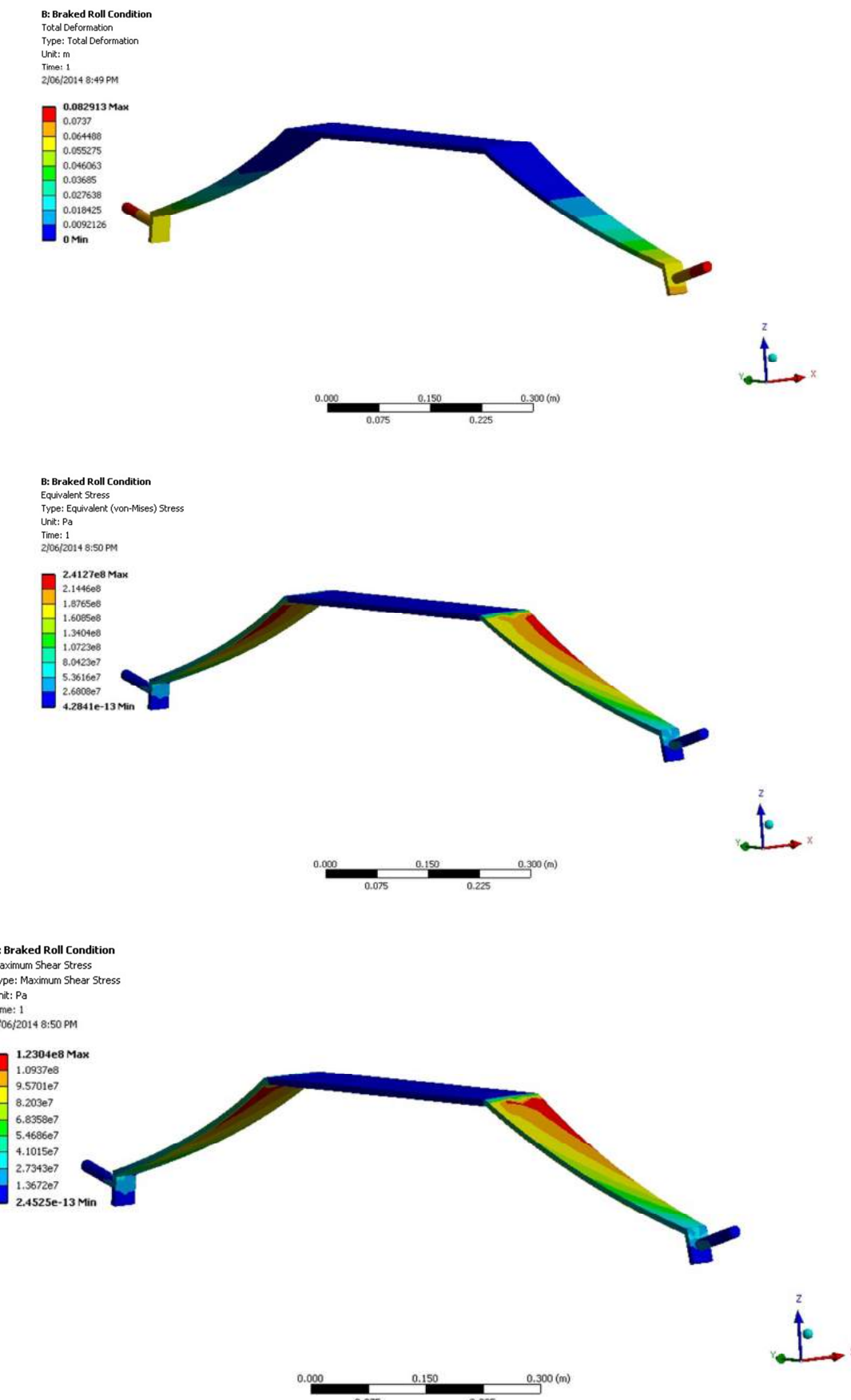
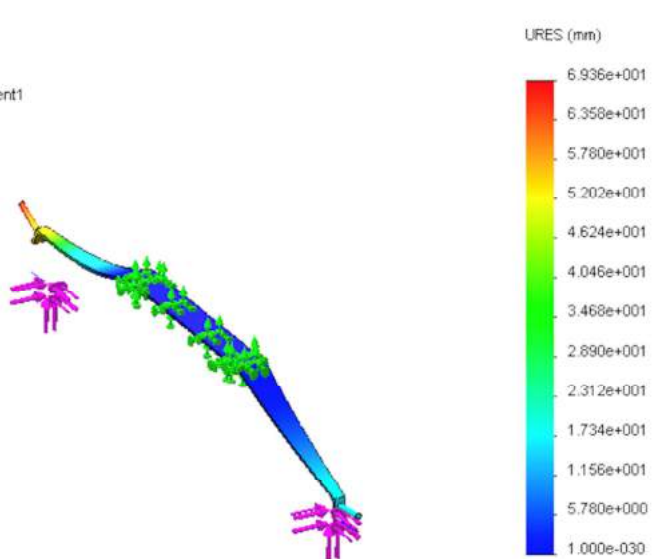


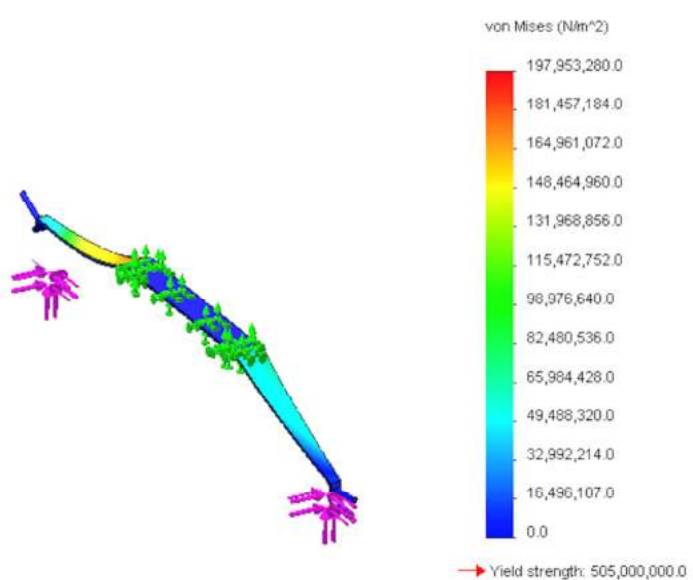
Figure E-3 Braked Roll - ANSYS

## Side Load Conditions

Model name: Landing Gear Real  
 Study name: Side Load Conditions  
 Plot type: Static displacement Displacement1  
 Deformation scale: 2.48432



Model name: Landing Gear Real  
 Study name: Side Load Conditions  
 Plot type: Static nodal stress Stress1  
 Deformation scale: 2.48432



Model name: Landing Gear Real  
 Study name: Side Load Conditions  
 Plot type: Static nodal stress Stress2  
 Deformation scale: 2.48432

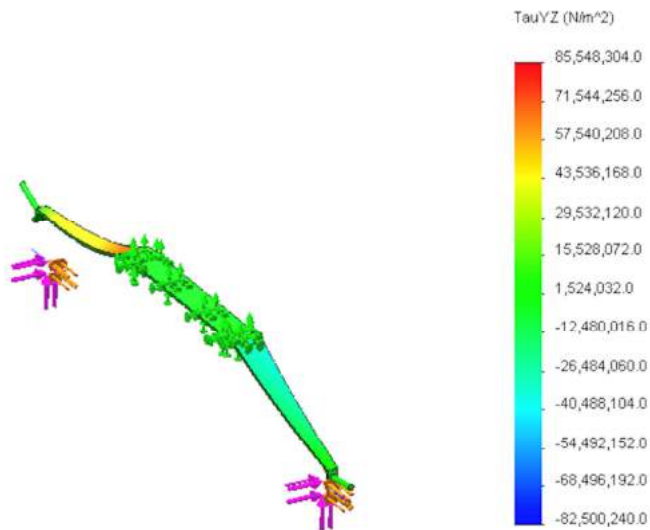
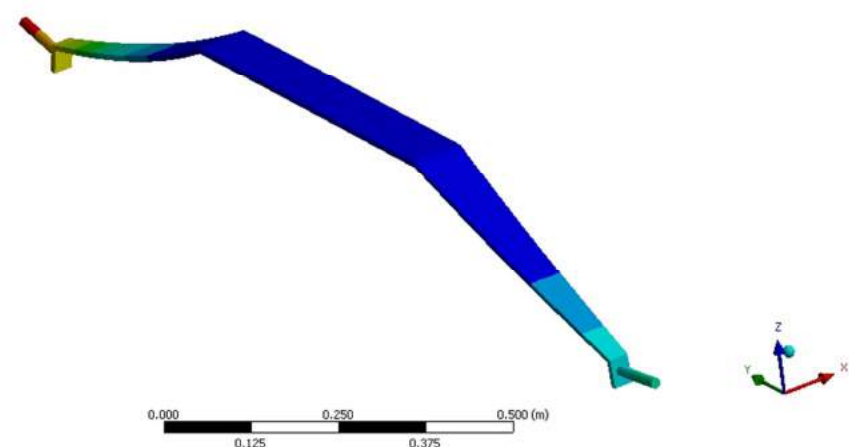
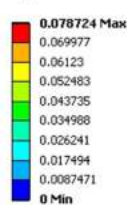


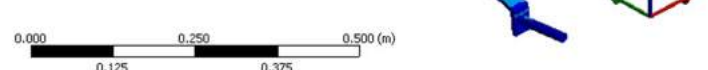
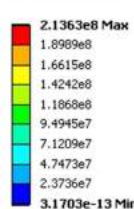
Figure E-4 Side Loading - SolidWorks

**C: Side Loading Condition**

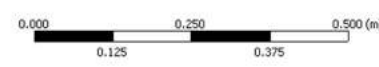
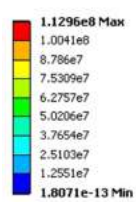
Total Deformation  
Type: Total Deformation  
Unit: m  
Time: 1  
2/06/2014 8:55 PM



Equivalent Stress  
Type: Equivalent (von-Mises) Stress  
Unit: Pa  
Time: 1  
2/06/2014 8:56 PM



Maximum Shear Stress  
Type: Maximum Shear Stress  
Unit: Pa  
Time: 1  
2/06/2014 8:57 PM



## References

- [1] L. M. Nicolai and G. E. Carichner, Fundamentals of Aircraft and Airship Design, Virginia: AIAA, 2010.
- [2] S. Gudmunsson, General Aviation Aircraft Design Applied Method and Procedure, First edition ed., Oxford: Elsevier, 2014.
- [3] UIUC, “UIUC airfoil database,” 2014. [Online]. Available: [http://aerospace.illinois.edu/m-selig/ads/coord\\_database.html](http://aerospace.illinois.edu/m-selig/ads/coord_database.html). [Accessed 3 May 2014].
- [4] D. P. Raymer, Aircraft Design: A Conceptual Approach, Washington DC: AIAA, 1992.
- [5] D. Stinton, The Design of the Aeroplane, London: Oxford, 1983.
- [6] X. International, “Xoar International - Sport Propellers,” 2014. [Online]. Available: <http://www.xoarintl.com/rc-propellers/gas-props/PJA-Sport-Prop-Type-A-Beechwood-Propeller/>. [Accessed 1 June 2014].
- [7] Zenith Aircraft Company, “Zenith Air, STOL CH 701 Design Revision 2.1,” Zenith Aircraft Co. , 2008.
- [8] N. S. Currey, Aircraft Landing Gear Design: Principles and Practices, Washington DC: AIAA, 1988.
- [9] J. Roskam, Airplane Design Part V: Component Weight Estimation, Kansas: Roskam Aviation and Engineering Corporation, 1985.
- [10] University of Minnesota, “UAV Research Group - Avionics and Sensors,” 2014. [Online]. Available: [http://www.uav.aem.umn.edu/index.php?option=com\\_content&view=article&id=47&Itemid=78](http://www.uav.aem.umn.edu/index.php?option=com_content&view=article&id=47&Itemid=78). [Accessed 1 June 2014].
- [11] J. Roskam, Airplane Design: Part VII, Kansas: Roskam Aviation and Engineering Corporation, 1985.
- [12] National Bureau of Statistics of the People's Republic of China, “National Bureau of Statistics of the People's Republic of China,” 2014. [Online]. Available:

- [http://www.stats.gov.cn/tjsj/zxfb/201405/t20140527\\_558611.html](http://www.stats.gov.cn/tjsj/zxfb/201405/t20140527_558611.html). [Accessed 28 May 2014].
- [13] 3W International, “2-Stroke Heavy Fuel and Gasoline Engines, 3W-157XIB2,” 2014. [Online]. Available: <http://www.3w-international.com/3W-157xiB2.php>. [Accessed 3 May 2014].
- [14] 3W International, “2-Stroke Heavy Fuel and Gasoline Engines, 3W-170XIB2,” 2014. [Online]. Available: <http://www.3w-international.com/3W-170xiB2.php>. [Accessed 3 May 2014].
- [15] Hirth Motors, “Gobler-Hirth F41,” 2014. [Online]. Available: <http://www.hirth-motoren.de/en/engine-f41.html>. [Accessed 3 May 2014].
- [16] UAS Engines, “Quadra-Aerrow,” 2014. [Online]. Available: [http://media.aero.und.edu/uasresearch.org/documents/195-197\\_Reference-Section\\_Engines.pdf](http://media.aero.und.edu/uasresearch.org/documents/195-197_Reference-Section_Engines.pdf). [Accessed 1 May 2014].
- [17] Desert Aircraft, “DA-100L,” 2014. [Online]. Available: [http://www.desertaircraft.com/engines\\_detail.php?Page=DA-100](http://www.desertaircraft.com/engines_detail.php?Page=DA-100). [Accessed 1 May 2014].
- [18] Desert Aircraft, “DA-120,” 2014. [Online]. Available: [http://www.desertaircraft.com/engines\\_detail.php?Page=DA-120](http://www.desertaircraft.com/engines_detail.php?Page=DA-120). [Accessed 1 May 2014].
- [19] J. B. Brandt and M. S. Selig, Propeller Performance Data at Lower Reynolds Numbers, 2011.
- [20] UIUC, “UIUC Propeller Database,” 2014. [Online]. Available: <http://aerospace.illinois.edu/m-selig/props/propDB.html>. [Accessed 1 May 2014].
- [21] A. Web, “Aerospace Web - Aircraft Landing Gear Layouts,” 2014. [Online]. Available: <http://www.aerospaceweb.org/question/design/q0200.shtml>. [Accessed 8 May 2014].
- [22] J. Roskam, Cessna 172 - Stability and Control Derivatives, Airplane Flight Dynamics and Automatic Flight Controls Part 1, 2003.
- [23] B. W. McCormick, Aerodynamics, Aeronautics and Flight Mechanics, 1979.

- [24] L. Pazmany, Light Airplane Design, San Diego, California, 1963.
- [25] M. Sadraey, Landing Gear Design, Daniel Webster College, 2002.
- [26] J. Roskam, Airplane Design Part II: Preliminary Configuration Design and Integration of Propulsion System, Kansas: Roskam Aviation and Engineering Corporation, 1985.